Journal of Asian Earth Sciences 35 (2009) 199–231

Contents lists available at ScienceDirect

Journal of Asian Earth Sciences

journal homepage: www.elsevier.com/locate/jaes

Ultrahigh-pressure minerals and metamorphic terranes – The view from China

J.G. Liou [a,*], W.G. Ernst [a], R.Y. Zhang [a], T. Tsujimori [b], B.M. Jahn [c]

[a] *Department of Geological and Environmental Sciences, Stanford University, Stanford, CA 94305-2115, USA*
[b] *Pheasant Memorial Laboratory for Geochemistry and Cosmochemistry, Institute for Study of the Earth's Interior, Okayama University, Misasa, Tottori 682-0193, Japan*
[c] *Institute of Earth Sciences, Academia Sinica, Taipei 11529, Taiwan*

ARTICLE INFO

Article history:
Received 13 May 2008
Received in revised form 8 October 2008
Accepted 18 October 2008

Keywords:
Global UHP terranes
Microdiamond
Majoritic garnet
Garnet peridotite
SHRIMP U–Pb ages
Sulu

ABSTRACT

Ultrahigh-pressure (UHP) metamorphism refers to mineralogical modifications of continental and oceanic crustal protoliths ± associated mafic-ultramafic rocks initially formed or emplaced in shallow levels of the lithosphere, but which subsequently have experienced *P–T* conditions within or above the coesite stability field (>~2.7 GPa, ~700 °C). Typical products include eclogite, garnet peridotite, and UHP varieties of metapelite, quartzite, marble, paragneiss, and orthogneiss. UHP metamorphic assemblages require relatively cold lithospheric subduction to mantle depths; some recrystallization even occurs under "forbidden" *P–T* conditions, characterized by a geotherm of <5 °C/km. In appropriate bulk compositions, UHP metamorphism produces coesite, microdiamond and other indicator phases such as majoritic garnet, TiO_2 with α-PbO_2 structure, supersilicic clinopyroxene, high-*P* clinoenstatite, K-cymrite and stishovite. Globally, at least 20 coesite-bearing eclogitic, eight diamond-bearing, and five majoritic garnet-bearing UHP regions have been documented thus far; they are mostly of Phanerozoic ages. The presence of majoritic garnet, and even apparent stishovite pseudomorph in supracrustal rocks suggests continental subduction to mantle depths exceeding 300 km; such UHP metamorphic terranes should be distinguished from deep-seated mantle xenoliths that contain UHP minerals. Cold subduction zones may be sites of major recycling of H_2O back into the mantle; high-*P* experiments on mafic-ultramafic bulk compositions reveal that many important hydrous and formally anhydrous phases are stable under such UHP conditions.

The current explosion of research on continental UHP terranes reflects their significance for mantle dynamics and the tectonics of continental subduction, collision, exhumation, mantle–slab interactions, and geochemical recycling. A further characterization of UHP phases and positive identification of UHP minerals requires new experimental studies coupled with state-of-the-art analyses. For example, the very rare occurrence of microdiamond inclusions in zircons from Dabie–Sulu UHP rocks may reflect high f_{O_2} attending recrystallization inasmuch as epidote is rather common. Rutile needles within garnets from Sulu UHP eclogitic rocks may not be the result of exsolution, so in such cases the apparent UHP pressure may have been over estimated. Hadean igneous microdiamond inclusions in Jack Hills detrital zircons could have originated from mantle xenoliths whereas abundant detrital Phanerozoic diamonds containing inclusions of coesite and other eclogitic minerals from New South Wales might have been derived from unexposed UHP metamorphic terranes. Micro-mineral intergrowth and nano-size minerals may hold important key to deciphering the actual *P–T* paths of subduction and mantle return flow. Although most exhumed terranes have returned surfaceward relatively rapidly after short time of UHP condition, the long duration of storage at great depth and slow exhumation for the largest UHP terranes remain as major problems.

1. Introduction

The current explosion in research on continental UHP terranes reflects their significance regarding mantle dynamics and the global tectonics of continental subduction, collision, exhumation, mantle–lithospheric slab interactions, and geochemical recycling. Many comprehensive review articles and special issues related to UHP metamorphism and plate tectonics have recently been published (e.g., Chopin, 2003; Jahn et al., 2003a; Liou et al., 2004; Green, 2005a; Ernst et al., 2007; Zhang et al., 2007g; Ernst and Liou, 2000, 2008; Guillot et al., 2008). In this review for terranes in northern Tibet prepared for the 8th International Eclogite Conference in 2009, we update some of the most recent findings of UHP minerals and terranes; both UHP rocks and lawsonite eclogites occur in northern Tibet and require very low geothermal gradients, <~7 °C/km. Some even record recrystallization under "forbidden" *P–T* conditions (Liou et al., 2000; Tsujimori et al.,

* Corresponding author. Tel.: +1 (650) 723 2716; fax: +1 (650) 725 2199.
E-mail address: jliou@stanford.edu (J.G. Liou).

1367-9120/$ - see front matter
doi:10.1016/j.jseaes.2008.10.012

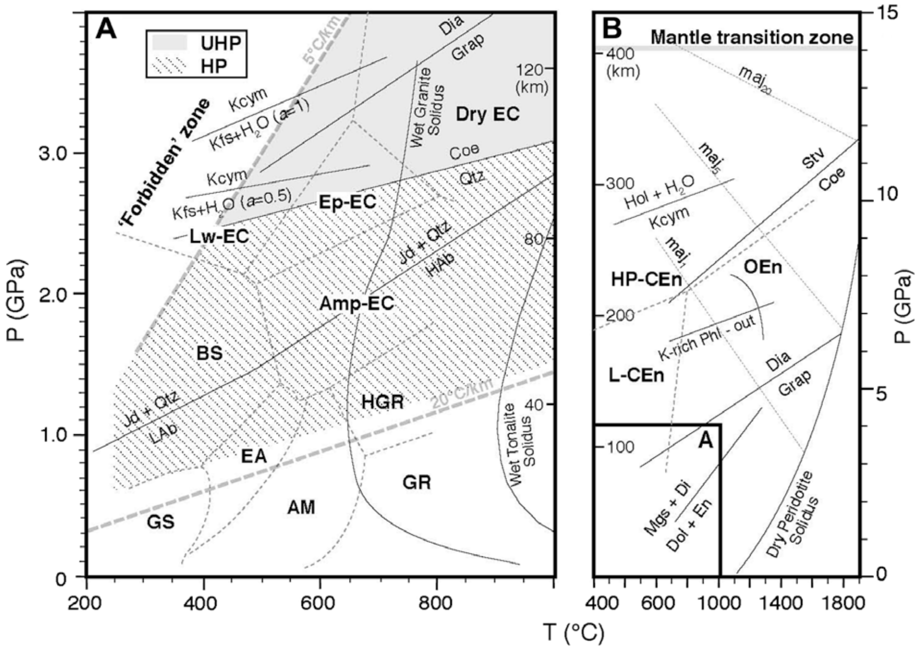

Fig. 1. (A) *P–T* regimes assigned to various metamorphic types: (1) ultrahigh-*P*, (2) high-*P*, (3) low-*P* and (4) "forbidden zone" and stabilities of coesite, diamond, jadeite and K-cymrite (modified after Liou et al. (2004)). (B) *P–T* stabilities of additional UHP index minerals including recently reported pseudomorphic stishovite, majoritic garnet, high-*P* clinoenstatite and pseudomorphic K-cymrite are shown (see text for references). Geotherms of 5 °C and 20 °C/km are indicated. *P–T* boundaries of various metamorphic facies [granulite (GR), amphibolite (AM), epidote amphibolite (EA), blueschist schist (BS), greenschist (GS) and subdivision of the eclogite (EC) into amphibole (Amp) eclogite, epidote (Ep) eclogite, lawsonite (Lw) eclogite and dry eclogite] are indicated (see text for explanation and references).

2006a) (Fig. 1). Occurrences of UHP minerals, including coesite and diamond have long been recognized in mantle xenoliths originating at great depths; however such occurrences should be distinguished from units formed at modest crustal levels and later subjected to UHP conditions in collisional orogens, as will be described in this review. Garnet peridotite as a new window to mantle wedge processes also requires attention. Reports of some previous findings of special UHP minerals will be reevaluated.

Among many recent exciting discoveries by Earth scientists, the following findings deserve to be highlighted: (1) stishovite pseudomorphs in a UHP pelitic gneiss from western China (Liu et al., 2007d, this issue), (2) coesite and/or clinopyroxene lamellae in ophiolitic chromite from the Luobusa ophiolite, southern Tibet, and from the classical Scottish Barrovian terrane (Yamamoto et al., 2007, 2009), (3) Hadean-age microdiamond inclusions in detrital zircons from the Jack Hills of western Australia (Menneken et al., 2007), and (4) multistage formation of majoritic garnet in a single Norwegian UHP garnet peridotite (Scambelluri et al., 2008).

Numerous UHP phases have been identified in deeply subducted supracrstal rocks since 2000. Rutile with α-PbO_2-type TiO_2 structure has been described from diamondiferous quartzofeldspathic rocks occurring in east-central China and in Bohemia (Hwang et al., 2000; Wu et al., 2005). K-cymrite ($KAlSi_3O_8 \cdot nH_2O$) was recently inferred to be the precursor phase of inclusions of K-feldspar aggregates in eclogitic garnet from the Dulan area of the North Qaidam terrane (Zhang et al., in press-a). These phases, as well as supersilicic titanite, Si- and/or K-bearing Cpx, and aragonite + magnesite inclusions in microdiamond-bearing paragneisses from northern Kazakhstan all suggest recovered subduction depths of ~190–280 km (Katayama et al., 2000; Ogasawara et al., 2002; Dobrzhinetskaya et al., 2006). More impressive still, textures in polycrystalline quartz with oriented inclusions of kyanite and hercynite, suggesting transformation from a precursor stishovite, have been documented for a sample of pelitic gneiss occurring along the Altyn Tagh fault, western China (Liu et al., 2007d). Thus, some continental crustal lithologies might have been exhumed from much deeper in the mantle (>350 km) than commonly accepted. Finally, diamond and coesite inferred as pseudomorphs of stishovite have been separated from chromitite layers in harzburgites from the Luobusa ophiolite, east-central Tibet (e.g., Yang et al., 2007b). Evidently, some oceanic crustal sections include UHP phases derived from deep mantle conditions.

Fig. 1 shows a subdivision of *P–T* regimes of the eclogite-facies into amphibole eclogite, epidote eclogite, lawsonite eclogite, and dry eclogite subfacies; UHP and high-pressure (HP) metamorphic domains are separated by the *P–T* boundary for the quartz–coesite equilibrium. Moreover, the equilibrium curves for (1) phase transformation of quartz–coesite, graphite–diamond and coesite–stishovite, (2) polymorphs of HP–clinoenstatite and ortho-clinoenstatite, (3) stability field of K-cymrite, and (4) isopleths of majoritic component are also shown. Mineral abbreviations are after Kretz (1983). Because this review was prepared for the 8th IEC in western China in 2009 and some participants may also visit the Dabie–Sulu UHP terrane, these regions have received the most intensive recent investigations including by the present authors; accordingly, we have used petrologic–geochemical–geochronologic data for Dabie–Sulu UHP rocks to exemplify many details discussed below.

2. Global distribution of UHP metamorphic terranes

Recognized global HP and UHP metamorphic terranes have been grouped into two types: (a) the Pacific type characterized by an oceanic assemblage consisting of first-cycle, mélanged volcaniclastic sedimentary rocks and widespread cherts ± deep-water carbonates, intimately mixed with structurally disaggregated ophiolites and (b) the Alpine collision-type characterized by protoliths including continental shelf carbonates, bimodal volcanics, peraluminous sediments, and granite-gneiss basement rocks (Maruyama et al., 1996; Ernst, 2006; Ernst et al., 2007). Thus far, all reported lawsonite eclogites are confined to Pacific-type orogens with typical MORB protoliths. Most UHP rocks have Alpine-type protoliths and consist mainly of felsic and intermediate gneissic rocks with minor mafic eclogites and ultramafic garnet peridotites; the mafic–ultramafic rocks appear to have originated from different tectonic settings but were subjected to coeval UHP metamorphism, deformation, and retrogression with the enclosing granitic gneisses and supracrustal rocks. Inasmuch as UHP eclogites and garnet peridotites most completely preserve petrological, geochemical and isotopic constraints on tectonic models of continental subduction, collision and subsequent exhumation, they have received the most intensive study.

Globally recognized UHP and lawsonite–eclogite terranes are shown in Fig. 2; a few examples of near-UHP terranes are also shown. Thus far, more than 20 coesite-bearing, eight diamond-bearing, five majoritic garnet-bearing UHP regions and five lawsonite eclogite-bearing HP belts have been documented in the world; most of them are of Phanerozoic ages, but a few are Neoproterozoic. These UHP and near-UHP terranes lie within major continental collision belts and extend for several hundred kilometers or more; most are in Eurasia, with rare examples in Africa, South, Central and North America and Antarctica. They share the following common structural and lithological characteristics. (1) UHP records are preserved mainly in eclogites and garnet peridotites enclosed as pods and slabs within quartzifeldspathic gneissic units. A few of those rocks contain minute inclusions of coesite in zircon, garnet and omphacite, microdiamonds in garnet, zircon and tourmaline, and inferred majoritic garnet based on exsolved lamellae of pyroxenes + Rt ± Ilm ± Ap. (2) The bulk-rock compositions of most lithologies are similar to the upper levels of the continental crust. (3) Exhumed UHP units are now present near the surface as thin subhorizontal slabs, bounded by normal faults on the top, and reverse faults on the bottom, and are sandwiched in with HP or lower grade metamorphic units. (4) Coeval island-arc volcanic and plutonic rocks are rare, whereas post-collisional or late-stage A-type granitic plutons are common.

UHP terranes, recognized based on the occurrence of stishovite pseudomorphs, majoritic garnet, diamond and coesite, are described below. Lithological and tectonic characteristics including index minerals, *P–T* conditions, size and peak metamorphic ages are summarized in Table 1. Because many of these UHP terranes have been extensively reviewed (e.g., Liou et al., 2004; Ernst et al., 2007; Ernst and Liou, 2008), only some new findings for each terrane since 2005 are described. Moreover, many of the UHP terranes contain microdiamond ± majoritic garnet in addition to coesite; in order to save space, each UHP terrane will be described only under one category.

2.1. Altun Tagh UHP terrane with possible stishovite pseudomorphs, western China

Stishovite is a HP polymorph of coesite stable at $P \sim 9$–10 GPa (Ono, 1998) and has been described from meteorites and impact craters (Chao et al., 1962; Sharp et al., 1999; El Goresy et al., 2000). This UHP silica phase may contain a few % Al_2O_3 in contrast to limited Al-solubility in both coesite and quartz (Irifune and Ringwood, 1993; Pawley et al., 1993). Pseudomorphs of stishovite were described recently as tiny inclusions in the Luobusa ophiolitic chromite of southern Tibet (Yang et al., 2007b) and in Altun Tagh UHP metapelites (Liu et al., 2007d), western China.

The Altun Tagh UHP terrane, about 200 km long, has been considered as a western extension of the North Qaidam belt of western China. Eclogitic lenses and blocks of various sizes together with garnet–lherzolite and clinopyroxenite are enclosed within a sequence of Early Proterozoic amphibolite, amphibole schist, garnet-bearing granitic gneiss, and pelitic gneiss. Garnet–lherzolite contains magnesite that reacted with aragonite to form dolomite; a *P–T* estimate of the peak magnesite-bearing assemblage yields >3.6 GPa and 850 °C (Liu et al., 2002b). Garnet porphyroblasts include exsolution lamellae of clinopyroxene and rutile, and are interpreted to have had majoritic garnet as a precursor phase.

The associated eclogites contain inclusions of coesite pseudomorphs in garnet with characteristic radial fractures; this, together with exsolved quartz rods in omphacite and *P–T* estimates of 820–850 °C and 2.8–3.2 GPa, provide additional evidence for

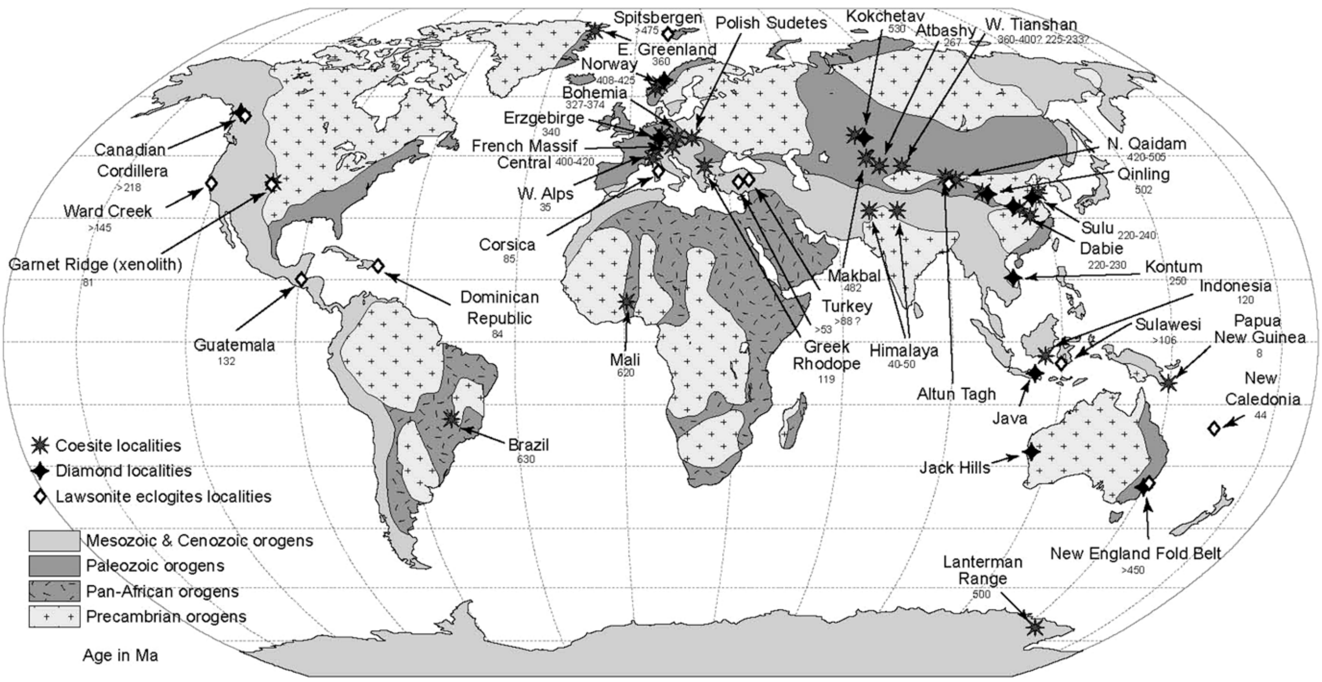

Fig. 2. Global distribution and peak metamorphic age of recognized coesite-, and diamond-bearing UHP terranes and lawsonite eclogite localities (modified after Liou et al. (2004) and Tsujimori et al. (2006a,b)).

Table 1
Worldwide occurrences of UHP metamorphic rocks (each UHP terrane is listed only once under the following four different categories).

Locality	UHP index minerals*	Peak-stage** (°C, GPa)	Metamorphic age in Ma	Selected recent references
(a) Inferred Stishovite pseudomorph-bearing UHP terrane				
Altun Tagh, western China	Coesite pseu. in Grt (eclogite); inferred stishovite pseudomorph (pelite)	820–850; 2.8–3.6	~493–504	Liu et al. (2001, 2007a,b,c,d), Zhang et al. (2001, 2005)
(b) Inferred Majoritic garnet-bearing UHP Terrane				
Western Gneiss Region, Norway	Coesite; diamond; majoritic Grt (peridotite)	>800; >3.2	408–425	Smith (1984), Scambelluri et al. (2008), Hacker (2007), Dobrzhinetskaya et al. (1995)
Dabie–Sulu, Eastern China	Coesite; majoritic Grt (eclogite and Grt peridotite); diamond in Grt (eclogite)	600–930; 2.7–5	220–240	Liou et al. (1998), Zheng et al. (2003a), Zhang et al. (2006a,b,c,d), Liu et al. (2008a,b)
N. Qaidam, western China	Coesite; diamond and majoritic Grt (peridotite)	620–740; 2.8–3.5	420–450	Yang et al. (2001), Song et al. (2005a,b), Mattinson et al. (2006)
Bohemian Massif	Coesite pseu.; majoritic Grt (peridotite)	>650–1100; >3.2–4.5	365–380	Massonne and Bautsch (2002), Massonne and O'Brien (2003)
Rhodope, Greece	Diamond + coesite pseu. (metapelite); magnesite + aragonite (marble); majoritic Grt (peridotite)	600–900; >3.1–3.9	149, 73, 51	Mposkos and Kostopoulos (2001), Liati et al. (2002), Liati (2005), Perraki et al. (2006), Mposkos et al. (2006), Bauer et al. (2007)
(c) Diamond-bearing UHP terrane				
Kokchetav Massif, Kazakhstan	Diamond (gneiss, marble); coesite (gneiss, whiteschist)	800–1000; 4–6	530–537	Sobolev and Shatsky (1990), Hermann et al. (2001), Katayama et al. (2002a,b), Parkinson et al. (2002), Okamoto et al. (2006),
Saxonian Erzgebirge, Germany	Diamond and coesite (gneiss); TiO_2 phase with α-PbO_2 structure	>900; >4	337	Massone (1999, 2001), Hwang et al. (2000), Massonne et al. (2007)
Maksyutov Complex, Ural Mtn	Diamond, diamond pseu., coesite pseu. (pelite)	640–690; 1.5–1.7 (annealed?)	375–400	Chesnokov and Popov (1965), Leech and Ernst (1998), Bostick et al. (2003)
Qinling, central China	Diamond in zircon (eclogite)	590–760; >2.6	507	Yang et al. (2003a)
Kontum, Vietnam	Diamond in zircon (HP granulite)	>900; 1.5–2 (>4?)	250	Nakano et al. (2006)
(d) coesite-bearing UHP Terrane				
Dora Maira, Italian Alps	Coesite in pyrope (whiteschist) and Cpx (eclogite); P–T–f_{O_2} estimates	>700; ~4.3 GPa	35–38	Chopin, 1984; Schertl et al. (2001), Hermann (2003), Castelli et al. (2007)
Western Tian-Shan, China	Coesite in garnet (eclogite)	500–600; 2.7–2.8	233–226	Zhang et al. (2007c,f), Lu et al. (2008)
Makbal, western Kyrgyzstan	Coesite pseu. in garnet (eclogite)	640–680; >2.6	482	Tagiri et al. (1995)
East Greenland Caledonides	Coesite in Grt, Cpx, Zrn (eclogite)	970; 3.6	330–390	Gilotti and Ravna (2002), McClelland et al. (2006), Gilotti and McClelland (2007)
Lanterman Range, Antarctica	Coesite in garnet (eclogite)	764–820; >2.9–3.3	500	Ghiribelli et al. (2002), Palmeri et al. (2003, 2007)
Gittidas, Pakistan Himalaya	Coesite in Grt, Omp, Zr (eclogite)	690–750; 2.7–2.9	40–50	O'Brien et al. (2001), Kaneko et al. (2003), Parrish et al. (2006)
Tso Morari, Himalaya	Coesite in garnet (eclogite)	700–800; >2.8	55	Sachan et al. (2004), Leech et al. (2005)
Papua New Guinea	Coesite in omphacite (eclogite)	700–750; 3.0	3–8	Baldwin et al. (2004, 2005), Monteleone et al. (2007)
Pohorje, eastern Alps	Coesite pseu. in Grt, Omp, Ky	760–820; 3.0–3.1	Cretaceous	Janak et al. (2004, 2006)
Zermatt-Saas, Switzerland	Coesite in tourmaline (quartzite)	590–630; 2.6–3.0	52	Reinecke (1991)
Massif Central, France	Coesite in garnet (kyanite eclogite)	700–800; >2.8	400–420	Lardeaux et al. (2001)
Mali, W. Africa	Coesite in omphacite (marble)	690–750; >2.9	620	Caby (1994), Jahn et al. (2001)
Sulawesi, Indonesia	Coesite in zircon (quartzite)	700–800; >4.0	20–27	Parkinson et al. (1998), Parkinson and Katayama (1999)
Sanbagawa, Japan	P–T estimate for Grt peridotite	700–810; 2.9–3.8	Cretaceous	Enami et al. (2004a,b)
Southwestern Brazil	Coesite in zircon (eclogite)	~800; >2.8	630–640	Parkinson et al. (2001)
Cuaba Gneiss, Dominican Republic	P–T estimates for both Grt peridotite + eclogite	~950; ~4.2	Cretaceous	Abbott and Draper (2007)
(e) Examples of near-UHP Terrane				
Chuacus complex, Guatemala	Coesite pseu. (?) in eclogitic Grt	700–750; 2–3	Cretaceous	Ortega-Gutiérrez et al. (2004)
South Motagua Fault Zone, Guatemala	P–T estimates for jadeite–laswsonite eclogite	450; ~2.7	135	Tsujimori et al. (2006a,b)
Pinchi Lake, British Columbia, Canada	P–T estimates for laswsonite eclogite	450; ~2.6	280	Ghent et al. (2009)
Qiangtang Belt, Central Tibet	P–T estimates for eclogite	480–625; 2.0–2.6	223–244	Zhang et al. (2006e), Pullen et al. (2008)

Abbreviation: pseu., pseudomorph.
* If index mineral appears in one specific rock type, the rock name is written in ( ); see text for details.
** Peak-stage P–T estimates are from eclogite and crust-derived Grt peridotite.

UHP (Zhang et al., 2001). A Sm–Nd mineral isochron for eclogitic garnet, omphacite, and whole rock yielded an age of 500 ± 10 Ma, whereas an U–Pb isochron for zircon separates from eclogite gave 504 ± 5 Ma (Zhang et al., 2001).

Pseudomorph of possible stishovite occurs in a pelitic gneiss that consists of garnet (20–25 vol%), kyanite (25–30%), perthite (30–35%) and quartz (10–15%) with minor retrograde biotite, plagioclase and sillimanite. Judging by oriented Al- and Fe-bearing oxide inclusions in the quartz, the single-phase precursor was interpreted as Al-bearing stishovite (Fig. 3A) based on experimental study as well as the measured tetragonal symmetry and lattice spacings consistent with those of stishovite. If such an interpreta-

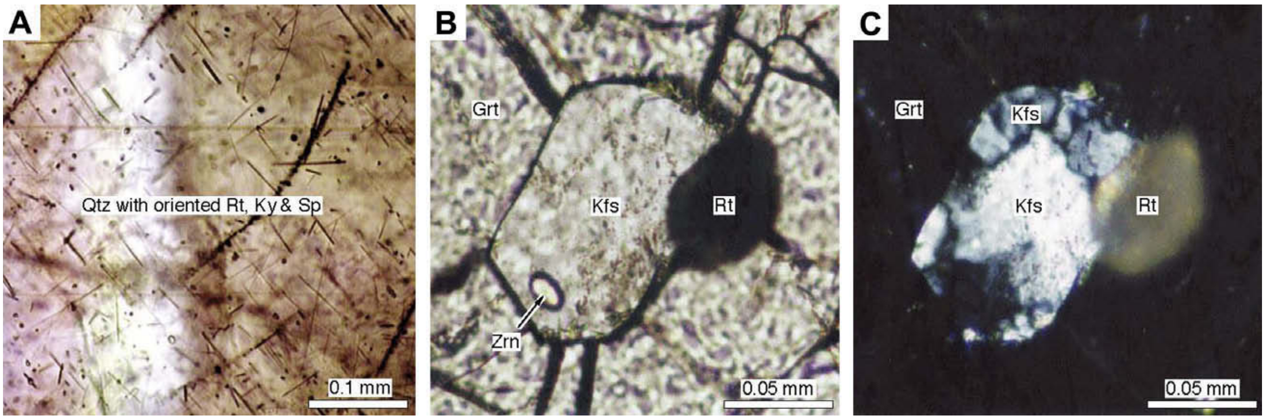

Fig. 3. Photomicrographs of newly recognized UHP minerals in western China: (A) oriented needles and rods of kyanite + hercynite + rutile in quartz interpreted as pseudomorphic stishovite from Altun Tagh pelitic gneiss (Liu et al., 2007d); (B and C) euhedral prismatic-shaped inclusion of pseudomorphic K-cymrite as K-feldspar polycrystalline aggregates in eclogitic garnet from Dulan associated with rutile showing palisade texture (B, plane polarized light; C, cross polarized light) (Zhang et al., 2008a).

tion is correct, the pelitic gneiss must have been subducted to depths >350 km; such depths are close to the "point of no return" where continental materials would have density comparable to the mantle, and would descend at least to the base of the mantle transition zone where they could contribute to the continental trace element signal in ocean island basalts (for details, see Liu et al. (2007d)). The occurrence of stishovite pseudomorphs in Altun Tagh UHP metapelites and recent geochronological dates about 30–80 Myr older than those of UHP rocks in North Qaidam led Liu et al. (this issue) to suggest that the Altun Tagh terrane may be a discrete separate collision orogen rather than a western extension of the North Qaidam UHP terrane displaced by the Altun Tagh strike-slip fault (e.g., Yang et al., 2001; Mattinson et al., 2007).

2.2. Inferred majoritic garnet-bearing UHP terranes

Majorite is a supersilicic garnet end-member that contains one fourth of its silicon in octahedral coordination and is stable well below depths >150 km (Ringwood and Major, 1971). Its occurrence in mantle xenoliths has been well documented (e.g., Haggerty and Sautter, 1990). It is recognized as having been an original single phase but is now present as host garnet containing topotaxially exsolved needles, rods or laths of pyroxenes ± Rt ± Ap. Such majoritic garnets with complex compositions have been characterized from eclogites and garnet peridotites from at least five UHP terranes as described below:

Western Gneiss Region, Norway: The Western Gneiss Region (WGR) lies within an Early Paleozoic collision zone; the gneissic unit, about 300 km long and 150 km wide, consists of interlayered pelite and migmatite, marble, quartzite, and amphibolite, with tectonic inclusions of gabbro, and peridotite. The gneissic unit exhibits mainly amphibolite-facies assemblages; eclogite boudins are widespread (e.g., Terry et al., 2000; Hacker, 2007). Since coesite was first reported by Smith in 1984, many new localities of coesite and coesite pseudomorphs have been found in both eclogites and the adjacent gneissic rocks (Wain, 1997; Carswell and Cuthbert, 2003; see Fig. 3 of Hacker, 2007). Microdiamond grains were described from residues separated from two gneisses (Dobrzhinetskaya et al., 1995) and in garnet peridotite (van Roermund et al., 2002; Brueckner et al., 2003). The suture zone occupied by WGR UHP/HP rocks reflects collision of the eclogite-bearing Greenland sialic crust-capped lithospheric plate (Laurentia) with Fennoscandia during the Caledonian orogeny (Gilotti, 1993; Krogh and Carswell, 1995; Brueckner and Medaris, 1998).

Radiometric ages for WGR eclogites are 408–425 Ma for the peak metamorphism, and 374–378 Ma for the retrogressive mid-crustal metamorphic overprinting (for reviews, see Carswell et al. (1999, 2003) and Hacker (2007)). A two-stage exhumation process is suggested: an initial exhumation to about 35 km depth by ~395 Ma at a mean rate of approximately 10 mm/yr, and subsequent exhumation to 8–10 km by ~375 Ma at a much lower rate of ~1.3 mm/yr. On the other hand, an exhumation rate of ~7 mm/yr from ~105 to ~20 km was constrained by a 390.2 ± 0.8 Ma titanite for the WGR UHP terrane (Kylander-Clark et al., 2008); these rates are slower than estimates from other, smaller UHP terranes such as the Dora Maira (Rubatto and Hermann, 2001) and Kaghan Valley terranes (Parrish et al., 2006) described below, but similar to other large UHP terranes, such as the Dabie–Sulu terrane of eastern China (>2 mm/yr, Hacker et al., 2000) (see Table 2 for a summary). This suggests that there might be a fundamental difference in the subduction and exhumation mechanisms between large and small UHP terranes.

Three generations of majoritic garnet were identified in WGR garnet peridotites on the islands of Otrøy and Flemsoy (Scambelluri et al., 2008), as shown in Fig. 4: (1) high-*T* Archean decompression melting within the mantle transition-zone (350 km; M1A) followed by upwelling and accretion to deep cratonic roots (100–125 km; M1B; van Roermund and Drury, 1998; Spengler et al., 2006); (2) isobaric cooling to 1000–1300 °C ending in Middle Proterozoic time (M2; Brueckner et al., 2003); and (3) deep subduction during the Caledonian orogeny (430–390 Ma; M3) when Baltic and Laurentian plate collision triggered the formation of microdiamond-bearing UHP rocks (van Roermund et al., 2002). Stages M1 (A–B) and M2 are recorded by the Grt peridotites and websterites where decimeter-sized garnets contain Opx and Cpx as intercrystalline grains and as intracrystalline lamellae, both exsolved from precursor majorite that contains up to 20 vol% Px component during evolution from M1A–M1B to M2 (Fig. 1 of Spengler et al., 2006). During M2, the M1B majorite exsolved intracrystalline pyroxene lamellae ~20–30 μm thick and hundreds of micrometers long. Together with the intercrystalline pyroxenes (also showing Px-Grt exsolution) and cm-sized Opx ± Cpx ± Ol ± spinel, they define the M2 assemblage. The resulting Cpx/Grt LREE partition coefficients indicate that exsolution occurred at 1280–1380 °C and ~7 GPa. The M3 assemblage consists of Grt + Opx + Cpx + Phl ± carbonate ± Spl. The M3 grain-boundary and vein garnets contain exsolved Cpx and Opx needles 1.5–3 μm thick and as long as 100 μm, much thinner than M2 Grt. The estimated abundance of

Table 2
Recent estimates of exhumation rate of selected UHP terranes.

UHP terrane	Age range (Ma)	Depth range 1st 2nd (Km)	Exhumation 1st 2nd Rates (cm/years)	Data source
WGR	408 to ~395–375	~105 to ~20	~1.0, ~0.13	Hacker (2007)
				Kylander-Clark et al. (2008)
Dabie	240 to ~220	~125 to ~30	>0.2	Hacker et al. (2000)
Sulu	239–225 to 219–210 to 209–207	120–60	0.3, 0.54	Liu et al. (2008a)
Qaidam				
Dora Mira	35.4–32.9–31.8–29.9	120–10	3.4–0.5	Gebauer et al. (1997)
Kokchetav	537–507–456	180–30 to ~10	~5, 0.4	Katayama et al. (2002a,b)
	535 to ~529	180–30	~10	Hacker et al. (2003)
Erzgebirge	336.8–330	>180–40	10, ~0.5	Massonne et al. (2007)
Kaghan Valley	~46	90–110 to		Kaneko et al. (2003)
Kaghan Valley	~50–46.4 to >44.0	108–36	~3.0–8.0	Kaneko et al. (2003), Parrish et al. (2006)
Tso Morari	55 to 48–45	~105 to 30	2.3–4.5	Massonne and O'Brien (2003)
East Papu New Guinea	7.9	>80 to surface	>1.0	Baldwin et al. (2005), Monteleone et al. (2007)

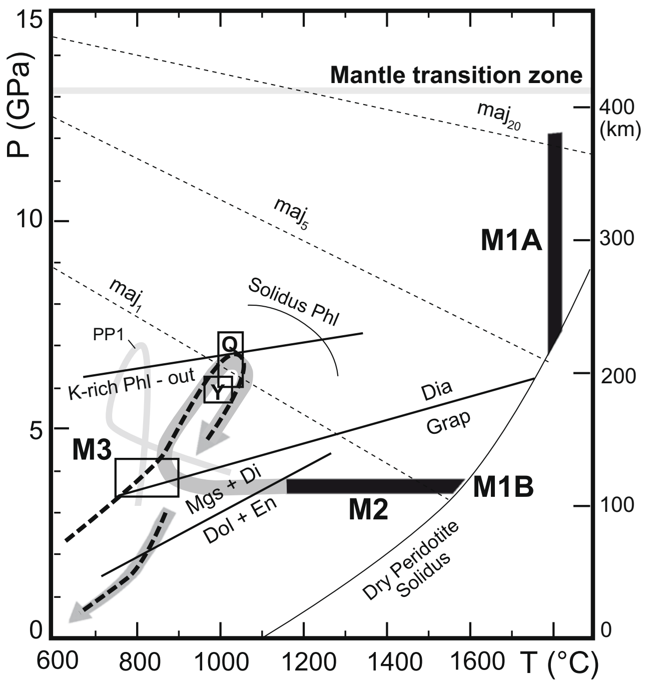

Fig. 4. *P–T* path of diamond- and majorite-bearing garnet websterite lens from Norway. Black path: Archean M1 (A and B) to Mid-Proterozoic M2 events. Light gray path – Scandian evolution. Dashed line – inferred *P–T* path of associated continental crust. White box – diamond crystallization conditions during M3. *P–T* conditions of majorite samples from Yangkuo (Y) (Ye et al., 2000) and North Quaidam (NQ) and *P–T* paths for garnet peridotite from North Qaidam (Song et al., 2005a,b) are shown. Thin solid lines labeled 1%, 5% and 20% are experimental isopleths for majorite component in garnet (modified after Fig. 1 of Scambelluri et al. (2008)).

pyroxene needles is 1–1.5 vol%; such pyroxene exsolution indicates that majoritic garnet crystallized during the M3 event at about 6.5 GPa (Dobrzhinetskaya et al., 2004; Scambelluri et al., 2008).

The M1 and M2 majoritic garnets were formed by solid-state transformation of pyroxene into garnet in a mantle setting. In contrast, M3 majorite localized in veins and along grain boundaries and its coexistence with phlogopite and carbonate suggest crystallization from aqueous-carbonate silicate fluids during deep continental subduction to >200 km. Such fluid-precipitated majoritic garnets may be similar to analogues in North Qaidam garnet peridotites described below.

Evidently, Archean (~3.5 Ga) deep-seated mantle containing majoritic garnets underwent exsolution during upwelling from a depth of 350 km or more, and was subjected to extensive partial melting; the residue formed a garnet-bearing cratonic root. These cratonic mantle assemblages of Proterozoic age (~1.8–1.4 Ga) were then incorporated into subducting sialic crust during the Caledonian continental collision at ~400 Ma. The conclusion of pre-subduction exsolution was based on detailed Re–Os and Sm–Nd age data (Brueckner et al., 2003, 2004), and on REE concentrations and partitioning between exsolved pyroxenes and the host garnets (Spengler et al., 2006). On the other hand, the M3 majoritic garnet recrystallized at about 6 GPa and 1000 °C, coeval with Caledonian UHP metamorphism of the associated supracrustal rocks.

Dabie–Sulu terrane, east-central China: The Triassic Dabie–Sulu UHP terrane marking the collision zone between the North China and South China blocks, has received the most intensive investigations in terms of manpower and resources, including the first Chinese continental scientific 5-km drilling project, completed in 2005 (described below; for a recent comprehensive review of the Dabie–Sulu orogen, see Zheng (2008)). Blocks, boudins and layers of eclogite and garnet peridotite occur as enclaves in UHP gneisses. Ubiquitous occurrences of coesite inclusions in zircons of felsic gneisses and eclogites from both surface and core samples indicate that the supracrustal rocks (>90% felsic gneisses, <10% eclogites) were subducted to depths >100 km (e.g., Zhang et al., 1995b). Drill core samples show the Sulu UHP slab to be >5 km thick; the Dabie–Sulu UHP terrane extends for >2000 km and is about 50 km wide. SHRIMP dating of zoned zircons identified four discrete age groups: mid-Neoproterozoic protolith ages (740–780 Ma) in inherited cores (Zheng et al., 2004; Liu et al., 2004a,b; Tang et al., 2008b), a UHP event in coesite-bearing mantles at 225–240 Ma (Liu et al., 2004a,b, 2005, 2006a,b; Wu et al., 2006), eclogite-facies assemblages at 215–225 Ma (Liu et al., 2006c; Zhao et al., 2006b) and amphibolite-facies overprint in quartz-bearing rims at 215–205 Ma (Liu et al., 2004a,b). These data constrain the rate of exhumation at >5 km/Ma (e.g., Hacker et al., 2006; Ernst et al., 2007). The presence of anomalously low $\delta^{18}O$ values in UHP minerals of eclogitic and felsic rocks suggests extensive meteoric water–rock interactions both prior to and under Snowball Earth conditions during the Neoproterozoic, and limited fluid infiltration during Triassic continental subduction and exhumation (Yui et al., 1995; Rumble et al., 2002; Zheng et al., 2003a, 2004; Chen et al., 2007a; Tang et al., 2008a). Such cold-climate effects also recorded in very negative $\delta^{18}O$ values of magmatic minerals such as garnet (Zheng et al., 2007a) and zircons (Tang et al., 2008a).

The Dabie–Sulu UHP rocks show several special characteristics. (1) Widespread occurrences of coesite and coesite pseudomorphs as inclusions in garnet, omphacite (Fig. 5A), zircon (Fig. 5B and C), kyanite, zoisite, epidote (Fig. 5D) and dolomite (e.g., Zhang and Liou, 1996); UHP hydrous minerals such as talc, zoisite/epidote, and

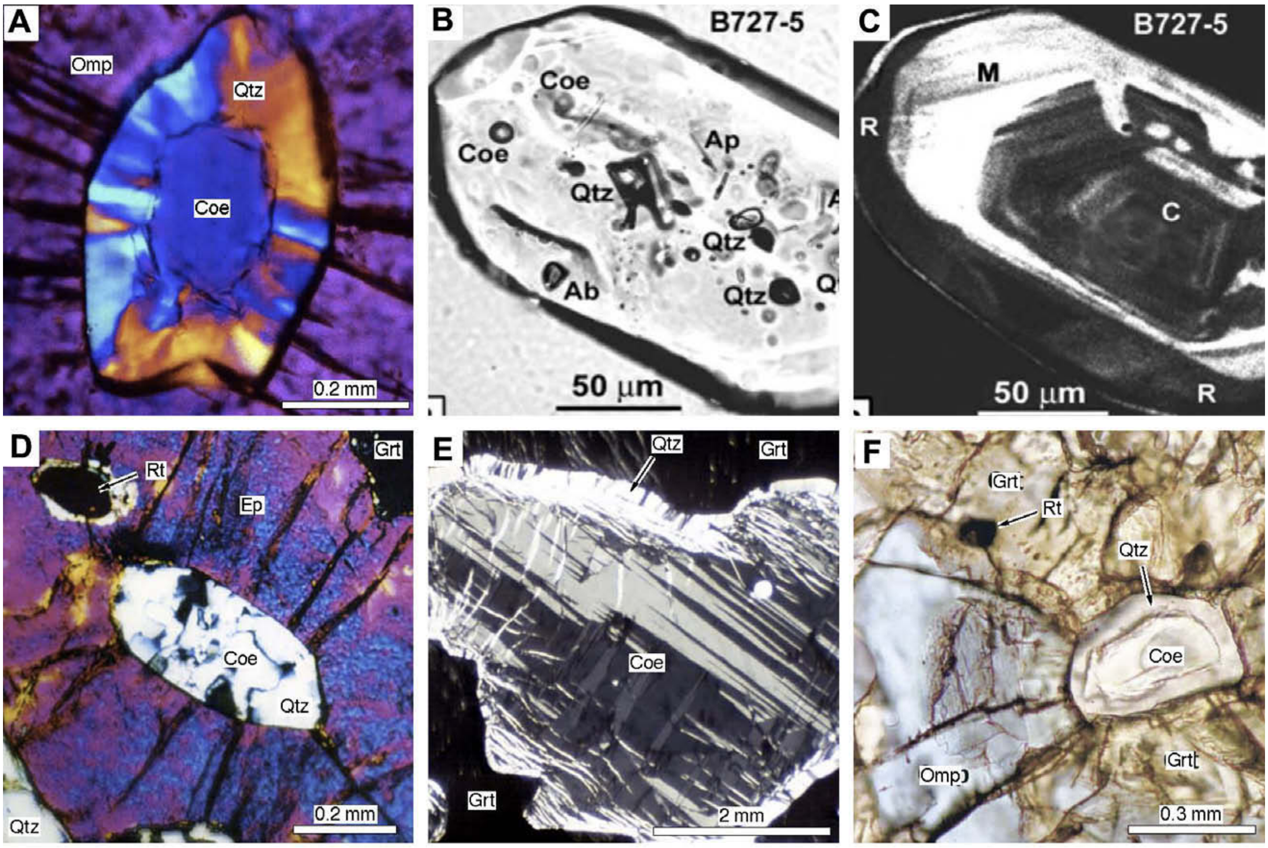

Fig. 5. Photomicrographs of coesite and coesite pseudomorphs in UHP rocks: (A) inclusion of coesite + palisade quartz in omphacite from Maowu omphacitite (Liou and Zhang, 1996), (B) plane polarized light image of mineral inclusions in zircon and (C) cathodoluminescence images of host zircon from epidote- and biotite-bearing two-feldspar granitic gneiss core of the CCSD-Main hole (B727, 1325.2 m depth). This zircon grain contains Qtz + Ap in the core, coesite in the mantle, and albite in the rim (Liu et al., 2007d), (D) inclusion of coesite pseudomorph in epidote from Qinglongshan eclogite (Zhang et al., 1995a), (E) inclusion of coarse-grained twinned coesite with palisade quartz at the margin in garnet of Dora Maira quartzite (courtesy from Werner Schreyer), and (F) intergranular coesite from Yangkou eclogite, Sulu (Zhang and Liou, 1997).

phengite are present in eclogites. (2) Both mantle-derived and crustal-hosted garnet peridotites occur (see below). (3) Abundant exsolution textures have been identified in UHP minerals from garnet peridotite and eclogite. (4) *P–T* estimates lie within the diamond *P–T* stability field, and minor diamond inclusions are contained in garnet and rare zircon from both eclogite and garnet peridotite (e.g., Okay, 1993). (4) Some garnet peridotites record much higher pressure than associated coesite-bearing eclogites, reaching 5–6 GPa (Yang et al., 1993; Zhang et al., 2000, 2003a, 2005c). (5) Various isotopic dating methods for UHP minerals and rocks including garnet peridotite yield a relatively long duration of UHP metamorphism, spanning from 240 to 220 Ma (see below for discussion).

The hypothesized occurrence of majoritic garnet has been described from two Sulu localities. (1) Ye et al. (2000) described abundant, evenly-distributed, oriented rutile needles along {1 1 1} of garnet and minor apatite inclusions in porphryroblastic garnets from a Yangkou eclogite layer within peridotite (*P–T* estimate shown as Y in Fig. 4). (2) Zhang and Liou (2003) found coarse Cpx grains from Rizhao garnet clinopyroxenites that contain up to 25 vol% exsolved garnet, 4 vol% ilmenite and minor amphibole (Fig. 6A). Experimental study of the Rizhao Grt clinopyroxenite at 4–15 GPa, 1000–1400 °C indicated that titanium solubility in garnet and Grt_{Ti}/Cpx_{Ti} ratios exhibit pronounced positive correlations with pressure, whereas the coexisting clinopyroxene contains small amounts of TiO_2 and shows no significant pressure effect (Zhang et al., 2003c). Petrologic and experimental studies suggest that the precursor of such intergrowths was majoritic garnet in which $Ca^{2+}Ti^{4+} \rightarrow 2Al^{3+}$, $Mg^{2+}Si^{4+} \rightarrow 2Al^{3+}$ in octahedral sites, and $Na^{+}Ti^{4} \rightarrow Ca^{2+}Al^{3+}$ (Zhang and Liou, 2003; Zhang et al., 2003c). The interpretation of these intergrowths as a majoritic garnet precursor phase was based on optical and SEM observations. However, recent analytical electron microscopic data obtained by Hwang et al. (2007) indicate a lack of a topotaxic relationship between rutile needles and the host Yangkou garnet. These data, together with the presence of nano-sized thin films of an amorphous phase at the contact between rutile needles and the surrounding garnet led them to question the exsolution origin of the rutile.

North Qaidam terrane, western China: Lenses and layers of garnet peridotite and eclogite occur in an amphibolite-facies gneissic terrane in the North Qaidam Mountains along the NE rim of the Qaidam Basin. This terrane extends westward for more than 1000 km to the Altun Mountains; the latter block is offset by left-lateral displacement along the Altyn-Tagh fault. This long, discontinuous UHP terrane was first established by identification of coesite inclusions in zircon from a paragneiss and *P–T* estimates of both eclogite (e.g., Yang et al., 2001; Song et al., 2003a,b, 2006; Yin et al., 2007) and garnet peridotite; (Song et al., 2004, 2005a,b, 2007 and this issue for a summary). Inclusions of K-cymrite ($KAlSi_3O_8 \cdot nH_2O$) pseudomorphs as K-feldspar polycrystalline aggregates (Fig. 3B and C) have been identified in Dulan eclogites where coesite occurs as includions in zircons of nearby gneissic rocks (Zhang et al., 2008; also see Fig. 4D and E of Song et al. (2003a,b)).

Inasmuch as this belt is covered in detail in this special issue, only some relevant garnet peridotites containing possible majoritic garnet described by Song et al. (2004, 2005a) are briefly described here. The Luliangshan garnet peridotite is the largest block, 500–800 m across within felsic gneisses (for details, see Song et al. (2004, 2005a,b, 2007) and this issue), and consists of Grt

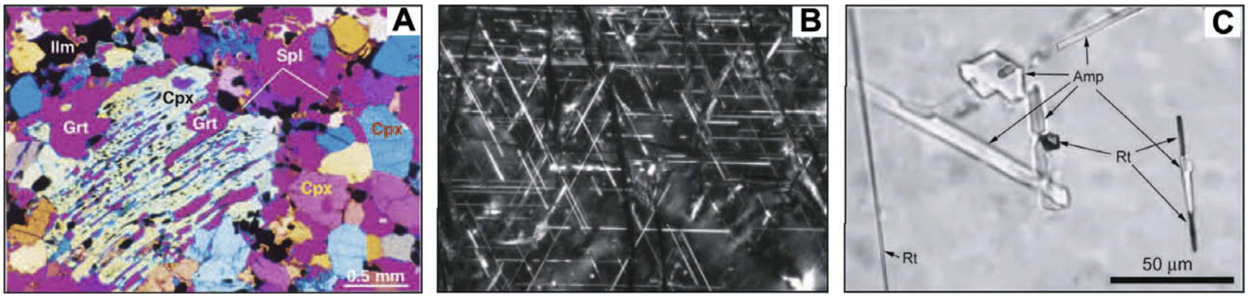

Fig. 6. Inferred majoritic garnet from the Sulu and North Qaidam UHP terranes: exsolution lamellae of (A) Grt + Ilm in relict clinopyroxene from Sulu peridotite (Zhang and Liou, 2003), (B and C) Rt + Amp in peridotitic garnet from North Qaidam (Song et al., 2005b).

(∼10–20 vol%), Ol (∼40–60%), Opx (∼15–25%), Cpx (∼5–15%) and minor Cr-rich spinel. Exsolution in porphryroblastic garnet consists of densely packed rods of Rt, Opx, Cpx, and two kinds of sodic amphibole (Fig. 6B and C). Exsolution in olivine includes rods of Ilm and Al-chromite. Pyroxene exsolution lamellae in garnet crystals suggest that the parent must have originally possessed excess silicon, i.e., they were majoritic garnets stable only at depths >150 km. Exsolution of rutile and sodic amphiboles further suggests that the inferred majoritic garnets must also have contained excess Ti, Na and hydroxyl (>1000 ppm) that are soluble only at UHP. The exsolution of ilmenite and Al-chromite rods from olivine is also consistent with the peridotite having once being equilibrated at very high pressures (>300 km). Estimation of Ti and Na contents in the reconstructed majoritic garnets yields $P > 8$ GPa. Thermobarometric calculations using matrix minerals of the peridotite yield re-equilibrium conditions of 960–1040 °C and 5.0–6.5 GPa. These observations and inferences, together with the occurrence of a microdiamond inclusion in the core of a zircon from garnet peridotite (Song et al., 2005b) and field observations, indicate that the North Qaidam garnet peridotite probably represents a mantle slice exhumed from depths >240 km. SHRIMP dating of zircon from one diamond-bearing garnet peridotite yields 457 ± 22 Ma in the cores, 423 ± 5 Ma in the outer zones and 397 ± 6 Ma in the rims representing, the cumulation, subduction and exhumation events (Song et al., 2005b).

However, recent petrologic study of mineral inclusions in porphyroblastic garnet, clinopyroxene and olivine from various ultramfic rocks of this body by Yang and Powell (2008) resulted in a very different conclusion. They described many low-P mineral inclusions such as Hbl + Chl, Spn + Opx forming symplectite after garnet in some garnet porphyroblasts, Act-Ed, calcite and lizardite in some Cpx porphyroblasts and Mg-rich olivine (Fo95-99), F-rich clinohumite, Pyx, chromite, anthophyllite-cummingtonite, Cl-rich lizadite, carbonates and "Ca-phlogopite" in olivine porphyroblasts. These findings and *P–T* estimates based on several pseudosections led them to suggest that these UHP ultramafic rocks were formerly mantle peridotites emplaced into the oceanic crust that was subjected to serpentinization by seawater-derived fluids near the sea floor prior to subduction to 3.0–3.5 GPa and 700 °C.

Bohemian Massif: The Bohemian Massif exposes the metamorphic core of the Variscan orogen along its eastern margin. It is a collage of several smaller basement areas differing in age and metamorphic evolution. Both eclogites and garnet peridotites have been extensively investigated (see a summary by Massonne and O'Brien (2003)). UHP rocks occur in all units characterized by HP rocks but so far, index minerals including coesite, and diamond have been found only in the Erzgebirge (see below) and coesite pseudomorphs in the Polish Sudetes (Bakun-Czubarow, 1991).

In the Bohemian Massif, Massonne and Bautsch (2002) described an unusual, meter-sized garnet pyroxenite from the Granulitgebirge, Germany. This rock is embedded in serpentinized garnet peridotite and consists of megacrysts which apparently were originally majoritic garnet from an upper portion of the mantle transition zone (>400 km). Exsolution lamellae of almost mm-wide garnet and clinopyroxene layers run parallel over several centimeters. Compositions of Grt and Cpx lamellae yield *P–T* estimate of ∼2.5 GPa and 1000 °C for the exsolution process. REE concentrations of minerals and the whole rock suggest that the host rock consisted essentially of garnet megacrysts; it might have been transported upward within a mantle plume, with upwelling facilitated by the presence of melt that interacted with the garnet pyroxenite.

Peridotites containing majoritic garnets have also been reported in other localities of the Bohemian Massif in both the Czech Republic and the Polish Sudetes (Bakun-Czubarow, 2007). Unfortunately, description of these occurrences is only in abstract form. Garnet porphyroblasts (up to 0.8 cm in diameter) in host lherzolite contain exsolved lamellae of Rt, Ilm, Opx and Ol, mainly along their {1 1 1} planes in the cores, and have estimated compositions of $Pyr_{72}Alm_{16}(Grs + Uvr)_7Ti\text{–}Mj_5$ where Ti–Mj stands for two possible Ti-equivalents of the majorite molecule: $Ca_2Na(AlTi)Si_3O_{12}$ and $M_3(MgTi)Si_3O_{12}$. Such majoritic garnets are not supersilicic either in terms of the amount of exsolved SiO_2, or in terms of stoichiometry (i.e., showing more than three Si atoms pfu). This garnet–lherzolite yielded UHP conditions of 4.5 ± 0.4 GPa and 1100 ± 30 °C, and is suggested to have been exhumed from depths in excess of 200 km (Bakun-Czubarow, 2007).

Greek Rhodope: The Greek Metamorphic Province (RMP) at the border between Greece and Bulgaria represents a synmetamorphic nappe-system that formed during the Cretaceous to mid-Tertiary collision of Apulia and paleo-Europe. The intermediate nappe complex comprises eclogites, orthogneisses, pelitic gneisses and minor mantle-derived ultramafic rocks. These units contain many mineralogical indicators of UHP metamorphism, such as inclusions of diamond in garnet porphyroblasts from pelitic gneiss, coesite pseudomorph inclusions in supersilicic eclogitic garnets containing quartz lamellae (Mposkos and Kostopoulos, 2001; Perraki et al., 2006), and coexistence of magnesite + aragonite in dolomitic marble (Mposkos et al., 2006). *P–T* conditions for diamond-bearing UHP metapelites were estimated at >850 °C and 4.3 GPa.

Liati (2005) obtained SHRIMP ages of 149 Ma for metamorphic zircons from a paragneiss of the Central Rhodope for which (U)HP conditions have been suggested, and 51 Ma for amphibolitized eclogite of the West Rhodope. These ages together with other (U)HP ages suggest that four distinct events of Alpine (U)HP metamorphism can be distinguished: 149, 73, 51 and 42 Ma. The Rhodope consists of different terranes, which resulted from multiple subductions and collisions of microcontinents, rather similar to the presently accepted picture in the Central and Western Alps.

Associated ultramafic rocks include garnet-spinel-bearing lherzolite and layers of spinel-garnet clinopyroxenite, garnet pyroxenite and clinopyroxene garnetite. These ultramafic rocks were subjected to UHP recrystallization at *P–T* conditions of ~1200 °C, >3.0 GPa. The occurrence of rods or needles of silica, rutile, biotite and apatite in sodic garnet suggests the former presence of majoritic garnet at ~7 GPa. These UHP rocks were reequilibrated at >800 °C at a SHRIMP-determined age of 171 ± 1 Ma (Bauer et al., 2007). Evidently the UHP metamorphism predated the Alpine suturing of Apulia and paleo-Europe by more than 100 Myr.

2.3. Diamond-bearing UHP terranes

Since metamorphic microdiamond was first discovered as inclusions in garnet and zircon in gneissic rocks of the Kokchetav Massif, northern Kazakhstan (Sobolev and Shatsky, 1990) (Fig. 7A and B), microdiamond inclusion has been increasingly recognized in other UHP terranes. For example microdiamond inclusions in Hadean zircons with an age range from 3058 ± 7 to 4252 ± 7 Ma were reported from the Jack Hills metasedimentary belt, western Australia (Menneken et al., 2007). This finding of the oldest known diamonds in terrestrial rocks introduces a new aspect to the debate on the origin of these zircons and the evolution of the early continental crust. The specific mineralogical features of these diamonds, including their occurrence in zircon, their association with graphite, and their Raman spectroscopic characteristics resemble UHP microdiamonds. These occurrences imply a relatively thick continental lithosphere and crust–mantle interaction at least locally in the Archean, and perhaps as long ago as 4.2 Ga.

In the Phanerozoic New England fold belt of eastern Australia, about 2 million diamonds have been mined from Tertiary alluvial deposits that are more than 1500 km from the nearest craton (Barron et al., 2005, 2008). Unlike diamonds from ancient cratons, these diamonds contain unique inclusions of eclogitic rocks of Phanerozoic ages. Some garnets exhibit unusual chemical characteristics and microstructures (oriented exsolution lamellae of rutile/apatite/ilmenite), implying the possible existence of an unexposed UHP metamorphic terrane in eastern Australia.

As shown in Table 1, at least seven terranes contain well-confirmed microdiamond occurrences in UHP rocks; these include paragneiss and marble of the Kokchetav Massif of Kazakhstan (Sobolev and Shatsky, 1990), metasedimentary rocks of the Erzgebirge Massif of Germany (Massonne, 1999), eclogites and garnet peridotites of the Dabie–Sulu (Xu et al. 1992, 2005), North Qaidam (Song et al., 2005a,b) and Qinling (Yang et al., 2003a) terranes of China, paragneiss and garnet peridotite of the Western Gneiss Region of Norway (Dobrzhinetskaya et al., 1995), metapelites of the Greek Rhodope (Mposkos and Kostopoulos, 2001), and garnet mica schist of the Maksyutov Complex of the South Ural Mountains (Leech and Ernst, 1998; Bostick et al., 2003). Other suspected diamond-bearing UHP terranes include the Central Indonesia

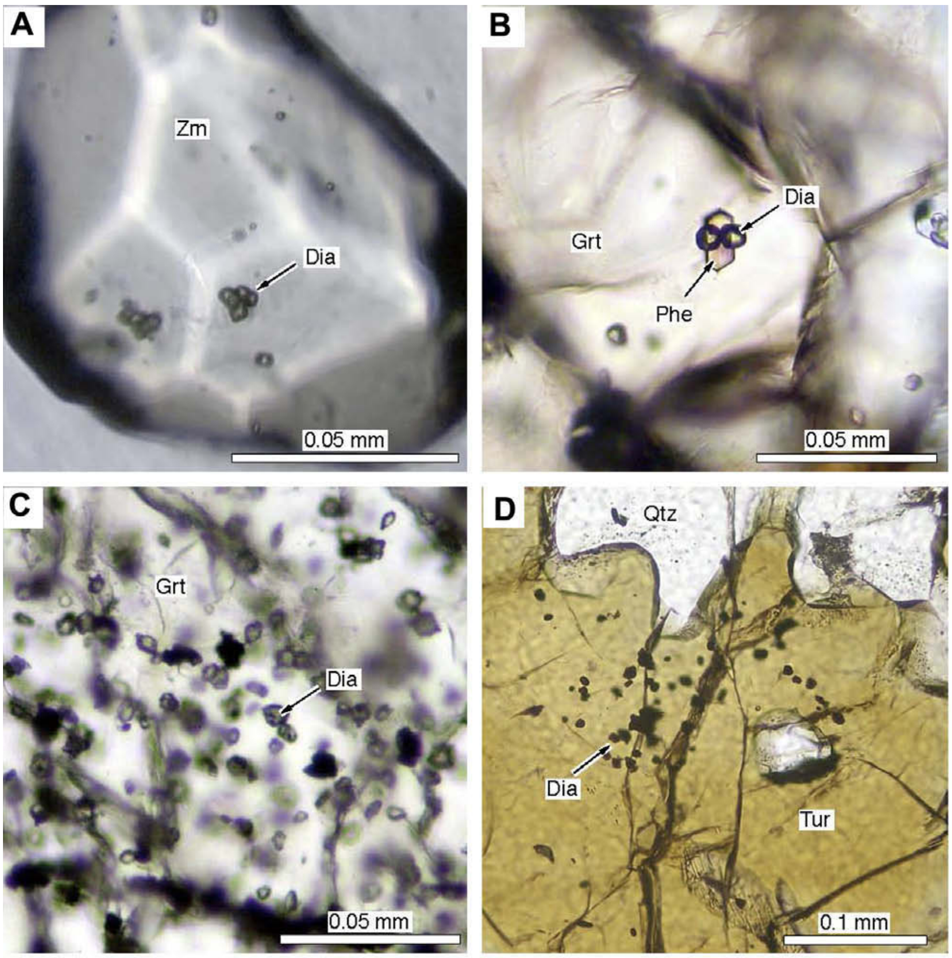

Fig. 7. Photomicrographs of microdiamonds from the Kokchetav Massif: (A) inclusions of microdiamond in zircon of Kochetav gneiss (Sobolev and Shatsky, 1990), (B) inclusions of diamond + phengite in garnet of Kokchetav gneiss (Ragozin et al., 2009), (C) inclusions of numerous microdiamonds in garnet of Kokchetav marble (Ogasawara et al., 2002), and (D) inclusions of microdiamond in K-rich tourmaline of Kokchetav gneiss (Ota et al., 2008).

UHP terrane in Sulawesi (Parkinson and Katayama, 1999), and the Kontum Massif of central Vietnam (Nakano et al., 2006).

Kokchetav Massif, northern Kazakhstan: The Kokchetav Massif is a large, fault-bounded metamorphic complex of Proterozoic protolith age, surrounded by Caledonian rocks of the Ural-Mongolian foldbelt (Dobretsov et al., 1996). The massif has been considered to be a mega-melange consisting of UHP, HP and low-pressure (LP) slices and blocks (Dobretsov et al., 1996) or alternatively, a stacking sequence of several fault-bounded UHP, HP and LP units (e.g., Parkinson et al., 2002). Both UHP and HP units extend for over more than 200 km, and are confined mainly to the western Kumdy-Kol and eastern Kulet areas. The UHP slab is composed of felsic paragneiss with eclogite lenses and minor orthogneiss, marble and rare garnet peridotite. The rock assemblage shows a range of Proterozoic protolith ages. Zoned zircons from diamond-bearing gneiss yield the following ages: quartz inclusion-bearing inherited cores yield 1100–1400 Ma for protolith age, coesite-bearing mantles 530 ± 7 Ma for the UHP metamorphism, and plagioclase-bearing rims 507 ± 8 Ma for the amphibolite-facies overprint (Hermann et al., 2001; Katayama et al., 2002b; Hacker et al., 2003; Katayama and Maruyama, in press). Many diamond-grade marble layers contain clinopyroxene with exsolution lamellae of quartz, K-feldspar, phengite and phlogopite (Katayama et al., 2002a); titanite contains coesite lamellae (Ogasawara et al., 2002). The mineralogy suggests that UHP metamorphism occurred at 6 GPa and 1000 °C.

Kokchetav microdiamonds occur as abundant minute inclusions in zircon (Fig. 7A), garnet (Fig. 7B and C), diopside, and K-tourmaline (Fig. 7D) from marble, pyroxene–carbonate–garnet rock, and garnet–biotite gneiss and schist in the western Kumdy-Kol area (e.g., Sobolev and Shatsky, 1990; Ogasawara et al., 2000) and from zoisite gneisses in the Bachi-Kol area. Drilling indicates that diamondiferous rocks a few hundred meters thick occur as slices in diamond-free granitic orthogneisses that lack HP phases. Microdiamond inclusions have also recently identified in the cores of tourmaline from biotite gneiss; this tourmaline contains ~2.7 wt% K_2O, suggesting that it was stable under UHP conditions (Shimizu and Ogasawara, 2005; Ota et al., 2008). Intergranular diamond occurs in some K-feldspar-quartz lenses and layers at Kumdy-Kol; some are partially pseudomorphed by graphite (Korsakov et al., 2004). Inclusions of coesite and its pseudomorphs also occur in garnet and zircon from eclogite and diamond-bearing gneiss.

Microdiamonds from the Kokchetav and other UHP terranes described below are characterized by small (1–80 μm) crystals of skeletal, cuboidal, subrounded and anhedral morphologies suggesting a short residence time at high-T (~900–1000 °C) (Shatsky and Sobolev, 2003). Carbon isotopic data for diamond suggest biogenic sources; inclusions of water, carbonate and nanometric oxides in diamonds indicate that the microdiamonds precipitated from C–O–H supercritical fluids (e.g., Stöckhert et al., 2001; Ogasawara, 2005; Dobrzhinetskaya et al., 2006, 2007). Ogasawara et al. (2002) suggested a two-stage growth mechanism for microdiamonds. Masago et al. (2003) report negative $\delta^{18}O$ values (−3.9 ‰) for minerals in Kokchetav eclogite and whiteschist, similar to those (−9 to −2 ‰) for regional UHP granitic gneiss throughout the Dabie–Sulu terrane (Zheng et al., 2003a, 2004; Tang et al., 2008a,b). The Kokchetav Massif is the second recognized UHP region that preserves a significant effect of the interaction of cold meteoric water with the protolith prior to subduction and closed-system UHP metamorphism.

Saxonian Erzgebirge, Germany: The Erzgebirge Crystalline Complex (ECC) on the northern margin of the Bohemian Massif is in fault contact with a low-grade Paleozoic unit at its margins. The Variscan ECC consists of abundant gneisses that include numerous eclogite lenses. The Gneiss-Eclogite Unit at the core of this massif contains UHP rocks typified by coesite pseudomorphic inclusions in eclogitic garnets (Schmädicke, 1991) and inclusions of 1–25 μm microdiamond, partially graphitized diamond, and graphite pseudomorph after diamond in garnet, kyanite, and zircon from the gneisses (Massonne, 2001; Massonne and Nasdala, 2003). Some of these inclusions contain additional hydrous phases including apatite, phengitic mica, and fluid inclusions; the morphologies of inclusions and mineral associations suggest that microdiamonds from both the Erzgebirge and the Kokchetav complexes crystallized from supercritical fluids under UHP conditions (Stöckhert et al., 2001; Hwang et al., 2001; Dobrzhinetskaya et al., 2001, 2003, 2006).

Schmädicke et al. (1995) reported Grt–Cpx-whole rock Sm–Nd isochrons at 360 ± 7 Ma for eclogite and 353 ± 6 Ma for garnet pyroxenite from the Erzgebirge UHP rocks. $^{40}Ar/^{39}Ar$ spectra of phengite from two eclogite samples gave plateau ages of 348 ± 2 and 355 ± 2 Ma. The similarity in age for garnet peridotite and eclogite enclaves in gneiss suggests a Variscan UHP *in situ* metamorphism of the ECC around 340–360 Ma. Recent systematic SHRIMP dating of various domains of zircon crystals from diamondiferous quartzofelspathic rocks yielded 337 ± 3 Ma for cores, 336.8 ± 2.8 Ma for diamond-bearing intermediate zones, 330 ± 6 Ma for rims and 332 ± 2 Ma for monazite (Massonne et al., 2007). These data were used to obtain a subduction rate at 2–5 cm/yr, an exhumation rate of the first stage from >180 to 40 km at >10 cm/yr and the second stage at the crustal level at ~0.5 cm/yr for the Erzgebirge UHP rocks. Such first-stage rates are comparable with that of Kokchetav (~5 cm/yr; Hermann et al., 2001), the Dora Maira Massif (3.4 cm/yr; Rubatto and Hermann, 2001), and the western Himalayan rocks (2.3–4.5 cm/yr; O'Brien and Sachan, 2000).

Maksyutov Complex, South Urals: This complex contains boudins of eclogite, layers of eclogitic gneiss, and rare ultramafic bodies within host metasedimentary mica schist and quartzite recrystallized at 594–637 °C at a minimum P of 1.5–1.7 GPa (Beane et al., 1995; Leech and Ernst, 1998). Documentation of UHP index minerals in the Maksyutov Complex has been more elusive (e.g., Beane and Leech, 2007). Chesnokov and Popov (1965) first interpreted quartz aggregates within garnet exhibiting radial cracks as coesite pseudomorphs, and Dobretsov and Dobretsova (1988) reported relict coesite in garnet from jadeite–quartzite. Leech and Ernst (1998) described mm- to cm-scale cuboid graphitized diamond in pelitic schist and foliation that wraps around these aggregates. Direct evidence for the presence of poorly crystallized microdiamond came from Raman spectroscopy. Bostick et al. (2003) identified what appeared to be three 2–3 μm cuboidal microdiamond inclusions in garnet from eclogite-facies gneiss samples. These microdiamonds were determined to be nanocrystalline aggregates with SEM, which accounted for the Raman broad spectral bands. Based on these spectra and kinetic data for crystallization, Bostick et al. (2003) suggested that these diamonds formed at low temperatures (~600 °C) relative to kimberlites or even the Kokchetav Massif described above. The UHP/HP metamorphism with peak metamorphic ages of 370–374 Ma (Shatsky et al., 1995; Beane and Connelly, 1998) may be related to Devonian collision of the Russian platform with a fragment of the Siberian craton, but was affected later by the Triassic suturing of the Kazakhstan block against the Russian platform.

Qinling belt, central China: Very small lenses and blocks of eclogite in the North Qinling terrane are enclosed in amphibolite-facies gneiss and garnet-bearing quartz and phengitic mica schist. Inclusions of coesite in eclogitic garnet (Hu et al., 1995) and of microdiamond in zircons from both eclogite and gneiss have been reported (Yang et al., 2003a). Although individual outcrops are no more than a few meters wide, the belt of eclogites extends more than 10 km. P–T estimates of amphibolitized coesite-bearing eclogite yield 590–758 °C and P > 2.6 GPa. U–Pb SHRIMP dating of zircons from granitic gneiss yields 507 ± 38 Ma for the peak UHP metamorphism

(Yang et al., 2003a). Since the report of microdiamond in 2003, extensive search for microdiamond by Chinese investigators has failed to confirm its presence; whether or not Qinling is a UHP terrane remains to be confirmed. The Early Paleozoic belt extends westward more than 4000 km to the North Qaidam-Altun Mountains (Yang et al., 2003a). Two discrete collision events may have occurred between the North and South China blocks: an Early Paleozoic North Qinling UHP belt, and a Triassic suture along with the Dabie–Sulu UHP–HP belt (e.g., Hacker et al., 2004 and references therein).

2.4. Coesite-bearing and new UHP terranes

More than 20 coesite-bearing UHP terranes have been described and extensively reviewed (e.g., Carswell and Compagnoni, 2003; Liou et al., 2004). Other than the UHP terranes described above and below, they include: (a) the Zermatt-Saas area, Western Alps (52 ± 18 Ma, Bowtell et al., 1994; Reinecke, 1991), (b) Mali, Africa (620 Ma, Jahn et al., 2001), (c) Makbal (480 Ma) and Atbashy (270 Ma), Kazakhstan (Tagiri et al., 1995), (d) Central Indonesian UHP terrane (Parkinson et al., 1998; Parkinson and Katayama, 1999), (e) the French Massif Central (Lardeaux et al., 2001), and (f) Neoproterozoic nappes in SE Brazil (640–630 Ma) (Parkinson et al., 2001). These UHP terranes were established by the discovery of inclusions of coesite or coesite pseudomorphs in rigid host minerals such as zircon, garnet or omphacite. Petrologic, geochemical and geochronologic data for these terranes have been described in a previous review (e.g., Liou et al. 2004; Table 1). Several recently recognized near-UHP belts are also listed in Table 1; this includes the Triassic (244–223 Ma) Qiangtang metamorphic belt in central Tibet (Zhang et al., 2006e; Pullen et al., 2008), lawsonite eclogites from Pinchi Lake, British Columbia (Ghent et al., 2009) and from the South Motagua fault zone, Guatemala (Tsujimori et al., 2006a,b). Recent significant findings of a few UHP terranes are summarized below.

Dora Maira Massif, Western Alps: This classical UHP massif (Chopin, 1984) consists of Late Paleozoic and older continental basement rocks metamorphosed under UHP and HP conditions as a result of Mesozoic–Cenozoic convergence of the European and African plates. A coesite-bearing, UHP subunit containing kyanite-eclogites (Fig. 5E) has estimated peak *P–T* conditions close to the diamond *P–T* stability field (Compagnoni and Rolfo, 2003). Hermann (2003) integrated experiments in the KCMASH model system with petrological information from white schist, metapelite and eclogite, and obtained a petrogenetic grid suggesting peak metamorphic conditions of ~730 °C and ~4.3 GPa, well within the diamond stability field for the UHP Brossasco-Isasca unit of the southern Dora Maira Massif. The lack of diamond or graphite in marbles, white schists, and other lithologies probably is due to the low temperature of metamorphism, the absence of a free fluid phase in the metapelites, oxidizing conditions, and/or the short residence time of UHP metamorphism under diamond-facies conditions. Recent petrological studies of marbles (Castelli et al., 2007) and phengite-bearing eclogites (Groppo et al., 2007) confirm such *P–T* conditions and provided calculated f_{O_2} conditions too high for the formation of either diamond during UHP metamorphism or graphite during exhumation.

SHRIMP dating of zircons extracted from gneiss, schist, pyrope inclusions, and pyrope quartzite indicates 240–275 Ma zircon cores and newly formed 35 Ma rims. Thus, UHP metamorphism took place during Oligocene time, with an estimated exhumation rate of 2–2.4 cm/yr (Gebauer et al., 1997). Similar data were obtained by Rubatto and Hermann (2001) who applied *in situ* ion microprobe U–Pb dating of titanite from calc-silicates. The inherited titanite core yields 253–87 Ma, whereas the UHP titanite rim formed at 35.1 ± 0.9 Ma; two distinct stages of titanite formation during decompression are at 32.9 ± 0.9 and 31.8 ± 0.5 Ma. These data provide an unambiguous *P–T–t* path for the Dora-Maira UHP rocks with a two-stage exhumation rate changing from 3.4 to 0.5 cm/yr.

Western Tianshan, China: The Chinese Western Tianshan HP–UHP belt extends for about 200 km between the Central Tianshan–Yili plate and the Tarim plate; this belt continues westward to the Atbashy HP–UHP belt, where inclusions of coesite pseudomorphs occur in eclogitic garnet (Tagiri et al., 1995). Recent discovery of coesite inclusions in garnet from a Western Tianshan eclogite (Lu et al., 2008) confirms the earlier suggestion of UHP conditions (Zhang et al., 2002c, 2003d, 2005g). SHRIMP ages of zircons (310–413 Ma protolith ages, and 233–226 ± 4 Ma for UHP) from HP–UHP eclogites and metapelites indicate a Triassic collision event (Zhang et al., 2007c). *P–T* estimates of the peak UHP stage metamorphism are 500–600 °C and 2.6–2.7 GPa (Wei et al., 2003).

North-East Greenland Caledonides: This UHP terrane was first established by the finding of coesite pseudomorphic inclusions in eclogitic garnet and omphacite, and in garnet of the host gneisses, yielding *P–T* estimates of ~972 °C and 3.6 GPa (Gilotti and Ravna, 2002). Inclusions of coesite were subsequently reported in zircons from both rock types (McClelland et al., 2006). At such high-*T*, dehydration melting of phengitic pelites yielded minor leucosomes; metapelites retain inclusions of polycrystalline quartz aggregates, suggesting the former presence of coesite (Lang and Gilotti, 2007). SHRIMP dates for coesite-bearing zircon domains range from 330 to 390 Ma for host gneiss and 330–370 Ma for kyanite eclogite. Combining U–Pb and REE data with observed CL domains of the inclusions suggests that (1) Caledonian metamorphic zircon formed by both new zircon growth and recrystallization, (2) UHP metamorphism occurred near the end of the Caledonian collision, and (3) the 30–50 Myr span of ages records an unusually long duration of eclogite-facies conditions for the UHP rocks (McClelland et al., 2006).

Lanterman Range, Antarctica: In this range, the more than 50 km long Gateway Hills Metamorphic Complex occurs as lenses and pods of UHP eclogite and garnet peridotite within felsic gneisses. Some less-foliated eclogites have inclusions of coesite and coesite pseudomorphs in garnet (Ghiribelli et al., 2002) and were subjected to UHP metamorphism at >850 °C and >2.9 GPa, followed by an amphibolite-facies overprint. Palmeri et al. (2003, 2007) described prograde, peak and retrograde assemblages of felsic gneiss and mantle-derived garnet peridotites interlayered with coesite-bearing eclogite, and documented *in situ* UHP metamorphism for these rocks: the felsic gneiss garnets contain inclusions of coesite pseudomorphs, and the garnet peridotite mineralogy suggests estimated *P–T* conditions of 3.2–3.3 GPa and 764–820 °C. The UHP event was dated by Grt–Omp-whole rock Sm–Nd and zircon ^{238}U–^{206}Pb ages at 500 Ma, and the ^{40}Ar–^{39}Ar ages of Ca-amphibole at 490–486 Ma for the amphibolite-facies overprint. This Paleozoic UHP terrane resulted from the subduction of a paleo-Pacific plate under the pre-Gondwana continental margin.

Himalayan UHP terrane: The Himalayan orogen has long been regarded as a classic locality, reflecting ongoing continental collision between Indian and Eurasian continents since the Eocene. Inclusions of coesite in omphacite, garnet and zircon of eclogites from the Upper Kaghan Valley, Pakistan (O'Brien et al., 2001; Kaneko et al., 2003) and the Tso Morari area, India (Mukherjee et al., 2003; Sachan et al., 2004) have been documented. Garnet-pyroxene-phengite barometry applied to the eclogites yielded peak *P–T* conditions of 2.7–2.9 GPa and 690–750 °C (O'Brien et al., 2001). Similar to other UHP terranes, UHP relics are volumetrically minor constituents of the metamorphic belts, which are dominated by retrograde assemblages. In these rocks, hydration related to Barrovian-zone metamorphism resulted in remarkably pervasive recrystallization during later exhumation; this event has almost entirely masked the UHP mineralogy.

SHRIMP U–Pb dates of zoned zircons containing mineral inclusions formed at different stages indicate the ages of non-UHP mineral-bearing mantle domains of zircon and UHP mineral-bearing rims, are ~50 and ~46 Ma, respectively (Kaneko et al., 2003). New U–Pb ages of 46.4 ± 0.1 Ma for zircon growth at the peak-stage of metamorphism of coesite-bearing eclogite, and 46.4 Ma for retrogressive growth of titanite yield rapid exhumation rates of ~3–8 cm/yr within the mantle (Parrish et al., 2006). This rapid rate is similar to the diffusion modeling estimates of exhumation rate by Massonne and O'Brien (2003). The HP–UHP metamorphic age of ~55 Ma for Tso Morari eclogites was obtained by Lu–Hf and Sm–Nd methods on garnet, omphacite, glaucophane and the whole rock (de Sigoyer et al., 2000). SHRIMP ages of zoned zircons from Tso Morari UHP felsic gneiss are 53, 50, and 48 Ma, respectively, for zircon growth at the prograde, peak, and retrograde stages (Leech et al., 2005). However, no evidence linking zircon growth to specific metamorphic conditions (O'Brien, 2006) was presented, and the extent to which any of these ages represent UHP conditions or just three distinct phases of zircon growth remains uncertain.

2.5. Recently recognized UHP terranes

Eastern Papua New Guinea terrane: The world's youngest coesite-bearing eclogite terrane (2–8 Ma) was discovered on Fergusson Island, Eastern Papua New Guinea (Baldwin et al., 2004, 2008). A metamorphic core complex in this region lies in a zone of extension west of the Woodlark Basin spreading center; it consists of a lower plate of complexly deformed gneissic domes and an upper plate of largely undeformed mafic-ultramafic rocks. The metamorphic basement includes a core zone of eclogites, migmatites, gneisses, and mylonitic rocks. Mafic eclogite occurs as lenses in gneisses, has a MORB composition, and records near-UHP conditions of 870–930 °C and >2.4 GPa. Identification of coesite inclusions in eclogitic omphacite was reported in Baldwin et al. (2005, 2008); its occurrence in a 7.9 Ma eclogite indicates that the UHP rocks were subducted to mantle depths and exhumed very rapidly, on the order of cm per year (Baldwin et al. 2005, 2008; Monteleone et al., 2007). The occurrence of Late Miocene–Pliocene HP–UHP eclogite provides a new opportunity to examine UHP processes in the context of neotectonics in the active Australian-Woodlark plate boundary zone.

Pohorje terrane, Eastern Alps: Cretaceous eclogites (quartz-, zoisite-, and kyanite-eclogites) and garnet peridotites crop out in the Pohorje Mountains of Slovenia. Some of these rocks contain evidence of UHP metamorphism, with estimated *P–T* conditions of 3.0–3.1 GPa for eclogite and 760–820 °C, and up to 4 GPa and 900 °C for garnet peridotites (Janak et al., 2004, 2006; de Hoog et al., in press). The eclogites are enclosed in mica schists and gneisses as well as in a large ultramafic complex. UHP evidence includes inclusions of coesite pseudomorphs in garnet, omphacite and kyanite, and a high content of H_2O in Cpx.

Caribbean region: (Hispaniola, Cuba, Guatemala, etc.) A new UHP terrane has been suggested from the Chuacús metamorphic belt in central Guatemala (Ortega-Gutiérrez et al., 2004). The Chuacús complex contains blocks, lenses and layers of HP–UHP eclogites and amphibolitized eclogites in quartzofeldspathic gneiss. Evidence for UHP conditions includes radial fractures around polycrystalline quartz inclusions in garnet and kyanite, and the identification of Na-bearing garnet (0.12 wt% Na_2O). However, the Grt–Cpx–Phn thermobarometry record only near-UHP conditions at ~2.3 GPa and ~700–750 °C (Martens et al., 2007). Although the Chuacús metamorphic belt was displaced by left-lateral strike-slip along the Motagua–Polochic fault system, available geochronologic data suggest the presence of Cretaceous subduction zones along the paleo-North American–Caribbean plate boundary.

Available geochronologic data indicates the presence of abundant Cretaceous subduction zones marking the North American–proto-Caribbean plate boundary, coeval with the last metamorphic event recorded in Chuacús rocks (Martens et al., 2007). The Motagua fault system has displaced the HP complex relative to other Caribbean terranes. Which of these was the collider that triggered Chuacús subduction and eclogite-facies metamorphism remains a matter of debate. It may have been thickened proto-Caribbean oceanic crust (e.g., Rosenfeld, 1993), the Cretaceous Antillean arc (Pindell et al., 2005; García-Casco et al., 2008), or the continental Chortís block (Ortega-Obregón et al., 2008).

Sutures and collisional belts that contain serpentinite-hosted eclogites occur throughout the North American–Caribbean plate boundary, including Cuba (e.g., Schneider et al., 2004), Dominican Republic (e.g., Krebs et al., 2008), and Guatemala (e.g., Harlow et al., 2004; Tsujimori et al., 2006b). Minor mantle-derived UHP garnet-peridotites and eclogites have been documented in Hispaniola (Abbott et al. 2006, 2007). Garnet clinopyroxenite and Cpx garnetite contain the only known natural occurrence of coexisting Grt + Cpx + Spl + corundum as a magmatic assemblage crystallized in a magma chamber under asthenospheric conditions (3.4 GPa, >1550 °C). These mantle-derived ultramafic rocks were subsequently isobarically cooled, included in a Cretaceous subduction-zone, and subjected to coeval UHP metamorphism with the subducted oceanic rocks. Thermobarometry for the ultramafic equilibrium assemblage Ol + Cpx + Grt + Spl suggests that UHP recrystallization took place at >4.2 GPa and ~850 °C. These UHP conditions were further constrained by the growth of symplectitic minerals (Pl + Cpx and Pl + Ep) in amphibolite-facies retrograded eclogites. The symplectitic minerals are interpreted to be the products of the decomposition of two types of omphacite with calculated *P–T* conditions between ~2.8 GPa, ~850 °C and ~4.2 GPa, ~950 °C (Abbott and Draper, 2007). These UHP rocks from the Dominican Republic are unusual inasmuch as they formed at an ocean–ocean convergent plate boundary, without the involvement of continental crust, and the garnet peridotite records in unusual detail UHP magmatic crystallization.

North America cordillera: Garnet peridotites and associated eclogites occur sparsely in some collisional orogens of the western North America cordillera. However, UHP conditions were not demonstrated until detritus of UHP (>2.8 GPa) garnet peridotite and eclogite was documented from the Lower Jurassic Laberge Group sediments in northern British Columbia (MacKenzie et al., 2005). Both coarse-grained graywackes and pebble conglomerates contain angular detrital garnet, pyroxene and olivine. Compositions of some clasts of these minerals and *P–T* estimates (>2.8 GPa; 650–1080 °C) and regional geology (distant from potential mantle xenoliths in alkaline volcanics) suggest that host garnet peridotite and eclogite were products of continental collision. This result suggests that collision in this part of the North American cordillera must have been thick skinned, involving a Proterozoic continental mass with a lithosphere >100 km thick. This finding, similarly to the one in western Australia involving detrital microdiamonds in eclogitic zircons, encourages the search for other evidence of UHP mantle and crustal rocks. Inasmuch as most global UHP terranes are confined to the Phanerozoic (Maruyama and Liou, 1998), the hypothesized Proterozoic UHP orogeny for the North American cordillera requires unambiguous age constraints.

Sanbagawa belt, Japan: The Cretaceous Sanbagawa belt is a classical HP belt of the Pacific-type. This accretionary complex hosts eclogitic metagabbro + UHP garnet peridotites in the Higashi-akaishi ultramafic body (Enami et al., 2004b; Ota et al., 2004; Terabayashi et al., 2005). The massif is mainly dunite with lenses, boudins and layers of clinopyroxenite, wehrlite and websterite as a cumulate sequence. Orthopyroxene coexisting with garnet shows bell-shaped Al zoning with a continuous decrease of Al from core to rim, consistent with rims recording peak metamorphic conditions. Estimated *P–T* conditions using core and rim compositions of Opx are 1.5–2.4 GPa/700–800 °C and 2.9–3.8 GPa/700–810 °C, respectively, implying a low geothermal gradient during prograde metamorphism (Enami et al., 2004b). The mafic–ultramafic body may have originated either as an ocean island or as a fragment of thick oceanic lithosphere.

Kontum Massif, central Vietnam: The metamorphic basement of the Kontum Massif in central Vietnam includes a variety of ultrahigh-*T* (UHT) pelitic and mafic granulites marking Permo-Triassic (~270–249 Ma) collision between the Indochina and South China blocks. Some UHT mafic granulites record more than five stages of metamorphic recrystallization, characterized by decompression and subsequent cooling from eclogite- through UHT granulite- to amphibolite-facies conditions (Nakano et al., 2007). The mafic granulite consists of coarse-grained granoblastic Grt + Cpx + Rt + Qtz together with a fine-grained symplectite of Opx + Pl ± Mag ± Spl around garnet, and has *P–T* estimates of 1.3 GPa at 1050 °C and 0.8 GPa at 850 °C. Quartz rods in Cpx, and Rt needles in Grt, with recalculated supersilicic and Ti-rich compositions, respectively, for precursor Cpx and Grt, are suggested as UHP relics. Of course, the occurrence of quartz rods in omphacite is not a reliable UHP indicator as pointed by Page et al. (2005). But in support of UHP conditions, inclusions of microdiamond were identified in zircons of the associated pelitic gneiss; the *P–T* condition of the peak-pressure stage was estimated to be ~900–930 °C and >4 GPa (Nakano et al., 2006). Sm–Nd internal isochron ages of the host gneiss and a mafic block yield 247 and 240 Ma, respectively. In addition, a U–Pb SHRIMP age of 268 Ma was obtained for zircon from the diamond-bearing pelitic gneiss. Unfortunately, the description of latter is in abstract form only. These petrologic and geochronologic data suggest that both mafic and pelitic granulites underwent coeval UHP recrystallization during continent collision with UHT overprinting during subsequent exhumation. Such a complex multiple-stage metamorphic recrystallization may be common for many collision orogens such as the Bohemian Massif of Eastern Europe and the North Dabie complex of east-central China.

Xenoliths from the Colorado Plateau, USA: Xenoliths of jadeitite, omphacite, zoisite-eclogite, kyanite-eclogite, and lawsonite eclogite occur in kimberlitic pipes at Garnet Ridge in the Colorado Plateau; they may have been generated by Cretaceous subduction of the Franciscan Complex in western California, and carried beneath the North American continent on the Fallon plate (Usui et al., 2003, 2006). Lawsonite eclogite with zircon U–Pb ages of 81–33 Ma has a MORB-like bulk-rock composition, and contains Grt + Omp (~43 mol% Jd) + Lws + Rt ± Phe (~3.8 Si pfu) + Coe. Coesite occurs as micro-inclusions in omphacite. Lawsonite is partly replaced by zoisite aggregates. Grt–Cpx–Phe thermobarometry yields ~3.5 GPa at 540 °C.

3. Chinese continental scientific drilling project (CCSD) in Sulu, east-central China

Completed in 2005, the CCSD project was established in 2001 in order to study the size, protoliths and structures of the subducted continental slab, and the formation and exhumation of Sulu UHP rocks, particularly garnet peridotites. Fig. 8 shows locations of several pilot holes drilled to depths of up to 2 km, as well as the 5-km main hole; nearly continuous core samples of felsic gneiss, eclogite and garnet peridotite were recovered. Wide ranging geophysical and geological studies of the regional and local drill sites were undertaken; the results have been or are in process of being published in numerous special issues related to the CCSD project, both in Chinese and western journals (e.g., APS, 2004, 2005, 2006, 2007). Local journals, written in Chinese, contain many non-referred papers with raw petrologic, geochemical, geochronologic, and geophysical data, plus preliminary findings and interpretations. Some of these papers were rewritten later in English and published either in Chinese or western journals using some of the same data sets and diagrams. These results provide new insights into the tectonics and geodynamics of continental collision and UHP metamorphism, especially concerning problems unresolved from study of surface outcrops. Petrologic and geochemical studies of continuous, unweathered drill core samples add important constraints on the nature and scale of fluid activity and element mobility during the continental subduction-zone metamorphism and exhumation. Many crust-hosted and mantle-derived garnet peridotite cores were recovered and will be described in a later section. The major petrologic and geochemical results for mafic and felsic rocks are outlined below:

Regional UHP metamorphism: Ubiquitous occurrence of coesite inclusions in zircons of felsic gneisses, amphibolites, and eclogites from core samples indicate that the supracrustal rocks (>90% felsic gneisses, <10% eclogites) were subducted to depths >100 km and were subjected to *in situ* UHP metamorphism; the cumulate thickness of the Sulu UHP slab is >5 km (Liu et al. 2001, 2004a,b, 2005, 2006a,b, 2007c; Zhang et al. 2006a,b; Zheng et al. in press). CL images of these zircons reveal low-*P* inclusions in the cores, coesite and other UHP phases in the mantles, and low-*P* phases in the rims (Fig. 5B and C). SHRIMP dating of zoned zircons identified three discrete age groups: latest Proterozoic protolith ages (780–750 Ma) in inherited cores, a UHP event in coesite-bearing mantles at 220–240 Ma, and an amphibolite-facies overprint in quartz-bearing rims at 210 ± 10 Ma; these data constrain the rate of exhumation to >5 km/Ma (Liu et al. 2001, 2004a,b, 2007c, 2008a) (Fig. 9). Combined with *P–T* estimates of mineral inclusions (732–839 °C; 3–4 GPa) and SHRIMP ages of 236–225 Ma for coesite-bearing zircon domains and Ar–Ar ages of 209–207 Ma of matrix amphibole of amphibolites from the CCSD-MH (131.6 m deep), Liu et al. (2008a) further obtained an average rate of 0.3 cm/yr for early exhumation from a mantle depth of 120–100 km to about 40 km; this rate is considerably lower than those obtained for UHP rocks in the Dora Maira and Kochetav massifs (2–3 cm/yr) described above.

Bimodal mid-Neoproterozoic protoliths of UHP rocks: Petrologic and geochemical data, zircon U–Pb ages, and Hf isotopes of UHP bimodal meta-igneous rocks suggest that they were formed during supercontinental rifting in response to the breakup of Rodinia at about 750–780 Ma (e.g., Zheng et al., 2004, 2007c, in press; Chen et al., 2007c). Both major and trace element profiles of continuous drill core segments indicate high mobility of LILE and LREE, but immobility of HFSE and HREE (Zhao et al., 2007d). Some eclogites have andesitic bulk-rock compositions with high SiO_2, alkalis, LREE, and LILE, but low CaO, MgO, and FeO contents. These features likely resulted from chemical exchange, possibly due to metasomatism of felsic melt produced by decompression partial melting of parental gneisses during exhumation. Other eclogites have geochemical affinities to refractory rocks formed by melt extraction, as indicated by strong LREE and LILE depletions and the absence of hydrous minerals (Zhao et al., 2007c). These results provide evidence for relatively dry melt-induced element mobility in UHP metamorphic rocks. Significant variations in the abundance of SiO_2, LREE, and LILE at the contact between eclogite and gneiss indicate small-scale mobility between different lithologies.

Selective and extensive Neoproterozoic meteoric water–rock interactions: The presence of anomalously low $\delta^{18}O$ values in UHP minerals of eclogitic and felsic rocks and granitic minerals mentioned in previous sections suggests extensive meteoric

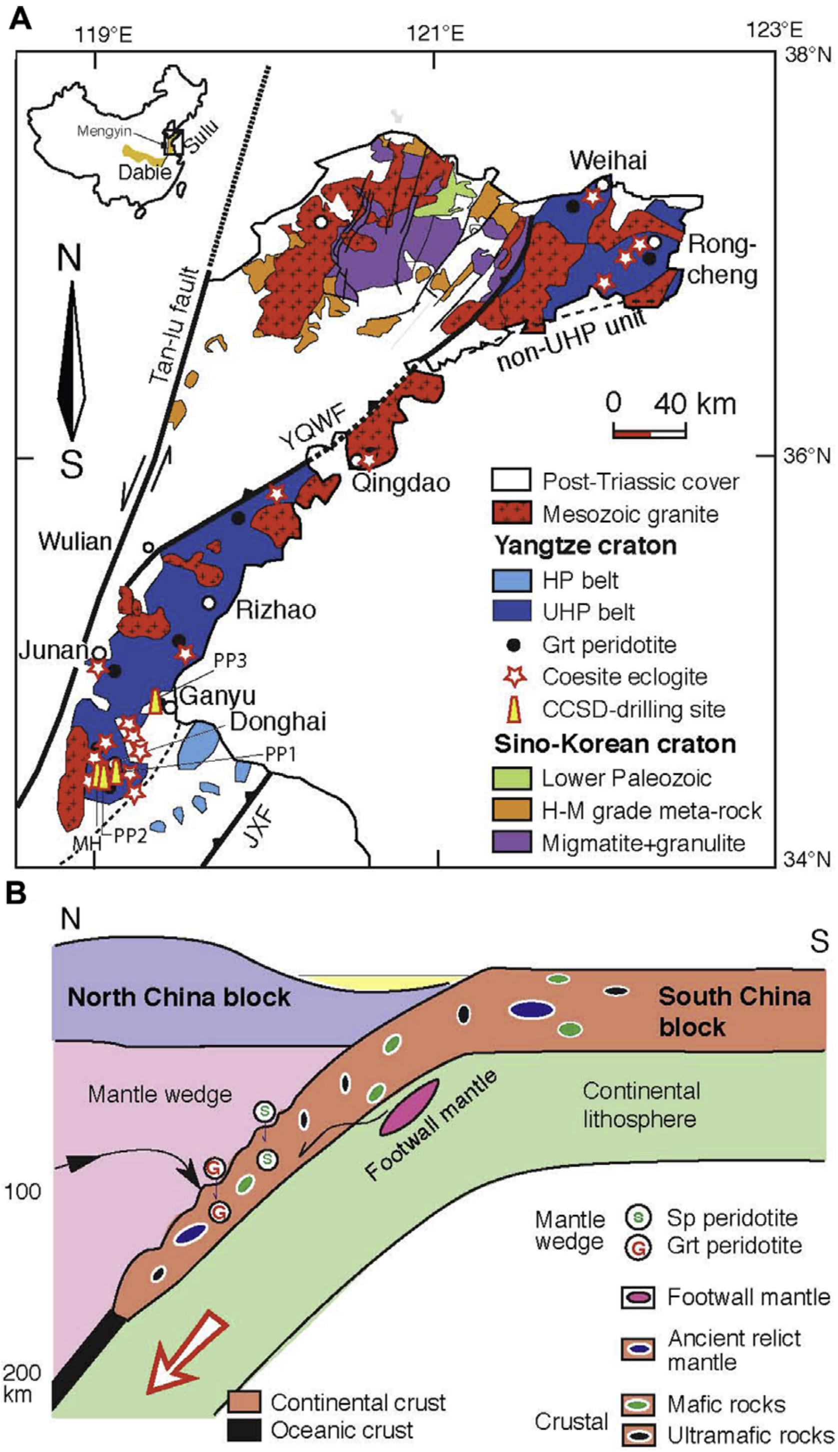

Fig. 8. (A) A schematic geologic map of the Sulu UHP and HP belts showing locations of Grt peridotite, coesite eclogite and CCSD drilling sites. Diamond-bearing kimberlite in Mengyin is about 155 km northwest of Donghai. (B) Tectonic model for Triassic subduction of the South China Block beneath the North China Block showing the tectonic setting for mantle-derived (Type A) and crust-hosted (Type B) Grt peridotite (modified after Zhang et al. (1998, 2000)).

water–rock interactions both prior to and attending Snowball Earth conditions during mid-Neoproterozoic rift magmatism, and limited fluid infiltration during Triassic continental subduction and exhumation (e.g., Yui et al., 1995; Rumble et al., 2003; Zheng et al., 2003a, Chen et al., 2007a; Zhang et al., 2005d). Established $\delta^{18}O$ profiles for UHP minerals from the depth interval 100–5000 m of the CCSD main hole, coupled with $\delta^{18}O$ depletion as deep as 3320 m (Zhang et al., 2006c; Chen et al., 2007a), and regional $\delta^{18}O$ depletion of over 30,000 km^2 along the Dabie–Sulu belt (Zheng et al., 2004; Tang et al., 2008a,b; Zhao et al., 2008), have documented a three-dimensional pattern of $\delta^{18}O$ depletion in a crustal volume of over 100,000 km^3 for the northern margin of the South China Block (Wu et al., 2007; Zheng et al., in press).

Extensive amphibolite-facies retrogression during exhumation: Petrologic data for both eclogite and country rocks indicate ubiquitous amphibolite-facies overprinting. Any retrograde fluid present was internally buffered in terms of stable isotope compositions, and the retrograde fluid was of deuteric origin as well as derived

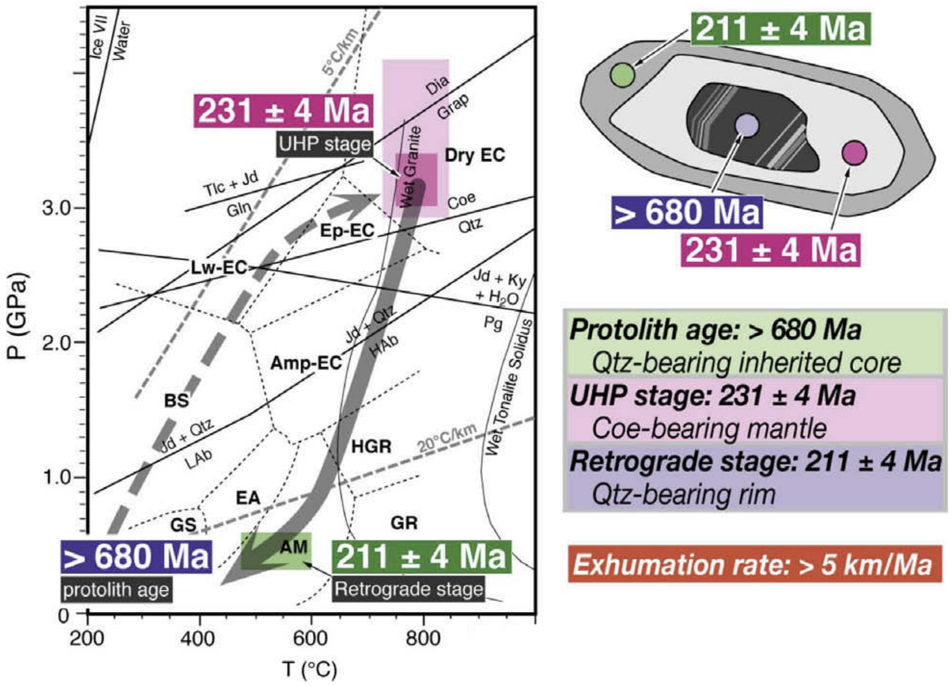

Fig. 9. A *P–T* path and zircon growth model for Dabie–Sulu eclogitic and gneissic rocks from the prograde stage through UHP stage to retrograde stage with estimated exhumation rate at >5 km/Ma (e.g., Liu et al., 2002a,b).

from the decomposition of structural hydroxyl and molecular water in nominally anhydrous minerals (Chen et al., 2007b; Zhao et al., 2007d). Changes in O- and H-isotopes and water contents of minerals occur at lithologic contacts; retrograde recrystallization of eclogites was principally caused by aqueous fluid from country rock gneisses. Local O isotope heterogeneities between different and similar lithologies on scales of 20–50 cm correspond to the maximum length scales of fluid mobility during exhumation (Chen et al., 2007a,b; Zhao et al., 2007d). Zhang et al. (2003b) documented metasomatic transformation of Dabie eclogite to dark-colored epidote–biotite-rich gneiss, hence the original proportion of UHP mafic eclogite exceeded than those shown on detailed geologic maps. Such features appear to be very limited in Sulu UHP rocks. The suggestion of very limited fluid mobility in Sulu is consistent with the preservation of gabbroic minerals and textures in coesite-bearing eclogite blocks (Zhang and Liou, 1998), the occurrence of matrix coesite in the Yangkou eclogite (Liou and Zhang, 1996), and the preservation of extremely high εNd values (+260) in Weihai eclogites with very low Nd concentrations (~0.5 ppm; Jahn et al., 1996).

Lack of microdiamond in drill hole cores: Zircon, as the most effective container for UHP minerals (e.g., Katayama and Maruyama, in press) has been separated from most core and many surface samples in Sulu, and has been subjected to intensive Raman studies for identification of coesite and microdiamond as well as for SHRIMP age dating. However, to our knowledge, except for a single report of a microdiamond inclusion in zircon from a North Dabie eclogite (Liu et al., 2007b), its *in situ* occurrence has not been documented in any other Dabie–Sulu rocks, including the thoroughly investigated CCSD core samples. Six coarse-grained diamond grains (>500 μm size) were separated from drill cuttings of the CCSD-main hole at depths between 100–1000 m and 1000–2000 m where eclogites are common (Zhang et al., 2007d,e). These coarse-grained diamonds should be studied to obtain isotopic fingerprints (both C and N) in order to identify their origin as either products of the drilling, or naturally occurring phases (e.g., Cartigny, 2005). Dabie–Sulu microdiamond occurrences are restricted to both eclogites and garnet peridotites as inclusions in garnet (Xu et al., 1992, 2005). The very limited occurrences of microdiamond in Sulu–Dabie UHP rocks may be related to lack of supracrustal fluids necessary for its formation (e.g., Dobrzhinetskaya and Green, 2007) or to high f_{O_2} UHP metamorphic conditions, as documented by the common occurrence of epidote in eclogites and gneissic rocks (Enami et al. 2004a; Mattinson et al. 2004; Zhang et al., 2005e). Such oxidized protoliths probably reflect the widespread Neoproterozoic meteoric water–rock interactions noted previously.

A host of unusual minerals (moissanite, wustite, kamacite, etc.) and native elements including Fe, Au, Zn, Ni and alloys such as FeSi, FeNi, SiFe and many other phases were identified in drill cuttings of garnet peridotites at depths between 603.2 and 683.5 m of the CCSD-MH (Yang et al., 2005; Zhang et al., 2007e). Several inclusions of moissanite (SiC) in garnets of retrograde eclogites from CCSD-PP2 were also identified by Raman spectroscopy; its occurrence was used to imply that some Sulu eclogites were subjected to UHP metamorphism at extremely high *P–T* (>1300 °C, >6.0 GPa) and extremely reduced conditions at subduction depths >200 km (Qi et al., 2007). The 1000 m core of PP2 comprises mainly gneissic rocks with minor eclogites; *in situ* UHP metamorphism was well documented by ubiquitous occurrence of coesite inclusions in zircon (Liu et al., 2001, 2002a). Natural moissanite has also been described by Xu et al. (2006a) in a southern Dabie serpentinite. Because this phase has been reported mainly as inclusions in kimberlitic diamond elsewhere (e.g., Leung, 1990; Mathez et al., 1995), its possible metastable or detrital origin in Dabie–Sulu HP–UHP rocks remains to be investigated.

4. Orogenic garnet peridotites

Our knowledge concerning the composition of the subcontinental lithospheric mantle (SCLM) is mainly based on mantle xenoliths, xenocrysts and mantle-derived volcanic rocks. Detailed, integrated petrochemical, mineralogic and geochronologic studies of orogenic garnet peridotites provide additional constraints on mantle processes, and the composition and evolution of the mantle wedge lying above a subduction zone. In most of the UHP terranes described above, garnet peridotites are widespread as a minor but significant component (Fig. 10). They have been intensively investigated inasmuch as many exhibit long-preserved histories in both mantle settings and deep continental subduction zones. The discovery of deep-seated minerals in garnet peridotites from several UHP terranes mentioned in the previous sections (see Table 3 and Fig. 10 for a summary) provides important information about mantle dynamics. How are these deep (>200 km) mantle rocks transported to shallow levels of the lithosphere, and how are they incorporated into subducted continental slabs (e.g., Brueckner, 1998, 2006; Brueckner and Medaris, 2000)?

Furthermore, some garnet peridotites and their host UHP continental rocks have experienced subduction-zone UHP metamorphism under *P*–*T* "forbidden zone" conditions involving very low thermal gradients (⩽5 °C/km) (e.g., Liou et al., 2000; Zhang et al., 2003a, 2004a,b). High-pressure experiments reveal that numerous hydrous dense magnesian silicates (HDMS) could be stable in this low-*T*, high-*P* environment (e.g., Ulmer and Trommsdorff, 1999; Komabayashi et al., 2005). Therefore, cold subduction zones are sites of major recycling of H_2O into the mantle, as described in the following sections. These findings have advanced our knowledge of the thermal structure of subduction zones, and the recycling of volatiles back into the mantle (e.g., Ohtani, 2005; Ernst and Liou, 2008, and references therein).

4.1. Mantle- vs. crust-derived garnet peridotites

The distributions, petrologic–geochemical characteristics, and origins of garnet peridotites in UHP terranes have been extensively reviewed (e.g., Brueckner and Medaris, 1998; Medaris, 1999; Zhang et al., 2004a, 2007a; Liou et al., 2007; Reverdatto et al., 2008). Most of these rocks are Mg–Cr types, derived from depleted upper mantle, but some are Fe-rich, and originated by crystallization of mafic-ultramafic complexes. The peridotites are polymetamorphic, with UHP garnet-bearing assemblages followed by a succession of retrograde assemblages related to exhumation and cooling; some also contain evidence for a pre-UHP stage, such as spinel inclusions in garnet and the Archean-stage majoritic garnet shown in Fig. 4 (Brueckner et al., 2004; Beyer et al., 2004; Scambelluri et al., 2008).

Garnet peridotites occur as m-to-km sized blocks and lenses in gneiss, and show massive, granoblastic or porphyroblastic textures. Most garnet peridotites are partially to completely serpentinized and deformed; only 0–30 vol% relict Grt-bearing assemblages are preserved in the central parts of such ultramafic bodies. The CCSD project in Sulu has recovered many drill cores of slightly serpentinized Grt peridotites. Exsolution microstructures in olivine, garnet and diopside, and high-*P* clinoenstatite are common (Zhang and Liou, 2003, 1998; Zhang et al., 1994, 1999, 2002a, 2003c; Hacker et al., 1997).

Table 3 summarizes petrologic, geochemical and geochronologic data for recognized Grt peridotites beyond that presented by Medaris (1999) and summarized by Ernst et al. (2007). Numerous tectonic origins for Grt peridotites in UHP terranes have been suggested. For simplicity, we suggested three different types based on their origin as (a) continental lithosphere, (b) low-*P* crustal mafic–ultramafic cumulate bodies, and (c) oceanic lithosphere.

Type A mantle-derived garnet peridotites from continental lithosphere: Type A mantle-derived peridotites are either residual mantle fragments, or peridotite and pyroxenite differentiated from mantle-derived magma in the uppermost mantle; they possess isotopic and geochemical signatures of the mantle subduction-zone hanging wall. Most Type A Grt peridotites are the Mg–Cr types of Medaris and Carswell (1990) and contain higher MgO, Cr_2O_3 and NiO and lower "fertile" elements (such as TiO_2, Al_2O_3, CaO, and FeO) than those of the primitive mantle as defined by Sun and McDonough (1989).

For example, massive-to-layered peridotites of the Western Gneiss Region are fragments of ancient depleted mantle, and were subsequently included in the Caledonian UHP terrane (e.g., Brueckner, 1998; Carswell et al., 2006). The early assemblages in the WGR peridotites have Sm–Nd Proterozoic ages (Brueckner and Medaris, 1998; Brueckner et al., 2003) and Archean (2.7–3.1 Ga) Re–Os ages

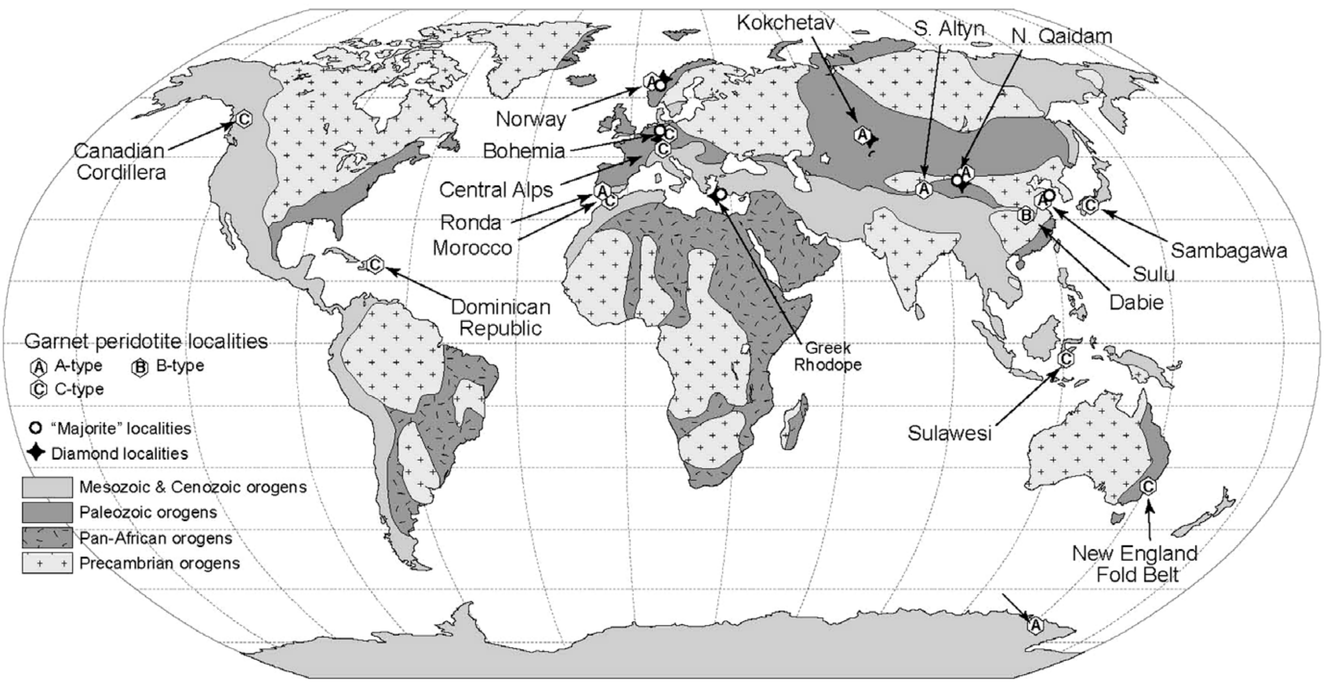

Fig. 10. Global distribution and peak metamorphic age of various types of garnet peridotites (see Table 3 and text for details) (modified after Ernst et al. (2007)).

Table 3
Characteristics of garnet peridotites in UHP metamorphic belts worldwide (mineral abbreviations after Kretz (1983)).

Terrane	Type	Modes of occurrence	Rock types*	Mineral assemblage	Peak-stage *T–P* (°C, GPa)	Metamorphic age in Ma**	References
Sulu, Eastern China							
Rongcheng	A	Blocks in gneiss	LZ, DN	Grt + Ol + Opx + Cpx	820–920; 4–6	242 ± 8	Zhang et al. (1994), Zhao et al. (2006)
Yangkou		Layers and blocks in gneiss	LZ, CP	Ol + Cpx + Opx + Grt + Amp	750 ± 50; >4	Triassic	Zhang et al. (2005b)
Rizhao	A	Lans and blocks in gneiss	DN, CP	Grt + Cpx + Ilm + Chl ± Ol	>820; >4	215–225 ± 2	Zhang et al. (1994, 2000), Zhang and Liou (2003), Zhao et al. (2007a,b)
Donghai: CCSD-PP1	A	118 m cores in gneiss	LZ, HZ, DN	Grt + Ol + Opx + Cpx ± Phl	~800; 4–6	221 ± 3	Zhang et al. (2005a), Yang et al. (2007a,b)
CCSD-PP3	B	480 m cores in gneiss	DN, HZ	Grt + Ol + Opx ± Cpx	~720; 5–6	240 ± 2	Chen et al. (2005), Yang et al. (2005)
CCSD-MH	B	Layered mafic–ultramafic	WR, DN	Grt + Ol + Cpx ± Opx	825; >6	220–240	Yang et al. (2007a,b), Zhang et al. (in press)
Dabie, Eastern China							
Bixiling	B	Layered mafic–ultramafic	LZ, WR, WB	Grt + Ol + Opx + Cpx ± Chu ± Mgs	820–950; 4.7–6.7	Triassic	Zhang et al. (1995b, 2000), Chavagnac and Jahn (1996)
Maowu	B	Layered ultramafic	HZ, CP, OP	Ol + Opx + Grt + Cpx + Rt ± Mz	750 ± 50; 4–6	~220–230	Liou and Zhang (1996), Zhang et al. (1998), Jahn et al. (2003a,b)
Raobazhai	?	Fault block	DN, HZ	Ol + Opx + Cpx + Spn ± Grt	>1100; 1.8–2.2	Triassic	Zhang et al., 1996; Tsai and Liou. (2000)
Western China							
Altun Tagh	A	Blocks in gneiss	LZ, WR, CP	Grt + Ol ± Opx + Cpx ± Mgs	890–970; 3.8–5.1	~493–500	Liu et al. (2002a,b), Zhang et al. (2005)
N Qaidam	A	Block, lens, layers in gneiss	LZ, DN, CP	Grt + Ol + Opx + Cpx	780–850; >2.7–4.5	420–423	Yang and Jahn (2000), Yang et al. (2003a), Song et al. (2004, 2005a,b), Zhang et al. (2004a,b)
Indonesia							
Sulawesi	C	Fault slice and xenolith in granite	LZ	Ol + Grt + Opx + Cpx	1025–1200; 2.6–4.8	Cretaceous	Kardarusman and Parkinson (2000)
SW Japan							
Sanbagawa	C	Lens, boudins or layers	DN, CP, WR, WB	Grt + Ol + Cpx + Cr–Sp ± Opx	700–810; 2.9–2.38	Cretaceous	Enami et al. (2004a,b), Mizukami et al. (2004)
Northern Kazakhstan							
Kokchetav	B	Block in gneiss	PD	Ol + Grt + Ti–Chu ± Ilm ± Cpx ± Phl	790–880; 4–6	554–494	Muko et al. (2002), Katayama et al. (2003)
Western Gneiss Region							
Kalskaret	A	Large body in gneiss	PD	Grt + Ol + Opx + Cpx	890–950; 4.2–4.4	Proterozoic – Archean	Medaris (1999, 1980, 1984), Jamtveit et al. (1991), Beyer et al. (2004)
Lien	A	Large body in gneiss	PD	Opx + Grt + Ol + Cpx	850–900; 3.6–3.9	Proterozoic – Archean	Medaris (1999, 1980, 1984)
Rodhaugen	A	Large body in gneiss	PD	Opx + Grt + Ol + Cpx	740–859; 2.3–3.6	Proterozoic – Archean	Medaris (1999), Carswell (1981)
Sandvika	A, B	Large body in gneiss	PD	Opx + Grt + Ol + Cpx	930–950; 4.4–5.0	Proterozoic – Archean	Medaris (1999), Jamtveit (1984, 1987)
Raudhaugene, Otroy, Flemsey, Fjortoft	A	Large body in gneiss		Opx + Grt + Ol + Cpx	740–890; 2.3–4.3	Proterozoic – Archean	Carswell (1986), van Roermund et al. (2002), Beyer et al. (2004), Spengler et al. (2006), Carswell et al. (2006)
Bohemian Massif							
Moldanubian	A, B, C	Lenses in gneiss and granulite	PD, CP	Ol + Grt + Cpx + Opx	815–1330; 2.4–5.6	~370–330	Medaris (1999), Medaris et al. (2005, 2006), O'Brien and Rötzler (2003)
Erzgebirge	A	Elongate body in gneiss and granulite	PD	Ol + Grt + Opx + Cpx	800–900; 2.9–3.2	Variscan	Schmadicke and Evans (1997)
S. Carpathians	A, B	Lenses in gneiss	PD	Opx + Grt + Ol + Cpx	1150–1300; 2.5–3.2	310–360	Medaris (1999), Medaris et al. (2005, 2006)
Ronda	A	Large massif	LZ	Grt + Ol + Opx + Cpx + Dia	1080–1240; 2.1–2.8	Alpine (21–25)	Reisberg et al. (1989), Medaris (1995, 2006)
Western Alps							
Lepontine Alps	C	Large boudins	PD	Grt + Ol + Opx + Cpx	775–820; 3.4–3.7	Alpine	Evans and Trommsdorff (1978)
Alpe Arami	A	Large lens	LZ	Grt + Ol + Opx + Cpx + Chu	840–1130; 3.4–5.2	Alpine	Dobrzhinetskaya et al. (1996), Brenker and Brey (1997)

(*continued on next page*)

Table 3 (*continued*)

Terrane	Type	Modes of occurrence	Rock types*	Mineral assemblage	Peak-stage *T–P* (°C, GPa)	Metamorphic age in Ma**	References
Eastern Alps							
Pohorje Mtns	A	Bounins in gneiss	HZ, DN	Grt + Ol + Opx + Cpx + Spn	~900; 4	Upper Cretaceous	Janak et al. (2006)
Antarctica							
Lanterman Range	A	Lenses in Eclogite + Gneiss	PD	Grt + Ol + Opx + Cpx	764–820; 3.2–3.4	486–490	Palmeri et al. (2007)
Dominican Republic	C	Boulders		Ol + Grt + Cpx + Spl ± Crn	1570–1540; >3.4	Late Cretaceous	Abbott et al. (2006)
British Columbia	C	Detrital Grt, Cpx and Ol in conglomerate	PD		800–950; 3–6	>192–183	MacKenzie et al. (2005)

* *Abbreviations for rock types:* LZ, Lherzolite; DN, Dunite; HZ, Harzburgite; CP, Clinopyroxenite; OP, Orthopyroxenite; WR, Wehrlite; WB, Websterite; PD, Peridotite.
** Most ages are SHRIMP data.

of sulfides (Beyer et al., 2004), close to the crystallization ages of the host gneisses. Archean ages imply a melt-extraction event in the lithospheric mantle that predated growth of the Proterozoic upper crust in the region. This finding suggests that some Proterozoic subcontinental lithospheric mantle may be refertilized Archean mantle.

On the other hand, Sulu massive, relatively homogeneous Grt peridotites from eastern China are in fault contact with country rock gneiss; they exhibit either near-equigranular or porphryroblastic textures, and contain lenses of bi-mineralic coesite-bearing eclogites. Type A Sulu Grt lherzolite and pyroxenite mainly preserve mantle $\delta^{18}O$ values ranging from +4.8 to +5.6, +4.7, and +4.5 to 5.6‰ for garnet, olivine and clinopyroxene, respectively (Zhang et al., 1998, 2000; Zheng et al., 2003b). The bulk rocks tend to have low $^{87}Sr/^{86}Sr$ (0.7038–0.7044) and $^{143}Nd/^{144}Nd$ values of 0.5123–0.5124. It should be noted that low *P*/*T* Grt peridotites of Medaris (1999) including those from the Bohemia Massif are included here; these bodies evolved from spinel peridotites and contain abundant inclusions of spinel in garnet, and equilibrated at temperatures ranging from 1000 to 1300 °C. SHRIMP U–Pb isotopic analyses and morphological characterization of zircon separates from surface and drill core samples of Sulu Grt peridotites provide important constraints regarding whether or not these mantle-derived rocks experienced subduction-zone metamorphism. Most zircons from Chinese Grt peridotites lack inherited magmatic cores with oscillatory zoning, implying a metamorphic origin. SHRIMP U–Pb dating of zircons from Sulu peridotites and enclosed eclogite lenses have yielded UHP metamorphic ages of 220–240 Ma (Yang et al., 2003b; Zhang et al., 2004a; Zhao et al., 2005, 2006a; Zheng et al., 2006a), consistent with the 230 ± 10 Ma UHP ages for the country rocks (Table 4).

However, reconnaissance study of Hf isotopic compositions and U–Pb upper-intercept ages of zircon separates yield Paleoproterozoic, even Archean, Hf modal ages for other Sulu Grt peridotites (Zheng et al., 2006a). This suggests that some peridotites had long residence times in the mantle wedge prior to involvement in the Triassic subduction. The peridotitic zircons have trace element characteristics similar to kimberlitic or carbonatitic zircons (Zheng et al., 2005a). Moreover, strong depletion of the CCSD-PP1 peridotite in basaltic components and the relatively non-radiogenic Hf isotopic compositions of peridotitic zircons indicate that this Sulu type A peridotite is a fragment of refractory Archean mantle that underwent Neoproterozoic metasomatism; it represents a tectonic insertion into a younger descending slab, and was subjected to UHP recrystallization involving fluids derived from the subducted continental crust (Zheng et al., 2006b). Multi-stage metasomatism was pointed out by Zhang et al. (2007b) involving a distinct parageneses of phlogopite, Ti–clinohumite, magnesite and dolomite in addition to garnet and clinopyroxene. Similarly, Malaspina et al. (2008) identified two discrete stages of UHP metamorphism and metasomatism of PP1 garnet peridotites in the mantle-wedge and in the subduction zone, respectively. The first-stage metasomatism involved a melt with alkaline character under high-temperature conditions ($T > 1000$ °C and $P > 5.0$ GPa) whereas the second-metasomatism resulted from interactions with an incompatible element- and silicate-rich fluid during Triassic UHP metamorphism. The *P–T* path of Dabie–Sulu Type A Grt peridotites is illustrated in Fig. 11A.

Type B garnet peridotites from ultramafic portions of crustal mafic–ultramafic complexes: Protoliths of these Grt peridotites were differentiated from mafic magma prior to continental subduction; they are interlayered with eclogites of various compositions. Those from Dabie (e.g., Bixiling and Maowu) and from the CCSD main-hole cores are characterized by (1) a well-developed banded or layered structure, (2) occurrence of low-*P* mineral inclusions in garnets, (3) preservation of relatively light isotope composition of oxygen ($\delta^{18}O < 5$‰), and (4) an earlier crustal intrusion age (~300–500 Ma), and a Triassic (~220–230 Ma) UHP metamorphic age (Chavagnac and Jahn, 1996; Jahn et al., 2003b; Yang et al., 2007a). Type B mafic–ultramafic complexes exhibit a large variation in major elements, and generally contain lower MgO and higher SiO_2, CaO, TiO_2, Al_2O_3, and FeO than type A peridotites (Zhang et al., 2000). The trace element characteristics of clinopyroxene and phlogopite from the Maowu websterite and orthopyroxenite (Malaspina et al., 2008) appear to be similar to the estimated residual fluid compositions in equilibrium with the country granitic gneiss (Xia et al., 2008). Such data led Malaspina et al. (2008) to conclude that the fluids produced from reactions at the slab–mantle interactions may produce phlogopite, which plays an important role in controlling LILE characteristics of the slab-derived fluid in subduction zones. The *P–T* path of Dabie–Sulu Type B Grt peridotites is shown in Fig. 11B.

Petrologic and geochemical studies of a variety of eclogites and layered ultramafics from both CCSD main hole cores and adjacent drill core, trench and surface samples have concluded that the protolith of the Maobei UHP complex was a Neoproterozoic (773 ± 8.0 Ma) layered intrusive consisting of a basal peridotite, and a main body of gabbro and minor granodiorite (e.g., Zhang et al., 2006b; Chen et al., 2007c). The bulk compositions of these rocks exhibit the characteristic trends of fractional crystallization as typified by the Skaergaard intrusion. On the other hand, SHRIMP dating of zircons from a wehrlite from the CCSD-MH yielded a Paleozoic age (~346–461 Ma) for mafic–ultramafic intrusions and a Mesozoic age (~220–240 Ma) for the UHP metamorphism (Yang et al., 2007a). These protolith ages are inconsistent with its interpretation as a Neoproterozoic layered intrusion. Such disagreement may result from incorrect assignment of concordant U–Pb data for the SHRIMP spot ages (Yang et al., 2007a). Alternatively, eclogite of various types and peridotite from the CCSD-MH may have been the products of fractional crystallization of a single magma or multiple mafic intrusions of different ages.

Table 4
Summary of U–Pb ages (in Ma) of different Sulu UHP rocks.

Locality	Rock type or sample[a]	Protolith	Prograde	Peak	Retrograde	References
Ultramafics						
CCSD-PP1	Grt PD (C24)			221 ± 3†		Zhang et al. (2005)
CCSD-PP1	Grt PD (C50)			220 ± 2**		Zhang et al. (2005)
CCSD-PP1	Grt PD (C27)				212 ± 3**	Zhang et al. (2005)
CCSD-PP3	Grt PD	726 ± 56		240 ± 3†		Yang et al. (2005)
CCSD-MH	Grt WR	346–461		223.3 ± 4.1		Yang et al. (2007a,b)
Xugou	Grt PD (XG13)		244.6 ± 7.6	227.8 ± 7.1		Liu et al. (2006)
Rongcheng	DN			242 ± 8		Zhao et al. (2006)
Rizhao	Grt CP			215 ± 2		Zhao et al. (2007a,b)
Rizhao	Grt CP			225 ± 1.8		Li et al. (2008)
Weihai	Grt PD	581 ± 44		221 ± 12		Yang et al. (2003a,b)
Zhimafang	Grt PD			216–233*		Rumble et al. (2002)
Eclogite in Grt peridotite						
Xugou				236 ± 3		Zhao et al. (2005)
Xugou	XG07		244.8 ± 2.8	224.8 ± 2.7		Liu et al. (2006)
Xugou	XG09			242.0 ± 2.9		Liu et al. (2006)
Rongcheng	CJ4A			238 ± 3		Zhao et al. (2006)
Rongcheng	CJ4C			232 ± 7		Zhao et al. (2006)
Rongcheng	CJ4D			218 ± 5		Zhao et al. (2006a)
Rongcheng	MC		225 ± 2			Zhao et al. (2007a,b)
Rongcheng	CD01		240.5 ± 4.7	227.0 ± 2.6	207 ± 6	Liu et al. (2006)
Eclogite or retrograded eclogite in gneiss						
CCSD-MH	G12 (131.6 m)	695–520		229 ± 3†	214 ± 3†	Liu et al. (2008a)
CCSD-MH	ZN76 (249.5 m)	647–446		221.6 ± 3.8		Zhang et al. (2006a,b,c,d)
CCSD-MH	511.2 m	774–508				Zhang et al. (2006a,b,c,d)
CCSD-MH	ZN73			220 ± 11		Zhang et al. (in press)
CCSD-MH	ZN77			222.0 ± 4.7		Zhang et al. (in press)
CCSD-MH	ZG64			221.5 ± 3.3		Zhang et al. (in press)
CCSD-MH	ZG65			214.2 ± 2.7		Zhang et al. (in press)
CCSD-MH	ZK66			218.2 ± 3.3		Zhang et al. (in press)
CCSD-MH	(543.6 m)	672–458		218 ± 9		Zhang et al. (2006)
CCSD-MH	ZD83 (728.0 m)	730–557		216.8 ± 8.7		Zhang et al. (2006)
CCSD-MH	736.01 m	767 ± 28		227 ± 24		Chen et al. (2007a,b,c)
CCSD-MH	930.52 m			221 ± 2		Chen et al. (2007a,b,c)
South Sulu	G13	659-520		231 ± 3†	214 ± 3†	Liu et al. (2008a)
South Sulu		762 ± 28**		217 ± 9**		Ames et al. (1996)
Weihai	SL-91-28	1822 ± 25**		232 ± 56**		Yang et al. (2003a,b)
Junnan	LJ-32		243.1 ± 1.4	227.2 ± 3.6		Liu et al. (2006)
Paragneiss						
CCSD-MH	736.46 m	785 ± 19		228 ± 3		Chen et al. (2007a,b,c)
CCSD-MH	930.32 m	783 ± 34		220 ± 12		Chen et al. (2007a,b,c)
CCSD-PP2	Paragneiss (S1)	743–345®		228 ± 5	208 ± 4	Liu et al. (2004a)
CCSD-PP2	Allanite-bearing (S27)	719 ± 12®		229 ± 7	210 ± 2	Liu and Xue (2007)
CCSD-MH	Paragneiss (ZK-2304)	751 ± 29		227 ± 9		Liu et al. (2005)
Paragneiss						
CCSD-PP2	S2	680–574		232 ± 4	213 ± 5	Liu et al. (2004a)
CCSD-PP2	Allanite-bearing (S28)	696–760		230 ± 7	211 ± 3	Liu and Xue (2007)
CCSD-MH	S2	810–910**		227 ± 2	209 ± 3	Liu et al. (2004b)
CCSD-MH	ZE83			220 ± 8		Zhang et al. (in press)
CCSD-MH	ZE85			220.5 ± 9.4		Zhang et al. (in press)
CCSD-MH	ZE87	777 ± 4.1†		217.4 ± 3.6		Zhang et al. (in press)
CCSD-MH	ZH64			223 ± 16		Zhang et al. (in press)
CCSD-MH	ZL44	767 ± 29				Zhang et al. (in press)
CCSD-MH	ZJ66			217.2 ± 1.8		Zhang et al. (in press)
CCSD-MH	ZO71			217.3 ± 3.4		Zhang et al. (in press)
CCSD-MH	ZM75			221.2 ± 3.7		Zhang et al. (in press)
CCSD-MH	ZO77	776 ± 19		217.3 ± 3.4		Zhang et al. (in press)
Weihai, Rongcheng				226 ± 2††	218 ± 2††	Hacker et al. (2006)
Weihai	SU45				215 ± 6	Leech et al. (2005)
Qinglongshan		684–754		221*		Rumble et al. (2002)
Qinglongshan	99QL19	702 ± 130**		218 ± 16**		Zheng et al. (2004)
Rizhao	00LS17	751 ± 72**		224 ± 27**		Zheng et al. (2004)
Yangkou	00YK10	798 ± 75**		224 ± 14**		Zheng et al. (2004)
Marble in gneiss						
Donghai	H4	1722–503	246 ± 3	234 ± 4	213 ± 6	Liu et al. (2006)

*, ages not included in Fig. #, due to the lack of uncertainty; **, Intercept age; ®, detrital; †, weighted mean age; ††, Concordia age; †††, ages for eclogite in gneiss except for that in Rongcheng (eclogite in garnetperidotite); CJ, Chijiadian; MC, Macaokuang.
[a] Abbreviations for ultramafics are the same as Table 3; MH: main hole.

Type C garnet peridotites from oceanic lithosphere: Protoliths of footwall mantle of a subducted slab could have been serpentinized prior to HP–UHP metamorphism. These ultramafics may be part of an ophiolitic sequence that was emplaced in the crust prior to sub-

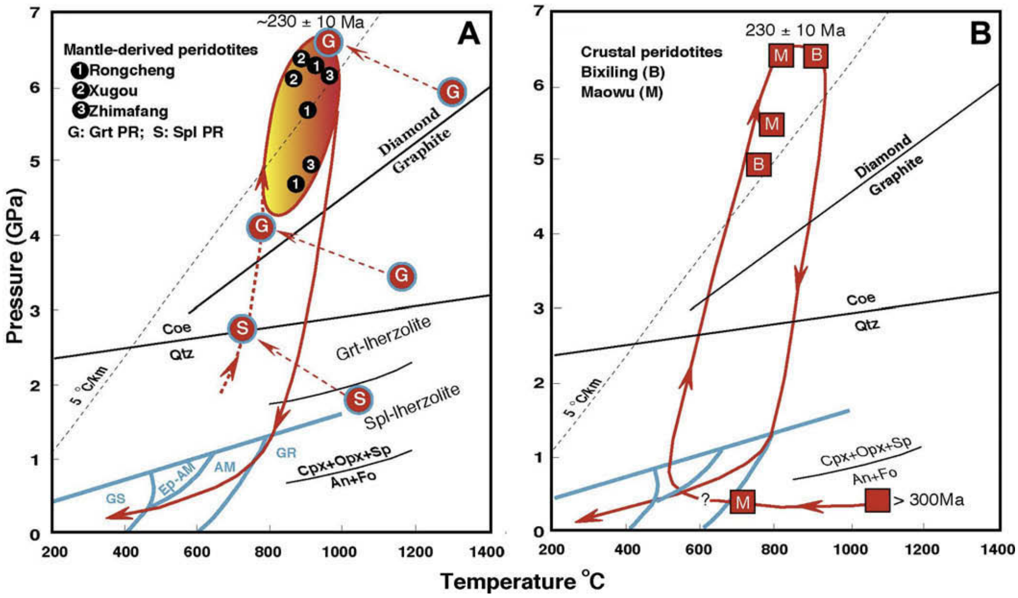

Fig. 11. *P–T* path of Types A (A) and B (B) garnet peridotites from the Dabie–Sulu terrane (after Zhang et al. (2004a,b)).

duction. Thus some Grt peridotites of the Western and Ligurian Alps may be associated with eclogites of HP transformed rodingitized gabbros and have geochemical evidence of seawater alteration. Geochemically, such Grt peridotites are difficult to differentiate from Type A mantle-derived from the hanging wall. Therefore, only a very few global Grt peridotites, chiefly from the Central Alps (e.g., Cima di Gagnone and Monte Duria bodies) have been assigned to this group. Similarly some North Qaidam Grt peridotites described by Song et al. (2007, this issue) and those in the Caribbean regions (Abbott et al., 2006) are of ophiolitic origin.

4.2. Microstructures of UHP minerals in garnet peridotites and other UHP rocks

Exsolution of anhydrous mineral lamellae: Studies of microminerals and exsolution structures have revealed numerous preserved deep-seated features formed at much higher *P* than values estimated using the conventional (e.g., Grt–Opx) geobarometer (Liou et al., 1998; Zhang and Liou, 1998). The best example was the report by Dobrzhinetskaya et al. (1996) of micron-sized $FeTiO_3$ rods and plates of chromite in olivine from the Alpe Arami garnet–lherzolite, Central Alps. These authors hypothesized that the lamellae exsolved from perovskite originally formed at 10–15 GPa (300–450 km). From the abundance, morphology, crystallography, and topotaxy of these oxides, they argued that the inferred very high solubility of highly-charged cations (Ti and Cr) represented previously unrecognized mantle conditions at $P > 10$ GPa. Subsequent UHP experiments (Dobrzhinetskaya et al., 2000) and observations of exsolved Ca-poor pyroxene displaying antiphase domains in diopside (Green et al., 1997; Bozilov et al., 1999, 2003) supported the idea of an extremely deep origin (>300 km) for the Alpe Arami Grt peridotite (Brenker and Brey, 1997). On the other hand, Ulmer and Trommsdorff (1997, 1999), Risold et al. (2001) and Hermann et al. (2005) interpreted the oriented ilmenite lamellae in olivine to indicate a prograde history for the host peridotite, in which Ti–clinohumite broke down to form olivine and ilmenite.

Precursor majoritic garnet that formed prior to and during UHP metamorphism was discussed in a previous section for Grt peridotites from the West Gneiss Region (Fig. 4; van Roermund et al., 2000; Spengler et al., 2006; Scambelluri et al., 2008), China (Zhang and Liou, 2003; Zhang et al. 2003a,c; Song et al., 2004, this issue), and the Bohemian Massif (Massonne and Bautsch, 2002). However, formation of such UHP solid-solution phases may have taken place either in the deep upper mantle, then sequestered in the mantle wedge such as in Norway, or in a subduction-zone such as in eastern China. The mechanism for the insertion of mantle–wedge fragments into a subducting slab remains to be further investigated.

Exsolution of hydrous phases: K-bearing pargasite lamellae in clinopyroxene inclusions within garnet megacrysts from the Rizhao Grt clinopyroxenite (Fig. 6A), and phlogopite lamellae in Donghai lherzolitic diopside show topotaxic intergrowths, and are confined to cores of the host clinopyroxene (Zhang et al., 2003c; Chen and Xu, 2005). These K- and OH-bearing exsolved phases suggest that the primary clinopyroxene could have incorporated a considerable amount of K_2O and H_2O under UHP conditions, as documented in clinopyroxene inclusions in Kokchetav zircons (Katayama et al., 2003). This conclusion is consistent with UHP experiments demonstrating the solubility of K in clinopyroxene (Luth, 1997; Harlow, 1997). Similar exsolution lamellae of sodic Amp + Rt in garnet from the North Qaidam Grt peridotite, western China, have been interpreted (Song et al., 2005b, this issue) to represent decompression products from depths >200 km of supersilicic majorite typified by high concentrations of Na_2O (0.3 wt%) and hydroxyl (up to 1000 ppm). Thus, majoritic garnet and supersilicic clinopyroxene could be important reservoirs of H_2O at mantle depths in addition to HDMS and other nominally anhydrous silicates. However, based on the observed inclusions of low-*P* minerals in porphyroblastic olivine, garnet and pyroxene of Grt peridotites described in previous sections, Yang and Powell (2008) argued against the exsolution model for the oriented amphibole lamellae in garnet and ultra-deep origin of Grt peridotites described by Song et al. (2004). Yang and Powell (2008) further posed an important question regarding the interpretation of oriented Rt + pyroxene ± Amp lamellae in garnet as ultra-deep origin (also see Hwang et al. (2007)).

Polymorphic transformations: Clinoenstatite lamellae (low-*P* $P2_1/c$ structure) in orthoenstatite may have formed either by inversion from Opx or by a displacive transformation from UHP Cpx during decompression of Chinese Grt peridotites. Low-*P* clinoenstatite lamellae have a composition identical with host enstatite from some Sulu–Dabie ultramafics (Zhang et al., 2002a, 2003a). Those in the Alpe Arami Grt peridotite apparently formed during mantle upwelling prior to Alpine subduction, and those in the Dabie Bixiling Type B Grt peridotite (Liu et al., 2007a) formed during exhumation of the UHP terrane. Experiments indicate that Opx transforms to UHP Cpx at $P > 8$ GPa, 900 °C, corresponding to a mantle depth of ~300 km (e.g., Ulmer and Stalder, 2001). Growth of UHP clinoenstatite and inferred precursor majoritic garnets may have formed at great depth in the mantle wedge long before insertion into the downgoing continental lithospheric plate, and then recrystallized during subduction-zone metamorphism. In Bixiling, lamellae of low-P Cpx with $P2_1/c$ space group symmetry present in diopside contain nanoscale antiphase domains indicating an original formation with $C2/c$ symmetry as high-P Cpx stable at $P > 9$ GPa. The Bixiling complex is a crustal cumulate; its occurrence extends the minimum depth of subduction of continental crust in the Dabie–Sulu orogen to >300 km (Liu et al. 2007a). However, this interpretation is based on Ca-free end-member experiments; natural clinoenstatite lamellae have a pigeonite composition, so this conclusion should be regarded with caution.

Nanometer-thick (<2 nm) lamellae of α-PbO_2-type TiO_2 occur between multiple twinned rutile crystals in both diamond-bearing felsic rocks from the Saxonian Erzgebirge (Hwang et al., 2000) and coesite-bearing Dabie eclogite (Wu et al., 2005); occurrence of this polymorph implies subduction of continental materials to a depth exceeding 200 km. Furthermore, possible former stishovite in metasediments exhumed from >300 km has been conjectured recently, based on the occurrence of Al- and Fe-bearing oxide inclusions (oriented kyanite and hercynite) in quartz from UHP pelitic rocks from the Altyn Tagh, western China (Liu et al., 2007d, this issue). These observations together with inferred supersilicic titanite in Kokchetav marble allow the conclusion that some continental supercrustal rocks have been subducted to depths of at least 300 km before being returned to the surface.

5. Discussion

5.1. In situ UHP recrystallization

The predominant rocks of UHP terranes are felsic gneisses and schists lacking obvious evidence of unusual metamorphism. Field observations indicate that not all Grt peridotites and eclogites are fault bounded, and that many contacts with gneissic rocks have retained structural coherence throughout subduction, metamorphism, and exhumation. Mineralogic indicators of UHP metamorphism are present in a variety of lithologies for wall rocks of eclogites and Grt peridotites, including gneisses, quartzites, and marbles. Detailed studies of mineral compositions and SHRIMP ages of zoned zircons in felsic gneisses + schists show that they were metamorphosed under P–T conditions and ages similar to those of the intercalated coesite-bearing eclogite and Grt peridotite bodies.

Evidence of UHP metamorphism is typically preserved as rare mineral inclusions and relict phase assemblages within host rocks that later reequilibrated under crustal conditions. Among the various types of evidence, zircons from UHP rocks provide the most useful information with regard to the P–T–time path of a subduction complex inasmuch as this mineral is extremely stable and mechanically–chemically resistant over a wide range of P–T conditions. During growth stages, individual zircon zonal domains may include and preserve inclusions of minerals in equilibrium with the matrix phase assemblage. Moreover, zircons which crystallized at mantle depths in equilibrium with garnet display characteristic HREE depletions and lack Eu anomalies, whereas those grown at crustal depths in equilibrium with plagioclase have pronounced HREE enrichments and marked negative Eu anomalies (Hermann et al., 2001; Rubatto and Hermann, 2001; Rubatto, 2002). Consequently, identification of mineral inclusions and characterization of REE patterns of zoned zircons have been used in conjunction with ion microprobe U–Pb dating in order to elucidate the P–T–time paths for some UHP terranes (e.g., Gebauer et al., 1997; Katayama et al., 2003; Hermann et al. 2001; Mattinson et al., 2006; McClelland et al., 2006; Katayama and Maruyama, in press).

For example, many new SHRIMP U–Pb ages support the hypothesis that Dabie–Sulu eclogites, Grt peridotites, and the surrounding wall rocks were subjected to coeval Triassic UHP metamorphism (Table 4). Metamorphic overgrowths on zircons from eclogites, Grt peridotites, and country rock gneisses and schists give virtually identical ranges of U–Pb Triassic ages (e.g., Liu et al., 2004a,b, 2005, 2006a,b; Zhang et al., 2005a, in press-b; Zhao et al., 2005, 2006a), demonstrating that all units were metamorphosed at the same time. Zircon separates from Dabie–Sulu UHP rocks retain low-P mineral-bearing (e.g., Qtz, Pl) inherited cores, UHP mineral-bearing (e.g., coesite) mantles, and low-P mineral-bearing (e.g., Qtz, Pl) rims (Liu et al., 2001, 2002a,b, 2005). Ion microprobe U–Pb analyses of these zoned zircons have identified three discrete age groups, shown schematically in Fig. 9. The presence of anomalously low $\delta^{18}O$ in UHP minerals, not only in coesite eclogites, but also in the wall rocks, suggests that both Dabie–Sulu mafic–ultramafic and felsic rocks remained in contact throughout subduction and underwent regional Triassic *in situ* UHP metamorphism (e.g., Rumble et al., 2003; Zheng et al., 2003a; Chen et al., 2007a).

5.2. Return of H_2O to the deep mantle attending subduction

Laboratory phase equilibrium studies have quantified the P–T stability fields for a wide range of hydrous minerals in peridotites, basalts, granites, and sedimentary rocks for conditions appropriate to the upper mantle (e.g., Schmidt and Poli, 1998; Poli and Schmidt, 2002). Under extremely low subduction-zone geothermal gradients (<5 °C/km), UHP hydrous phases such as lawsonite, micas, K-cymrite, OH-rich Topaz, Ti–clinohumite, serpentine and epidote group minerals (e.g., Wunder et al., 1993; Liou et al. 1998; Zhang et al., 2002b; Litasov and Ohtani, 2007; Tsujimori, 2006a,b; Frezzotti et al., 2007) can return H_2O to the deep upper mantle. For appropriate bulk-rock compositions, dense hydrous Mg-silicates may also transport a substantial quantity of H_2O to the mantle transition zone and perhaps into the lower mantle (Litasov and Ohtani, 2003; Maruyama and Liou, 2005; Komabayashi et al., 2005; Katayama et al., 2006). In addition, many nominally anhydrous minerals that make up the Earth's crust and mantle may accommodate small but measurable amounts of H_2O (Katayama and Nakashima, 2003; Zheng et al., 2003a; Keppler and Smyth, 2006; Chen et al., 2007b). For example, the β and γ polymorphs of olivine (wadsleyite and ringwoodite) can carry up to 2–3 wt% H_2O under UHP conditions, and are stable to depths of 510 and 660 km, respectively (e.g., Kohlstedt et al., 1996; Inoue et al., 1995, 1998). The potential storage capacity of the mantle transition zone is roughly five times that of the volume of seawater on the present-day Earth (Murakami et al., 2002; Ohtani, 2005; Maruyama and Liou, 2005). Transport of H_2O back into the deep mantle drastically lowers solidus temperatures and viscosities, both of which promote more rapid mantle circulation, overturn, and enhanced differential plate and plume tectonic processes (Bercovici and Karato, 2003; Ohtani, 2005).

However, double seismic wedge zones within subducting slabs at mantle depths between 300 and 600 km are related to the transformation of metastable olivine to wadsleyite and ringwoodite, suggesting that the downgoing plate has to be dry at depths >300 km (e.g., Green, 2005a). This observation requires that only inappreciable H_2O can be transported to the mantle transition zone and the lower mantle. Similarly, recent experimental data on the conductivity of wadsleyite and ringwoodite indicate that the contributions of proton (H^+) conduction are small at *P–T* conditions of the mantle transition zone and that of wadsleyite is considerably lower than that of ringwoodite (Yoshino et al., 2006, 2008). The dry model mantle shows considerable conductivity jumps associated with the olivine–wadsleyite and wadsleyite–ringwoodite transitions. Such a dry mantle model adequately explains the currently available conductivity–depth profiles obtained from geo-electromagnetic studies, and suggested that the water content of the mantle may not exceed 0.1 wt% (e.g., Kuvshinov et al., 2005; Yoshino et al., 2008). This conclusion is inconsistent with the idea of significant amount of water transport to the deep mantle. Further studies on the fate of subducted H_2O, the rupture mechanism of deep seismic zones, and conductivity of the mantle transition zone are necessary.

5.3. Duration of Dabie–Sulu UHP metamorphism

Storage times for crustal lithologies subducted into the deep upper mantle are largely unknown, but may be approximated by several ways: (1) kinetics of mineral O isotope exchange at mantle depths (Zheng et al., 2003a, 1998), (2) kinetics of radiogenic isotope diffusion between metamorphosed minerals (Zheng et al., 2003b; Zhao et al., 2006a,b), and (3) the measured age range of UHP mineral assemblages characterizing a particular terrane (Zheng et al., in press, this review). Geochronologic data indicate that most recognizable UHP terranes have experienced brief periods of maximum pressure. Ultrahigh-pressure durations lie in the range of 2–5 Myr for the exhumated complexes of northern Kazakhstan, the Western + Central Alps, the western Himalayas, and Eastern Papua, New Guinea (Sobolev and Shatsky, 1990; Gebauer et al., 1997; Katayama et al., 2003; Hermann et al., 2001; Rubatto and Hermann, 2001; Hacker et al., 2003; Massonne and O'Brien, 2003; Treloar et al., 2003; Baldwin et al., 2004, 2008; Leech et al., 2005; Massonne et al., 2007). In contrast, the largest UHP terranes, including those of east-central China, western China, East Greenland and coastal Norway appear to have been sequestered at great depth for ~15–20 Myr (Hacker et al., 2000, 2006; Wu et al., 2006; Hacker, 2007; Zhang et al., 2008a; Mattinson et al., 2006, 2007, this issue; McClelland et al., 2006; Gilotti and McClelland, 2007; Yin et al., 2007; Kylander-Clark et al., 2008). One example is described below for Sulu UHP rocks.

Numerous geochronological data for Sulu (± some Dabie) felsic, mafic and ultramafic rocks are summarized in Table 4 and Fig. 12. (1) U–Pb zircon studies have yielded Triassic ages (245–205 Ma) from a variety of Sulu gneisses and eclogites (Yang et al., 2003a,b; Li et al., 2004; Liu et al., 2004a,b, 2005, 2006a,b; Zheng et al., 2004, 2005a,b, 2006a,b,c, 2007b; Chen et al., 2007c; Wu et al., 2006; Zhao et al., 2006b; Tang et al., 2008b). This 245–205 Ma interval has also been confirmed by Sm–Nd isochron ages (228–209 Ma) on eclogites (Li et al., 1993) and on the Maowu Grt clinopyroxenite (221–236 Ma) (Jahn et al., 2003b). (2) Zircon rims that contain low-*P* inclusions such as Qtz and Ab from gneisses yield Late Triassic ages (213–208 Ma) (Liu et al., 2004a,b, 2005) representing the late amphibolite-facies retrograde event. On the other hand, Schmidt et al. (2008) report high precision Grt–Cpx Lu–Hf ages of 219.6 and 224.4 Ma for six Dabie–Sulu eclogites; such narrow and uniform Lu–Hf (and Sm–Nd) ages suggest rapid HP eclogitization of the Dabie–Sulu UHP terrane during exhumation.

SHRIMP U–Pb ages of Sulu Grt peridotites and their enclosing eclogites have been determined in spite of the scarcity of zircons in these rocks. Available ages for the mafic–ultramafic bodies range from 238 to 218 Ma (e.g., Zhao et al., 2006a; Zhang et al., 2005a,

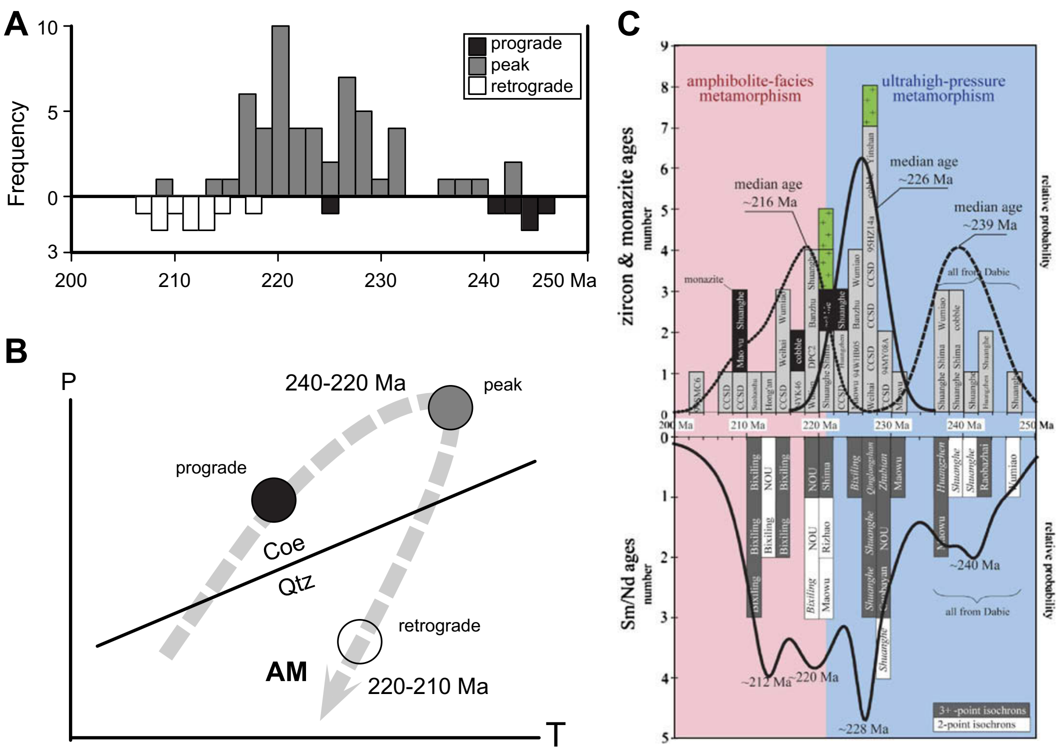

Fig. 12. Compilation of ages for Dabie–Sulu UHP rocks showing long duration of prograde, peak and retrograde metamorphism at UHP conditions: (A) histograms showing ages of Sulu rocks listed in Table 3, (B) schematic *P–T* path for Sulu UHP rocks with the prograde, peak and retrograde stages within the coesite stability for ~30 Myr (250–220) and the retrograde stage within the quartz stability between 220 and 210 Ma. (C) Histogram of ages for three-stage recrystallization of Dabie–Sulu UHP rocks (from Hacker et al. (2006)).

2006a; Yang et al., 2007a), and overlap the UHP metamorphic age range (240–220 Ma) for Dabie–Sulu gneisses and eclogites. Such consistent ages from mafic–ultramafic rocks and country rock gneisses demonstrate that the entire section was subjected to coeval UHP–HP metamorphism. The morphology, internal structure, and Th–U chemistry of analyzed mafic–ultramafic zircon grains are also consistent with metamorphic growth under UHP–HP conditions.

However, a large age range exists in samples from different areas and even in adjacent samples of the same body, resulting from several factors: (1) An insufficient number of spot analyses may result in a bias when calculating weighted mean ages of mafic–ultramafic rocks. (2) Absence of inclusions in most zircons makes it difficult to pin down the metamorphic conditions for each zircon growth zone. (3) Zircons may have recrystallized under different *P–T* conditions in the subduction zone, and their inclusions may or may not reflect the *P–T* conditions that reset the U–Pb system. (4) Zircons may have grown at different times during protracted residence of these mafic–ultramafic bodies at UHP–HP conditions. The close proximity and similar petrologic–geochemical characteristics of analyzed mafic–ultramafic rocks exclude the possibility that they record different metamorphic events and were later juxtaposed. Instead, the mafic–ultramafic rocks have experienced prolonged HP–UHP metamorphism between 238 and 218 Ma, similar to the country rock gneisses and eclogites. The long residence times of the mafic–ultramafic bodies at UHP conditions may be supported by the fact that each sample shows a similar range of spot ages in spite of different weighted mean ages. Moreover, probability diagrams that plot all spot analyses from the studied samples suggest a single population with a normal age distribution.

Evidence for 15–20 Myr duration under UHP conditions (Fig. 12) has been suggested by a growing number of U–Pb, Sm–Nd, and Rb–Sr ages from Dabie–Sulu UHP rocks (Hacker et al., 2004; Leech et al., 2005; Wu et al., 2006; Zheng et al., in press). A possible explanation for such a long duration is the episodic growth of zoned zircons during prograde and retrograde stages at UHP conditions in the presence of an aqueous fluid (e.g., Zheng et al., 2005a,b, 2007b, in press; Wu et al., 2006; Liu et al., 2006c; Rubatto and Hermann, 2007). Internal structures, mineral inclusions, U–Pb ages, and Lu–Hf isotope compositions of Dabie–Sulu zircons indicate that the zoned crystals may have grown during prograde and retrograde paths as shown, respectively, in the mantle and rim domains (Wan et al., 2005; Wu et al., 2006; Zheng et al., 2007b) (Fig. 12B). Inasmuch as some of these domains contain inclusions of coesite, they were formed at UHP conditions. Yet, they are different in terms of CL patterns, U and Th contents, Th/U ratios, abundance of mineral inclusions, and compositions of omphacite inclusions. One example of the proposed *P–T* paths is shown in Fig. 12B (modified from Wan et al. (2005)), based on SHRIMP U–Pb ages of zoned zircon and monazite; the exhumation rate is estimated at >6 km/Ma. The linking of zircon growth to specific metamorphic conditions is not an easy task. Inasmuch as the *P–T* path for recrystallization of UHP rocks from prograde, peak and retrograde stages could pass through the coesite stability field for a considerable length of time, unless the specific *P–T* conditions for each stage could be determined, the extent to which any of these ages represent prograde, peak and retrograde UHP stages of zircon growth remains uncertain (e.g., O'Brien, 2006).

The role of fluid in the growth of Dabie–Sulu zircons has been detailed by Zheng et al. (2004, 2005a,b, 2007b). For a very dry UHP eclogite block at Yangkou Beach of the Sulu terrane, both gabbroic minerals and textures (Zhang and Liou, 1997; Mosenfelder et al., 2005) and intergranular coesite (Fig. 5F) (Liou and Zhang, 1996) coexist. In such a dry eclogite body, zircons are fine-grained showing no metamorphic growth, and have Neoproterozoic U–Pb ages and isotopic compositions (Zheng et al., 2004). Depending on both *P–T* conditions and the amount of fluid, zircon overgrowth in some UHP rocks is generally too small to be analyzed by the ion microprobe. Some grains did not even grow under the peak metamorphic conditions. Hence, spot SHRIMP dating of "peak-stage" metamorphism should be used with caution, unless growth conditions are demonstrated by inclusions, trace element patterns, and/or Ti-thermometry. This is true particularly for the Dabie–Sulu eclogites because they have formed at relatively lower temperatures and much dryer conditions than those from some other UHP terranes (see Table 1).

The large range of SHRIMP ages for Sulu UHP rocks may also imply the juxtaposition of several UHP slices during exhumation from mantle to crustal depths. In fact, a multiple subduction–exhumation model was used to explain about 30 Myr period of successive exhumation of HP–UHP rocks in the western Dabie (Liu et al., 2004c). Slices of the subducting South China slab reached different depths and the successive descent of underlying slabs was accompanied by nearly concomitant uplift of overlying slabs.

6. Future study of UHP metamorphic minerals and rocks

The above review concludes that some sections of continental crust, involving passive-margin lithologies, including carbonate, felsic, pelitic, and minor mafic–ultramafic protoliths, have reached subduction depths approaching or even exceeding 300 km. However, the positive assignment of exsolution lamellae in minerals of mantle-derived garnet peridotites as resulting from decompression in a mantle–wedge setting, or as due to exhumation in a subduction zone remains to be confirmed, except in cases for which age constraints—such as those in the WGR of Norway—are conclusive. With recent breakthroughs in UHP technology and new-generation synchrotron, neutron, and laser facilities for characterization of nano-sized materials, in-depth researches on UHP minerals and rocks are now within reach; such studies are just beginning (see Dobrzhinetskaya et al. (2005, 2006, 2007) and Hwang et al. (2004, 2006, 2007)). Three general fields of mineral physics research are highlighted below to illustrate some of the challenges.

6.1. Identification of micron- and nano-sized minerals

Numerous peculiar minerals and mineral compositions have been identified since UHP metamorphism was first recognized (Chopin, 1984; Smith, 1984). Since then, many novel techniques have been developed for the study of UHP phases with high spatial, temporal, and energy resolutions; they should be applied in the microanalysis of solid and fluid inclusions in UHP minerals, including unexplored trace but widespread opaque (e.g., Fe–Ni sulfide) phases in garnet peridotites (Zhang et al., 2004b; Dobrzhinetskaya et al., 2005) and nano-sized diamond inclusions in eclogitic garnet from Maksyutov (Bostick et al., 2003). Similarly, isotopic characterization of reported microdiamonds (e.g., N-content and N-isotope) and moissanite (C-isotope) from Dabie–Sulu by nano-SIMS is essential because these occurrences are unique in UHP rocks that crystallized briefly at relatively low *T* compared with those in mantle xenoliths.

Nano- to micro-sized mineral and fluid inclusions are rare but ubiquitous in tough, rigid UHP mineral hosts including zircon, diamond, garnet, and pyroxenes (e.g., Langenhorst and Poirier, 2002; Langenhorst, 2003; Dobrzhinetskaya et al., 2005; Hwang et al., 2004, 2005; Zhang et al., 2005c, 2006d, 2007d,e, 2008b); they require *in situ* X-ray microprobe and/or Raman techniques employing synchrotron radiation, or analytical electron microscopy to characterize their structures and compositions. For example, kokchetavite, a new hexagonal polymorph of K-feldspar was discovered as a metastable phase together with α-cristobalite + phengite + siliceous glass ± phlogopite, titanite, calcite, and/or zircon as multiphase cloudy inclusions in Cpx and Grt from a diamond-grade Kokchetav garnet-pyroxene rock (Hwang et al., 2004, 2005). This phase (2–7 μm-sized plates) could be misidentified as K-feldspar by conventional techniques, and misinterpreted as an exsolved phase.

Available studies indicate that microstructures, micro- and nano-phases preserved in host minerals have provided useful information regarding petrotectonic processes of UHP rocks. However, such features are extremely difficult to study due to their submicron size. Moreover, the contribution of interface energies to their stabilities becomes substantial; for example, anatase nano-crystals are more stable than rutile, although rutile is the stable TiO_2 polymorph according to bulk-phase properties (e.g., Barnard and Zapol, 2004). The thermodynamic stabilities of nano-phase clinoenstatite lamellae and α-PbO_2-type TiO_2 within host pyroxene and rutile, respectively, and of nano-size diamond inclusion in garnet may be much different from the stabilities of the bulk phases that have been employed for *P–T* estimates. Clearly, the contribution of interface energies for nano-phases should be considered for occurrences in UHP rocks.

6.2. Characterization of mineral exsolution and phase transformations

Exsolution intergrowths are common in minerals of decompressed UHP rocks; however, exsolution mechanisms in UHP phases are poorly known. Each lamellae-bearing host mineral preserves information concerning the composition and physical conditions of formation of the homogeneous precursor phase, as well as a portion of the *P–T* path during decompression. Compositional and structural characterization of lamellae–host mineral pairs will provide important new constraints on the physical conditions of crystallization/recrystallization. Such studies could guide subsequent experimentation to delineate the *P–T* conditions and mechanisms for formation of the primary UHP minerals. However, the significance of oriented mineral inclusions in host UHP minerals remains unclear. The interpretation of several examples, including ilmenite rods in Alpe Arami olivine [e.g., Dobrzhinetskaya et al. (1996) vs. Hermann et al. (2005)], rutile lamellae in Yangkou eclogitic garnet [e.g., Ye et al. (2000) vs. Hwang et al. (2007)], amphibole lamellae in Qaidam peridotitic garnet [e.g., Song et al. (2005a,b) vs. Yang and Powell (2008)], and quartz rods in eclogitic omphacite of many UHP terranes (Page et al., 2005) remain problematic.

6.3. Experimental phase relations and compositional variations

Experimental investigations of the systems of KMASH, CMASH, and KNCMASH have revealed possible occurrences of hydrous phases in UHP pelitic and peridotitic rocks (Domanik and Holloway, 1996; Ulmer and Trommsdorff, 1999). Experimental investigation of hydroxyl solubility in clinopyroxene, orthopyroxene and olivine (e.g., Grant et al., 2006) indicates that OH content in these minerals is highly dependent on pressure and temperature. Many OH-bearing phases, such as OH-topaz and phase A, are stable only under "forbidden zone" *P–T* conditions (geotherms considerably less than 5 °C/km) (e.g., Wunder et al., 1993; Wunder, 1998). Because such conditions are essentially transient and inevitably are followed by thermal relaxation, these low-*T* phases have little chance to survive decompression accompanying return to the surface through tectonic and erosional processes. However, one possibility for their preservation is as minute inclusions in high-mechanical-strength, impervious containers like garnet, zircon, or diamond (e.g., O'Brien and Ziemann, 2008; Katayama and Maruyama, in press).

Interpretation of the occurrence of majoritic garnets in orogenic peridotites requires more complete experimental data. For example, as shown in Fig. 13, depths for their formation are based on reconnaissance experiments in the pseudobinary system $MgSiO_3$–$Mg_3Al_2Si_3O_{12}$. Although some experiments involve evaluating the effects of Fe and Ca, that of Ti has not been explored. Solubilities of Ti, K, OH, and other trace elements in olivine, garnet and pyroxene in mafic-ultramafic systems need to be examined inasmuch as these phases exhibit numerous microstructures. They also contain minute, as yet unidentified inclusions that may turn out to be UHP phases or DHMS previously synthesized only in diamond-

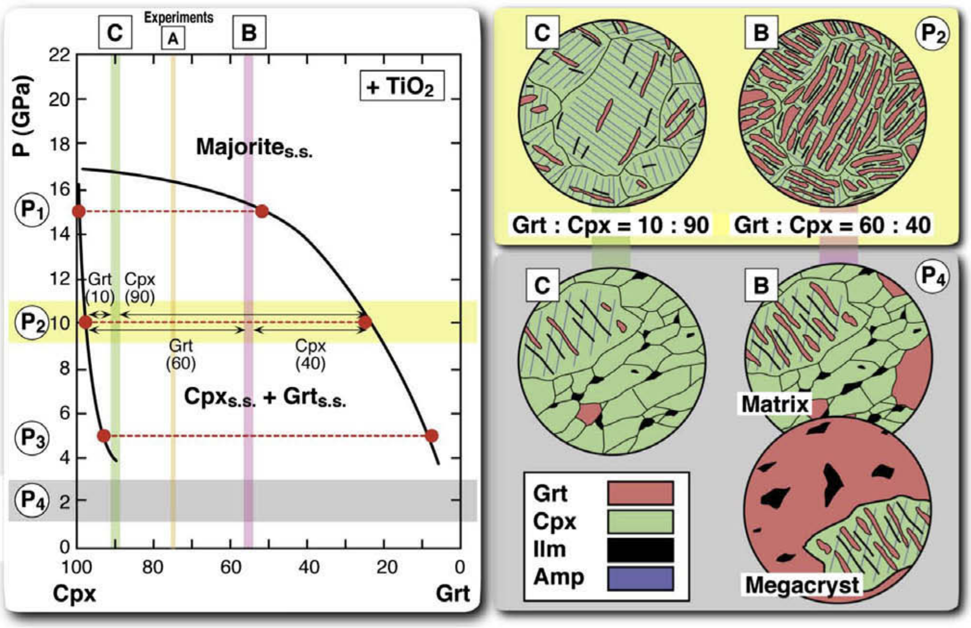

Fig. 13. Schematic *P–X* (Cpx–Grt) diagram and model proportions Grt and Cpx in the presence of ilmenite for isothermal decompression of majoritic garnet to form garnet + ilmenite lamellae in a clinopyroxene host. Path A is based on experiments using starting material of Fig. 6A (see Zhang et al., 2003c, for details); Paths B and C are, respectively, for high- and low-Al content, for Grt-rich and Grt-poor clinopyroxenites.

cell or multi-anvil experiments (e.g., see Bose and Navrotsky (1998)). Discovery of natural representatives of these synthetic phases would be a major step in understanding mantle processes, including the role of hydrous phases as storage sites for H_2O.

6.4. Subcontinental lithospheric mantle (SCLM)

The roots of subcontinental lithospheric mantle vary in thickness, composition and thermal state, all of which depend on the age and tectonothermal history of the overlying crust (e.g., Griffin, 2008; O'Reilly et al., 2001). Archean SCLM is typically strongly depleted in basaltic constituents, highly magnesian, thick (160–250 km), and has a low geotherm; Phanerozoic SCLM is typical fertile, Fe-rich, thin (50–100 km) and exhibits a range of relatively high geotherms; Proterozoic SCLM tends to be intermediate in most respects (O'Reilly and Griffin, 2006). Isotopic compositions and dating of mantle xenoliths and orogenic peridotites employing Lu–Hf and Re–Os system coupled with geochemical bulk-rock data are critical to understanding the processes effecting the secular and spatial variation of SCLM.

Comparison of petrologic, geochemical and isotopic compositions and ages of rocks and zircons from Sulu UHP peridotites and those from mantle xenoliths in east-central China should provide useful information for the evolution of the SCLM. Extensive studies of Sulu peridotites indicated that most Sulu garnet peridotites were derived from a depleted mantle (Type A peridotite), underwent metasomatism, and were subjected to Triassic subduction-zone UHP metamorphism at >150 km depth with a very low thermal gradient (Liou et al., 1998; Zhang and Liou, 1998; Zhang et al., 2000, 2003a, 2005b, 2007b; Malaspina et al., 2008). However, advanced isotope studies of the peridotites required to understand the age and evolution of the SCLM beneath the North and South China blocks are very limited. We are the first to have separated zircons from PP1 peridotites (Zhang et al., 2005a), and subsequently from surface exposures of Sulu peridotites for SHRIMP dates (Zhao et al., 2005, 2006a, 2007a,b; Zheng et al., 2006a).

P–T–time estimates and geochemical characteristics of Sulu mantle-derived Grt peridotites described above were compared with those from nearby diamond-bearing kimberlite (±Grt peridotite) xenoliths (457–500 Ma) in Mengyin, and Grt peridotite xenoliths from Neogene volcanics (16–18 Ma) in Shanwang (see Fig. 8 for locations) (Zheng et al., 2006a,b). Results indicate that a buoyant, refractory lithospheric keel present beneath the eastern North China Block in Paleozoic times was partly replaced by younger, hotter, more fertile lithospheric mantle during the Mesozoic–Cenozoic. Protoliths of UHP Grt peridotites were subjected to complex metasomatism by asthenosphere-derived melts or fluids and subsolidus re-equilibration involving fluids/melts derived from the subducted South China continental crust during Early Mesozoic UHP metamorphism. Tectonic extension of the SCLM of the North China Block and exhumation of the Sulu UHP terrane induced upwelling of the asthenosphere. Peridotites sampled by Neogene basalts represent new lithosphere derived by cooling of the ascending asthenospheric mantle in Jurassic-Cretaceous and Paleogene time (see Fig. 12 of Zheng et al., 2006b) for a model of lithospheric mantle evolution in eastern China).

However, our model of Type A peridotites from the North China mantle wedge (Fig. 8B) was recently challenged by Yuan et al. (2007), who reported preliminary whole-rock Re–Os modal ages of ~2.0 Ga for Xugou peridotites, Sulu terrane; the Paleoproterozoic ages suggest derivation of these Dabie–Sulu mantle peridotites from the South China Block. Systematic Hf isotope study of PP1 peridotite cores and Re–Os isotopic study of Ni–Fe sulfides in peridotites are necessary to better constrain the time and evolution of the SCLM, the dynamics of continental subduction and collision, and the geochemical affinity with the North and South China blocks (e.g, Xu et al., 2006b; Jahn and Chen, 2007; Yuan et al., 2007; Zheng, 2008).

7. Epilogue

Since the first findings of coesite in eclogites by Christian Chopin and Dave Smith in 1984, many UHP terranes have been identified in orogenic belts typified by the occurrence of coesite and/or micro-diamond inclusions in garnet, omphacite and/or zircons. During the last 25 years, much effort has been focused on the characterization of UHP rocks through petrologic, geochemical, and geochronologic studies. Zircon has been found to represent the best container recording the *P–T*–time path of UHP rocks. Fortunately, zircon occurs at least sparsely in almost all UHP rocks, including ultramafics. Many new micro-size phases including fluids and microtextures have been identified; subduction depths of supracrustal rocks are now recognized to extend from the coesite through diamond stability fields at ~150 km to majoritic garnet and possibly to stishovite as deep as 300 km. With new analytical tools characterized by high spatial, temporal, and energy resolutions, many new petrologic, geochemical, and isotopic surprises are expected.

Integrated approaches continue to provide better answers for some old but persistant questions, such as: (1) how are the UHP terranes formed and exhumed? What are the specific exhumation mechanisms that bring these deep-seated rocks from mantle depths back to the surface, and how have UHP minerals survived such long *P–T*–t journeys? (2) Is there a unique or a unified model to explain different terranes with different protoliths, formed at different subduction depths, and subjected to different durations of UHP conditions? (3) What are the effects of subducted continental materials and the effect of crust–mantle interactions on the geodynamics and heterogeneities of the upper mantle? (4) What are the effects of interface energy on the stabilities of nano- and micro-size phases as inclusions as well as lamellae or rods in common UHP minerals?

At the same time, new questions are being raised. For example: do UHP rocks occur in every continental collisional orogeny? What is the role of minor UHP fluids for the generation and preservation of UHP index minerals? When did UHP metamorphism first occur, and why? Geodynamic modeling for subduction, collision, and exhumation of UHP rocks with better thermal, temporal and spacial constraint is proceeding with a better exhumation model for UHP terranes (e.g., Boutelier and Chemenda, 2008; O'Brien and Ziemann, 2008; Yamato et al., 2008).

Green (2005b) concluded that "the story of ultrahigh-pressure metamorphism is a confused mixture of surprising, sometimes spectacular, discoveries and emotional reactions. Surprisingly, the process has been a repeating cycle of disbelief followed by confirmation, with little evidence that the community response in a given cycle has learned from the previous cycles". The explosion of research workshops and special sessions in many national and international meetings leads us to anticipate that UHP research will continue to flourish for the foreseeable future. Many new findings and manuscripts are being published each year. However, it is critical for Earth scientists to pay attention to the basic principles – precise field, mineralogical and petrologic data are essential for interpretations of geotectonic model and mantle dynamics.

This review has undoubtedly overlooked many important published papers inasmuch as more than dozen relevant papers/month and special issues appear in regional and international journals. For this we apologize, but hope that our review will spur additional research on this exciting and evolving topic.

Acknowledgements

This work was supported by Stanford University, the Institute of Earth Sciences, Academia Sinica in Taiwan, and the NSF Continental Dynamic Program, EAR 00-03355, 05-06901, and 0810969. We thank Zeming Zhang, Fulai Liu, Yong-Fei Zheng, Chris Mattinson, Uwe Martens, Tzen-Fu Yui, and other Chinese and Stanford colleagues, as well as Shige Maruyama, Hans-Peter Schertl, and Harry Green who have provided pre-prints and feedback for our review. A draft version of the manuscript was reviewed by Chris Mattinson. We particularly thank both Hans-Peter Schertl and Yong-Fei Zheng for comprehensive, constructive suggestions to improve the content of the manuscript. Bor-ming Jahn acknowledges the support of National Science Council of Taiwan through the following grants: NSC94-2116M-001-08, NSC95-2116M-001-20, and NSC96-2116M-001-004. Tatsuki Tsujimori thanks the support of the Japan Society for the Promotion of Science, Grant-in-Aid for Young Scientists (B) 13740312. We thank the above institutions and scientists for support and help.

References

Abbott, R.N., Draper, G., 2007. Petrogenesis of UHP eclogite from the Cuaba Gneiss, Rio San Juan Complex, Dominican Republic. International Geology Review 49, 1069–1093.

Abbott, R.N., Draper, G., Broman, B.N., 2006. *P–T* path for ultrahigh-pressure garnet ultramafic rocks of the Cuaba gneiss, Rio San Juan complex, Dominican Republic. International Geology Review 48, 778–790.

Abbott, R.N., Broman, B.N., Draper, G., 2007. UHP magma paragenesis revisited, olivine clinopyroxenite and garnet-bearing ultramafic rocks from the Cuaba Gneiss, Rio San Juan Complex, Dominican Republic. International Geology Review 49, 572–586.

APS, 2004. Special issue for Chinese continental drilling project. Acta Petrologica Sinica 20 (1), 1–191 (in Chinese with English abstract).

APS, 2005. Special issue for Chinese continental drilling project. Acta Petrologica Sinica 21 (2), 257–544 (in Chinese with English abstract).

APS, 2006. Special issue for Chinese continental drilling project. Acta Petrologica Sinica 22 (7), 1745–2111 (in Chinese with English abstract).

APS, 2007. Special issue for Chinese continental drilling project. Acta Petrologica Sinica 23 (12), 3041–3348 (in Chinese with English abstract).

Bakun-Czubarow, N., 1991. On the possibility of occurrence of quartz pseudomorphs after coesite in the eclogite–granulite rock series of the Zlote Mountains in the Sudetes, SW Poland. Archiwum Mineralogy 48, 3–25.

Bakun-Czubarow, N., 2007. Ultradeep origin of select Variscan garnet peridotites viewed through majoritic-like garnets, Moldanubian and Szothuringian zones of the Bohemian Massif. In: 29th International Eclogite Field Symposium in Lochalsh Scotland Programme and Abstracts, pp. 8–9.

Baldwin, S.L., Monteleone, B., Webb, L.E., Fitzgerald, G., Grove, M., Hill, E.J., 2004. Pliocene eclogite exhumation at plate tectonic rates in eastern Papua New Guinea. Nature 431, 263–267.

Baldwin, S.L., Webb, L.E., Monteleone, B., 2005. Late Miocene–Pliocene eclogites of eastern Papua New Guinea: the youngest know HP/UHP terrane on Earth. Mitteilungen der Osterreichischen Mineralogischen Gesellschaft 150, 16.

Baldwin, S.L., Webb, L.E., Monteleone, B., 2008. Late Miocene coesite-bearing eclogite exhumed in the Woodlark Rift. Geology 36, 735–738.

Barnard, A.S., Zapol, P., 2004. A model for the phase stability of arbitrary nanoparticles as a function of size and shape. Journal of Chemistry and Physics 121, 4276–4283.

Barron, B.J., Barron, L.M., Dungan, G., 2005. Eclogitic and ultrahigh-pressure crustal garnets and their relationship to Phanerozoic subduction diamonds, Ingara Area, New England Fold belt, eastern Australia. Economic Geology 100, 1565–1582.

Barron, L.M., Barron, B.J., Merbagh, T.P., Birch, W.D., 2008. Ultrahigh pressure macro diamonds from Copeton (New South Wales, Australia), based on Raman spectroscopy of inclusions. Ore Geology Review 34, 76–86.

Bauer, C., Rubatto, D., Krenn, K., Proyer, A., Hoinkes, G., 2007. Age constraints for the metamorphic evolution of the Rhodope Mountains, N-Greece. IEC abstract, pp. 10–11.

Beane, R.J., Connelly, J.N., 1998. $^{40}Ar/^{39}Ar$, U–Pb, and Sm–Nd constraints on the timing of metamorphic events in the Maksyutov Complex, southern Ural Mountains. Journal of Geological Society London 157, 811–822.

Beane, R.J., Leech, M., 2007. The Maksyutov Complex. The first UHP terrane 40 years later. In: Cloos, M., Carlson, W.D., Gilbert, M.C., Liou, J.G., Sorensen, S.S. (Eds.), Convergent Margin Terranes and Associated Regions. Geological Society of America Special Paper 419, 171–184.

Beane, R.J., Liou, J.G., Coleman, R.G., Leech, M.L., 1995. Petrology and retrograde *P–T* path for eclogites of the Maksyutov Complex, southern Ural Mountains, Russia. The Island Arc 4, 254–266.

Bercovici, D., Karato, S.I., 2003. Whole-mantle convection and the transition-zone water filter. Nature 425, 39–44.

Beyer, E.E., Brueckner, H.K., Griffin, W.L., O'Reilly, S.Y., Graham, S., 2004. Archean mantle fragments in Proterozoic crust, Western Gneiss Region, Norway. Geology 32, 609–612.

Bose, K., Navrotsky, A., 1998. Thermochemistry and phase equilibria of hydrous phases in the system $MgO–SiO_2–H_2O$: implications for volatile transport to the mantle. Journal of Geophysical Research 103, 9713–9719.

Bostick, B., Jones, R.E., Ernst, W.G., Chen, C., Leech, M.L., Beane, R.J., 2003. Low-temperature microdiamond aggregates in the Maksyutov metamorphic complex South Ural Mountains, Russia. American Mineralogist 88, 1709–1717.

Boutelier, D.A., Chemenda, A.I., 2008. Exhumation of UHPM/LT rocks due to the local reduction of the interplate pressure: thermomechanical modeling. Earth and Planetary Science Letters 271, 226–232.

Bowtell, S.A., Cliff, R.A., Barnicoat, A.C., 1994. Sm–Nd isotopic evidence on the age of eclogitization in the Zermatt-Saas ophiolite. Journal of Metamorphic Geology 12, 187–196.

Bozilov, K.N., Green, H.W., Dobrzhinetskaya, L.F., 1999. Clinoenstatite in the Alpe Arami peridotite: additional evidence of very high pressure. Science 284, 128–132.

Bozilov, K.N., Green, H.W., Dobrzhinetskaya, L.F., 2003. Quantitative 3D measurement of ilmenite abundance in Alpe Arami olivine: confirmation of high-pressure origin. American Mineralogist 88, 596–603.

Brenker, F.E., Brey, G.P., 1997. Reconstruction of exhumation path of the Alpe Arami garnet-peridotite body from depths exceeding 160 km. Journal of Metamorphic Geology 15, 581–592.

Brueckner, H.K., 1998. Sinking intrusion model for the emplacement of garnet-bearing peridotites into continent collision orogens. Geology 26, 631–634.

Brueckner, H.K., 2006. Dunk, dunkless and re-dunk tectonics: a model for metamorphism, lack of metamorphism, and repeated metamorphism of HP/UHP terranes. International Geology Review 48, 978–995.

Brueckner, H.K., Medaris Jr., L.G., 1998. A tale of two orogens – the contrasting *P–T–t* history and geochemical evolution of mantle in ultrahigh pressure (UHP) metamorphic terranes of the Norwegian Caledonides and the Czech Variscides. Schweizerische Mineralogische und Petrographische Mitteilungen 78, 293–307.

Brueckner, H.K., Medaris Jr., L.G., 2000. A general model for the intrusion and evolution of mantle peridotites in high-pressure and ultrahigh-pressure metamorphic terranes. Journal of Metamorphic Geology 18, 119–130.

Brueckner, H.K., Carswell, D.A., Griffin, W.L., 2003. Paleozoic diamonds within a Precambrian peridotite lens in UHP gneisses of the Norwegian Caledonides. Earth and Planetary Science Letters 203, 805–816.

Brueckner, H.K., Van Roermund, H.L.M., Pearson, N.J., 2004. An Archean (?) to Paleozoic evolution for a garnet peridotite lens with sub-Baltic affinity within the Seven Nappe Complex of Jämtland, Sweden, Central Scandinavian Caledonides. Journal of Petrology 45, 415–437.

Caby, R., 1994. Precambrian coesite from N Mali: first record and implications for plate tectonics in the trans-Saharan segment of the Pan-African belt. European Journal of Mineralogy 6, 235–244.

Carswell, D.A., 1981. Clarification of the petrology and occurrence of garnet lherzolites, garnet websterites and eclogite in the vicinity of Rodhaugen, Almklovdalen, West Norway. Norsk Geologisk Tidsskrift 61, 249–260.

Carswell, D.A., 1986. The metamorphic evolution of Mg-Cr type Norwegian garnet peridotites. Lithos 19, 279–297.

Carswell, D.A., Compagnoni, R. (Eds.), 2003. Ultra-High Pressure Metamorphism. European Mineralogical Union, Notes in Mineralogy, vol. 5, 508pp.

Carswell, D.A., Cuthbert, S.J., 2003. Reviews of representative UHPM terranes: the Western Gneiss Region of Norway. In: Carswell, D.A., Compagnoni, R. (Eds.), Ultra-High Pressure Metamorphism. European Mineralogical Union, Notes in Mineralogy, vol. 5, pp. 51–74.

Carswell, D.A., Cuthbert, S.J., Krogh Ravna, E.J., 1999. Ultrahigh-pressure metamorphism in the Western Gneiss Region of the Norwegian caledonides. International Geology Review 41, 955–966.

Carswell, D.A., Brueckner, H.K., Cuthbert, S.J., Mehta, K., O'Brien, J., 2003. The timing of stabilisation and the exhumation rate for ultra-high pressure rocks in the Western Gneiss Region. Journal of Metamorphic Geology 21, 601–612.

Carswell, D.A., van Roermund, H.L.M., Wiggers de Vries, D.F., 2006. Scandinavian ultrahigh-pressure metamorphism of Proterozoic basement rocks on Fjortoft and Otroy, Western Gneiss Region, Norway. International Geology Review 48, 957–977.

Castelli, D., Rolfo, F., Groppo, C., Compagnoni, R., 2007. Impure marbles from the UHP Brossaco-Isasca Unit (Dora-Maira Massif, western Alps): evidence for Alpine equilibration in diamond stability field and evolution of the $X(CO_2)$ fluid evolution. Journal of Metamorphic Geology 25, 587–603.

Cartigny, P., 2005. Stable isotopes and the origin of diamond. Elements 1, 79–84.

Chao, E.C.T., Fahey, J.J., Littler, J., Milton, D.J., 1962. Stishovite, a new mineral from meteorite crater, Arizona. Journal of Geophysical Research 67, 419–421.

Chavagnac, V., Jahn, B.-M., 1996. Coesite-bearing eclogites from the Bixiling complex, Dabie Mountains, China: Sm–Nd ages, geochemical characteristics and tectonic implications. Chemical Geology 133, 29–51.

Chen, J., Xu, Z., 2005. Pargasite and ilmenite exsolution texture in clinopyroxenes from the Hujianling garnet-pyroxenite, Sulu UHP terrane, central China: a geodynamic implication. European Journal of Mineralogy 17, 895–903.

Chen, S.Z., Yang, J.S., Xu, Z.Q., Li, T.F., Chen, F.Y., Zhang, Z.M., Zhang, W.L., 2005. Petrology and mineralogy of PP3 ultramafic rocks in the Sulu UHP belt and its significance. Acta Petrologica Sinica 21, 369–380 (in Chinese with English abstract).

Chen, R.-X., Zheng, Y.-F., Gong, B., Zhao, Z.-F., Gao, T.-S., Chen, B., Wu, Y.-B., 2007a. Oxygen isotope geochemistry of ultrahigh-pressure metamorphic rocks from 200–4000 m core samples of the Chinese continental scientific drilling. Chemical Geology 242, 51–75.

Chen, R.-X., Zheng, Y.-F., Gong, B., Zhao, Z.-F., Gao, T.-S., Chen, B., Wu, Y.-B., 2007b. Origin of retrograde fluid in ultrahigh-pressure metamorphic rocks: constraints from mineral hydrogen isotope and water content changes in eclogite-gneiss transitions in the Sulu orogen. Geochimica et Cosmochimica Acta 71, 2299–2325.

Chen, R.-X., Zheng, Y.-F., Zhao, Z.-F., Tang, J., Wu, F.-Y., Liu, X.-M., 2007c. Zircon U–Pb ages and Hf isotopes in ultrahigh-pressure metamorphic rocks from the Chinese continental scientific drilling project. Journal of Metamorphic Geology 25, 873–894.

Chesnokov, B., Popov, A., 1965. Increasing volume of quartz grains in eclogites of the south Urals. Doklady Akademii Nauk 162, 176–178 (in Russian).

Chopin, C., 1984. Coesite and pure pyrope in high-grade blueschists of the Western Alps: a first record and some consequences. Contributions to Mineralogy and Petrology 86, 107–118.

Chopin, C., 2003. Ultrahigh-pressure metamorphism: tracing continental crust into the mantle. Earth and Planetary Science Letters 212, 1–14.

Compagnoni, R., Rolfo, F., 2003. UHPM units in the Western Alps. In: Carswell, D.A., Compagnoni, R. (Eds.), Ultra-High Pressure Metamorphism. European Mineralogical Union, Notes in Mineralogy, vol. 5, pp. 13–49.

de Hoog, J.C.M., Janak, M., Vrabec, M., Froitzheim, N., in press. Serpentinised peridotites from an ultrahigh-pressure terrane in the Pohorje Mts. (Eastern Alps, Slovenia): geochemical constraints on petrogenesis and tectonic setting. Lithos.

de Sigoyer, J., Chavagnac, V., Blichert-Toft, J., Villa, I.M., Luais, B., Guillot, S., Cosca, M., Mascle, G., 2000. Dating the Indian continental subduction and collisional thickening in the northwest Himalaya: multichronology of the Tso Morari eclogites. Geology 28, 487–490.

Dobretsov, N.L., Dobretsova, L., 1988. New mineralogic data on the Maksyutov eclogite–glaucophane schist complex, southern Urals. Doklady Akademii Nauk 300, 111–116.

Dobretsov, N.L., Shatsky, S., Coleman, R.G., Lennykh, I., Valizer, M., Liou, J.G., Zhang, R.Y., Beane, R.J., 1996. Tectonic setting and petrology of ultrahigh-pressure metamorphic rocks in the Maksyutov Complex, Ural Mountains, Russia. International Geology Review 38, 136–160.

Dobrzhinetskaya, L.F., Green II, H.W., 2007. Diamond synthesis from graphite in presence of water and SiO_2: implications for diamond formation in quartzites from Kazakhstan. International Geology Review 49, 389–400.

Dobrzhinetskaya, L.F., Eide, E.A., Larsen, R.B., Sturt, B.A., Tronnes, R.G., Smith, D.C., Taylor, W.R., Posukhova, T., 1995. Microdiamond in high-grade metamorphic rocks of the Western Gneiss region, Norway. Geology 23, 597–600.

Dobrzhinetskaya, L.F., Green II, H.W., Wang, S., 1996. Alpe-Arami: a peridotite massif from depth of more than 300 kilometers. Science 271, 1841–1845.

Dobrzhinetskaya, L.F., Bozhilov, K.N., Green II, H.W., 2000. The solubility of TiO_2 in olivine: implication to the mantle wedge environment. Chemical Geology 163, 325–338.

Dobrzhinetskaya, L.F., Green II, H.W., Mitchell, T.E., Dickerson, R.M., 2001. Metamorphic diamonds: mechanism of growth and inclusion of oxides. Geology 29, 263–266.

Dobrzhinetskaya, L.F., Green II, H.W., Weschler, M., Darus, M., Wang, Y.C., Massonne, H., Stöckert, B., 2003. Focused ion beam technique and transmission electron microscope studies of microdiamonds from the Saxonian Erzgebirge, Germany. Earth and Planetary Science Letters 210, 399–410.

Dobrzhinetskaya, L.F., Green II, H.W., Renfro, A.P., Bozhilov, K.N., Spengler, D., Van Roermund, H.L.M., 2004. Precipitation of pyroxenes and olivine from majoritic garnet: simulation of peridotite exhumation from great depth. Terra Nova 16, 325–330.

Dobrzhinetskaya, L.F., Wirth, R., Green II, H.W., 2005. Nanometric inclusions of carbonates in Kokchetav diamonds from Kazakhstan: a new constraint for the depth of their origin. Earth and Planetary Science Letters 243, 85–93.

Dobrzhinetskaya, L.F., Liu, Z., Cartigny, P., Zhang, J., Tchkhetia, N.N., Hemley, R.J., Green II, H.W., 2006. Synchrotron infrared and Raman spectroscopy of microdiamonds from Erzgebirge, Germany. Earth and Planetary Science Letters 248, 340–349.

Dobrzhinetskaya, L.F., Wirth, R., Green II, H.W., 2007. A look inside of diamond forming media in deep subduction zones. Proceedings of the National Academy of Sciences 104, 9128–9132.

Domanik, K.J., Holloway, J.R., 1996. The stability and composition of phengitic muscovite and associated phases from 5.5 to 11 GPa: Implications for deeply subducted sediments. Geochimica et Cosmochimica Acta 60, 4133–4150.

El Goresy, A., Dubrovinsky, L., Sharp, T.C., Saxena, S.K., Chen, M., 2000. A monoclinic post-stishovite polymorph of silica in the Shergotty Meteorite. Science 288, 1632–1634.

Enami, M., Liou, J.G., Mattinson, C., 2004a. Epidote minerals in high- and ultrahigh-pressure metamorphism. In: Liebscher, A., Franz, G. (Eds.), Epidotes, Review in Mineralogy and Geochemistry, vol. 56, pp. 347–398.

Enami, M., Mizukami, T., Yokoyama, K., 2004b. Metamorphic evolution of garnet-bearing ultramafic rocks from the Gongen area, Sanbagawa belt, Japan. Journal of Metamorphic Geology 22, 1–15.

Ernst, W.G., 2006. Preservation/exhumation of ultrahigh-pressure subduction complexes. Lithos 92, 321–335.

Ernst, W.G., Liou, J.G., 2000. Ultrahigh-pressure Metamorphism and Geodynamics in Collision-type Orogenic Belts: International Book Series, vol. 4. Geological Society of America. p. 293.

Ernst, W.G., Liou, J.G., 2008. High- and ultrahigh-pressure metamorphism—past results, future prospects. American Mineralogist 93, 1771–1786.

Ernst, W.G., Hacker, B.R., Liou, J.G., 2007. Petrotectonics and geochronology of ultrahigh-pressure crustal and upper mantle rocks—implications for Phanerozoic orogeny. In: Sears, J.W., Harms, T.A., Evenchick, C.A. (Eds.), Whence the Mountains? Enquiries into the Evolution of Orogenic Belts. Geological Society of America Special Paper, vol. 433, pp. 27–49.

Evans, B.W., Trommsdorff, V., 1978. Petrogenesis of garnet lherzolite, Cima di Gagnone, Lepontine Alps. Earth and Planetary Science Letters 40, 415–424.

Frezzotti, G., Ferrando, S., Dallai, L., Compagnoni, R., 2007. Intermediate alkali-alumino-silicate aqueous solutions released by deeply subducted continental crust: fluid evolution in UHP OH-rich topaz-kyanite quartzites from Donghai (Sulu, China). Journal of Petrology 48, 1219–1241.

García-Casco, A., Iturralde-Vinent, M., Pindell, J., 2008. Latest Cretaceous collision/accretion between the Caribbean plate and Caribeana: origin of metamorphic terranes in the Greater Antilles. International Geology Review 50, 781–809.

Gebauer, D., Schertl, H.-P., Brix, M., Schreyer, W., 1997. 35 Ma old ultrahigh-pressure metamorphism and evidence for very rapid exhumation in the Dora Maira Massif, western Alps. Lithos 41, 5–24.

Ghent, E., Tinkham, D., Marr, R., 2009. Lawsonite eclogites from the Pinchi Lake area, British Columbia – new P – T estimates and interpretation. Lithos 109, 248–253.

Ghiribelli, B., Frezzotti, M.-L., Palmeri, R., 2002. Coesite in eclogites of the Lanterman range, Antarctica: evidence from textural and Raman studies. European Journal of Mineralogy 14, 355–360.

Gilotti, J.A., 1993. Discovery of a medium-temperature eclogite province in the Caledonides of North-East Greenland. Geology 21, 523–526.

Gilotti, J.A., Ravna, E.J.K., 2002. First evidence for ultrahigh-pressure metamorphism in the Northeast Greenland Caledonides. Geology 30, 551–554.

Gilotti, J.A., McClelland, W.C., 2007. Characteristics of, and a tectonic model for, ultrahigh-pressure metamorphism in the overriding plate of the Caledonian orogen. International Geology Review 49, 777–797.

Grant, K.J., Kohn, S.C., Brooker, R.A., 2006. Solubility and partitioning of water in synthetic forsterite and enstatite in the system $MgO–SiO_2–H_2O \pm Al_2O_3$. Contributions to Mineralogy and Petrology 151, 651–664.

Green II, H.W., 2005a. Psychology of a changing paradigm: 40+ years of high-pressure metamorphism. International Geology Review 45, 439–456.

Green II, H.W., 2005b. New light on deep earthquakes. Scientific American, 1–9.

Green II, H.W., Dobrzhinetskaya, L.F., Bozhilov, K.N., 1997. Determining the origin of ultra-high pressure lherzolites. Science 278, 704–707.

Griffin, W.L., 2008. Research focus. Major transformations reveal Earth's deep secrets. Geology 36, 95–96.

Groppo, C., Lombardo, B., Castelli, D., Compagnoni, R., 2007. Exhumation history of the UHPM Brossasco-Isaca Unit, Dora Maira Massif, as inferred from a phengite-amphibole eclogite. International Geology Review 49, 142–182.

Guillot, S., Hattori, K., Schwartz, S., Vidal, O., 2008. Exhumation processes in oceanic and continental contexts: a review. In: Lallemand, S., Funiciello, F. (Eds.), Subduction Zone Dynamics? Springer-Verlag, Berlin, Heidelberg, pp. 1771–1786.

Hacker, B.R., 2007. Ascent of the ultrahigh-pressure Western Gneiss Region, Norway. In: Cloos, M., Carlson, W.D., Gilbert, M.C., Liou, J.G., Sorensen, S.S. (Eds.), Convergent Margin Terranes and Associated Regions. Geological Society of America Special Paper, vol. 419, pp. 171–184.

Hacker, B.R., Sharp, T., Zhang, R.Y., Liou, J., Hervig, R.L., 1997. Determining the origin of ultrahigh-pressure lherzolite? Science 278, 702–704.

Hacker, B.R., Ratschbacher, L., Webb, L., McWilliams, M.O., Ireland, T., Calvert, A., Shuwen, D., Wenk, H.-R., Chateigner, D., 2000. Exhumation of ultrahigh-pressure continental crust in East-central China: Late Triassic-Early Jurassic tectonic unroofing. Journal of Geophysical Research 105, 13339–13364.

Hacker, B.R., Calvert, A., Zhang, R.Y., Ernst, W.G., Liou, J.G., 2003. Ultrarapid exhumation of ultrahigh-pressure diamond-bearing metasedimentary rocks of the Kokchetav Massif, Kazakhstan. Lithos 70, 61–75.

Hacker, B.R., Ratscnbacner, L., Liou, J.G., 2004. Subduction, collision, and exhumation in the qinling-dabie orogen: a review. In: Malpas, J., Fletcher, C.J.N., Ali, J.R., Aitchison, J.C. (Eds.), Aspects of the Tectonic Evolution of China, Geological Society of London Special Paper, vol. 226, pp. 157–175.

Hacker, B.R., Wallis, S.R., Ratschbacher, L., Grove, M., Gehrels, G., 2006. High-temperature geochronology constraints the tectonic history and architecture of the ultrahigh-pressure Dabie–Sulu orogen. Tectonics 25, TC5006. doi:10.1029/2005TC001937.

Haggerty, S.E., Sautter, V., 1990. Ultradeep (greater than 300 kilometers) ultramafic upper mantle xenoliths. Science 248, 993–996.

Harlow, G.E., 1997. K in clinopyroxene at high pressure and temperature: an experimental study. American Mineralogist 82, 259–269.

Harlow, G.E., Hemming, S.R., Avé Lallemant, H.G., Sisson, V.B., Sorensen, S.S., 2004. Two high-pressure–low-temperature serpentinite-matrix mélange belts, Motagua fault zone, Guatemala: a record of Aptian and Maastrichtian collisions. Geology 32, 17–20.

Hermann, J., 2003. Experimental evidence for diamond-facies metamorphism in the Dora-Maira massif. Lithos 70, 163–182.

Hermann, J., Rubatto, D., Korsakov, A., Shatsky, V.S., 2001. Multiple growth during fast exhumation of diamondiferous deeply subducted continental crust (Kokchetav Massif, Kazakhstan). Contributions to Mineralogy and Petrology 141, 66–82.

Hermann, J., O'Neill, H.S.C., Berry, A.J., 2005. Titanium solubility in olivine in the system TiO_2–MgO–SiO_2: no evidence for an ultra-deep origin of Ti-bearing olivine. Contributions to Mineralogy and Petrology 148, 746–760.

Hu, N., Zhao, D., Xu, B., Wang, T., 1995. Petrography and metamorphism study on high-ultrahigh pressure eclogite from Guanpo area, northern Qinling Mountain. Journal of Mineralogy and Petrology 15, 1–9 (in Chinese).

Hwang, S.L., Shen, P., Chu, H.T., Yui, T.F., 2000. Nanometer-size α-PbO_2-type TiO_2 in garnet: a thermobarometer for ultra-high pressure metamorphism. Science 288, 321–324.

Hwang, S.L., Shen, P., Chu, H.T., Yui, T.F., Lin, C.C., 2001. Genesis of microdiamonds from melt and associated multiphase inclusions in garnet of ultrahigh-pressure gneiss from Erzegebirge, Germany. Earth and Planetary Science Letters 188, 9–15.

Hwang, S.L., Shen, P., Chu, H.T., Yui, T.F., Liou, J.G., Sobolev, N., Zhang, R.Y., Shatsky, S., Zayachkovsky, A.A., 2004. Kokchetavite, a new potassium-feldspar polymorph from the Kokchetav ultrahigh-pressure terrane. Contributions to Mineralogy and Petrology 148, 380–389.

Hwang, S.L., Shen, P., Chu, H.T., Yui, T.F., Liou, J.G., Sobolev, N.V., 2005. Crustal-derived potassic fluid in terrestrial diamonds. Earth and Planetary Science Letter 231, 295–306.

Hwang, S.L., Chu, H.T., Yui, T.F., Shen, P.Y., Schertl, H.P., Liou, J.G., Sobolev, N.V., 2006. Nanometer-size P/K-rich silica glass (former melt) inclusions in microdiamond from gneisses of Kokchetav and Erzgebirge massifs: diversified characteristics of the formation media of metamorphic microdiamond in UHP rocks. Earth and Planetary Science Letter 243, 94–106.

Hwang, S.-L., Chu, H.-T., Yui, T.-F., Shen, P., Schertl, H.-P., Liou, J.G., Sobolev, N.V., 2007. On the origin of oriented rutile needles in garnet from UHP eclogites. Journal of Metamorphic Geology 25, 349–362.

Inoue, T., Yurimoto, H., Kudoh, K., 1995. Hydrous modified spinel $Mg_{1.75}SiH_{0.5}O_4$: a new water reservoir in the mantle transition region. Geophysical Research Letters 22, 117–120.

Inoue, T., Weidner, D.J., Northrup, A., Parise, J.G., 1998. Elastic properties of hydrous ringwoodite (gamma-phase) in Mg_2SiO_4. Earth and Planetary Science Letters 160, 107–113.

Irifune, T., Ringwood, A.E., 1993. Phase transformations in subducted oceanic crust and buoyancy relationships at depths of 600–800 km in the mantle. Earth and Planetary Science Letters 117, 101–110.

Jahn, B.-m., Chen, B., 2007. Dabieshan UHP metamorphic terrane: Sr–Nd–Pb isotopic constraint to pre-metamorphic subduction polarity. International Geology Review 49, 14–29.

Jahn, B.-m., Cornichet, J., Cong, B.L., Yui, T.F., 1996. Ultra-high εNd eclogites from an ultra-high pressure metamorphic terrane of China. Chemical Geology 127, 1–24.

Jahn, B.-m., Caby, R., Monie, P., 2001. The oldest UHP eclogites of the world: age of UHP metamorphism, nature of protoliths and tectonic implications. Chemical Geology 178, 143–158.

Jahn, B.M., Rumble, D., Liou, J.G., 2003a. Geochemistry and isotope tracer study of UHPM rocks. In: Carswell, D.A., Compagnoni, R. (Eds.), Ultrahigh-pressure Metamorphism. European Mineralogical Union, Notes in Mineralogy, vol. 5, pp. 365–414.

Jahn, B.M., Fan, Q.C., Yang, J.J., Henin, O., 2003b. Petrogenesis of the Maowu pyroxenite-eclogite body from the UHP metamorphic terrane of Dabieshan: chemical and isotopic constraints and tectonic implications. Lithos 70, 243–267.

Janak, M., Froitzherim, N., Luptak, B., Vrabec, M., Krogh Ravna, E.J., 2004. First evidence for ultrahigh-pressure metamorphism of eclogites in Pohorje, Slovenia: tracing deep continental subduction in the Eastern Alps. Tectonics 23, TC5014. doi:10.1029/2004TC001641.

Jamtveit, B., 1984. High-*P* metamorphism and deformation of the Gurskebotn garnet peridotite, Sunnmore, Western Norway. Norsk Geologisk Tidsskrift 64, 97–110.

Jamtveit, B., 1987. Metamorphic evolution of the Eiksunddal eclogite complex, Western Norway, and some tectonic implications. Contributions to Mineralogy and Petrology 95, 82–99.

Jamtveit, B., Caswell, D.A., Mearns, E.W., 1991. Chronology of the high-pressure metamorphism of Norwegian garnet peridotites/pyroxenites. Journal of Metamorphic Geology 9, 125–139.

Janak, M., Froitzheim, N., Vrabec, M., Krogh Ravna, E.J., De Hoog, J.C.M., 2006. Ultrahigh-pressure metamorphism and exhumation of garnet peridotite in Pohorje, Eastern Alps. Journal of Metamorphic Geology 24, 19–31.

Kadarusman, A., Parkinson, C.D., 2000. Petrology and P-T evolution of garnet peridotites from central Sulawesi, Indonesia. Journal of Metamorphic Geology 18, 193–210.

Kaneko, Y., Katayama, I., Yamamoto, H., Misawa, K., Ishikawa, M., Rehman, H.U., Kausar, A.B., Shiraishi, K., 2003. Timing of Himalayan ultrahigh-pressure metamorphism: sinking rate and subduction angle of the Indian continental crust beneath Asia. Journal of Metamorphic Geology 21, 589–599.

Katayama, I., Maruyama, S., in press. Inclusion study in zircon from ultrahigh-pressure metamorphic rocks in the Kokchetav massif: an excellent tracer of metamorphic history. Journal of the Geologic Society of London Special Publication.

Katayama, I., Nakashima, S., 2003. Hydroxyl in clinopyroxene from the deep subducted crust: evidence for H_2O transport into the mantle. American Mineralogist 88, 229–234.

Katayama, I., Parkinson, C.D., Okamoto, K., Nakajima, Y., Maruyama, S., 2000. Supersilicic clinopyroxene and silica exsolution in UHPM eclogite and pelitic gneiss from the Kokchetav massif, Kazakhstan. American Mineralogist 85, 1368–1374.

Katayama, I., Ota, M., Ogasawara, Y., 2002a. Phengite exsolution in diopside in diamond-bearing marbles from Kumdy-Kohl. In: Parkinson, C.D., Katayama, I., Liou, J.G., Maruyama, S. (Eds.), The Diamond-bearing Kokchetav Massif, Kazakhstan: Petrochemistry and Tectonic Evolution of a Unique Ultrahigh-pressure Metamorphic Terrane. Universal Academy Press Inc., Tokyo, Japan, pp. 181–190.

Katayama, I., Maruyama, S., Parkinson, C.D., Terada, K., Sano, Y., 2002b. Pressure-temperature-time path of the Kokchetav UHP metamorphism deduced from mineral inclusions and SHRIMP geochronology of zircons. In: Parkinson, C.D., Katayama, I., Liou, J.G., Maruyama, S. (Eds.), The Diamond-bearing Kokchetav Massif, Kazakhstan: Petrochemistry and Tectonic Evolution of a Unique Ultrahigh-pressure Metamorphic Terrane. Universal Academy Press Inc., Tokyo, Japan, pp. 381–396.

Katayama, I., Mukou, A., Iizuka, T., Maruyama, S., Terada, K., Tsutsumi, T., Sano, S., Zhang, R.Y., Liou, J.G., 2003. Dating of zircon from Ti–clinohumite-bearing garnet peridotite: implication for timing of mantle metasomatism. Geology 31, 713–716.

Katayama, I., Nakashima, S., Yurimoto, H., 2006. Water content in natural eclogite and implication for water transport into the deep upper mantle. Lithos 86, 245–259.

Keppler, H., Smyth, J.R. (Eds.), 2006. Water in Nominally Anhydrous Minerals. Reviews in Mineralogy and Geochemistry, vol. 62, 478pp.

Kohlstedt, D.L., Keppler, H., Rubie, D.C., 1996. Solubility of water in the a, b and g phases of $(Mg, Fe)_2SiO_4$. Contributions to Mineralogy and Petrology 123, 345–357.

Komabayashi, T., Omori, S., Maruyama, S., 2005. Experimental and theoretical study of stability of dense hydrous magnesium silicates in the deep upper mantle. Physics of the Earth and Planetary Interiors 153, 191–209.

Korsakov, A.V., Theunissen, K., Smirnova, L.V., 2004. Intergranular diamonds derived from partial melting of crustal rocks at ultrahigh-pressure metamorphic conditions. Terra Nova 16, 146–151.

Krebs, M., Maresch, W.V., Schertl, H.-P., Münker, C., Baumann, A., Draper, G., Idleman, B., Trapp, E., 2008. The dynamics of intra-oceanic subduction zones: a direct comparison between fossil petrological evidence (Rio San Juan Complex, Dominican Republic) and numerical simulation. Lithos 103, 106–137.

Kretz, R., 1983. Symbols for rock-forming minerals. American Mineralogist 68, 277–279.

Krogh, E.J., Carswell, D.A., 1995. HP and UHP eclogites and garnet peridotites in the Scandinavian Caledonides. In: Coleman, R.G., Wang, X. (Eds.), Ultrahigh Pressure Metamorphism. Cambridge University Press, pp. 244–298.

Kuvshinov, A., Utada, H., Avdeev, A., Koyama, T., 2005. 3-D modeling and analysis of Dst C-responses in the North Pacific Ocean region, revisited. Geophysical Journal International 160, 505–526.

Kylander-Clark, A.R.C., Hacker, B.R., Mattinson, J.M., 2008. Slow exhumation of UHP terranes: titanite and rutile ages of the Western Gneiss Region, Norway. Earth and Planetary Science Letters 272, 531–540.

Lang, H.M., Gilotti, J.A., 2007. Partial melting of metapelites at ultrahigh-pressure conditions, Greenland Caledonides. Journal of Metamorphic Geology 25, 129–148.

Langenhorst, F., 2003. Nanostructures in ultra-high pressure metamorphic coesite and diamond: a genetic fingerprint. Mitteilungen der Osterreichischen Mineralogischen Gesellschaft 48, 401–412.

Langenhorst, F., Poirier, J-P., 2002. Transmission electron microscopy of coesite inclusions in the Dora Maira high-pressure metamorphic pyrope-quartzite. Earth and Planetary Science Letters 203, 793–803.

Lardeaux, J.M., Ledru, D.I., Duchene, S., 2001. The Variscan French Massif Central – a new addition to the ultrahigh pressure metamorphic 'club': exhumation processes and geodynamic consequences. Tectonophysics 332, 143–167.

Leech, M.L., Ernst, W.G., 1998. Graphite pseudomorphs after diamond? A carbon isotope and spectroscopic study of graphite cuboids from the Maksyutov complex, south Ural Mountains, Russia. Geochimica et Cosmochimica Acta 62, 2143–2154.

Leech, M.L., Singh, S., Jain, A.K., Klemperer, S.L., Manickavasagam, R.M., 2005. The onset of India–Asia continental collision: early, steep subduction required by the timing of UHP metamorphism in the western Himalaya. Earth and Planetary Science Letters 234, 83–97.

Leung, I.S., 1990. Silicon carbide cluster entrapped in a diamond from Fuxian, China. American Mineralogist 75, 1110–1119.

Li, S., Chen, Y., Cong, B., Zhang, Z., Zhang, R., Liou, D., Hart, S.R., Ge, N., 1993. Collision of the North China and Yangtze Blocks and formation of coesite-bearing eclogites: timing and processes. Chemical Geology 109, 70–89.

Li, X.-P., Zheng, Y.-F., Wu, Y.-B., Chen, F.K., Gong, B., Li, Y.-L., 2004. Low-*T* eclogite in the Dabie terrane of China: petrological and isotopic constraints on fluid activity and radiometric dating. Contributions to Mineralogy and Petrology 148, 443–470.

Li, T., Yang, J.S., Zhang, R.Y., 2008. Geochemical characteristics and UHP metamorphic age of the Hujialing garnet clinopyroxenite from the Sulu terrane, China and the bearing on its genesis. International Geology Review 50, 48–60.

Liati, A., 2005. Identification of repeated alpine ultrahigh pressure metamorphic events by U/Pb SHRIMP geochronology and REE geochemistry of zircon; the Rhodope Zone of northern Greece. Contributions to Mineralogy and Petrology 150, 608–630.

Liati, A., Gebauer, D., Wysoczanski, R., 2002. U–Pb SHRIMP-dating of zircon domains from UHP garnet-rich mafic rocks and late pegmatoids in the Rhodope Zone (N Greece): evidence for Early Cretaceous crystallization and Late Cretaceous metamorphism. Chemical Geology 184, 281–299.
Liou, J.G., Zhang, R.Y., 1996. Occurrence of intergranular coesite in ultrahigh-*P* rocks from the Sulu region, eastern China: implications for lack of fluid during exhumation. American Mineralogist 81, 1217–1221.
Liou, J.G., Zhang, R.Y., Ernst, W.G., Rumble III, D., Maruyama, S., 1998. High pressure minerals from deeply subducted metamorphic rocks. Reviews in Mineralogy 37, 33–96.
Liou, J.G., Hacker, B.R., Zhang, R.Y., 2000. Into the forbidden zone. Science 287, 1215–1216.
Liou, J.G., Tsujimori, T., Zhang, R.Y., Katayama, I., Maruyama, S., 2004. Global UHP metamorphism and continent subduction/collision. The Himalayan model. International Geology Review 46, 1–27.
Liou, J.G., Zhang, R.Y., Ernst, W.G., 2007. Very-high-pressure orogenic garnet peridotites. Proceedings of the National Academy of Sciences 104, 9116–9121.
Litasov, K.D., Ohtani, E., 2003. Stability of various hydrous phases in CMAS pyrolite–H_2O system up to 25 GPa. Physics and Chemistry of Minerals 30, 147–156.
Litasov, K.D., Ohtani, E., 2007. Effect of water on the phase relations in Earth's mantle and deep water cycle. In: Ohtani, E. (Ed.), Advances in High-Pressure Mineralogy. Geological Society of America Special Paper 421, pp. 115–156.
Liu, F.L., Xue, H.M., 2007. Geochemical characteristics and SHRIMP U-Pb dating of metamorphic zircons from allanite-bearing para- and ortho-gneiss in Sulu ultrahigh-pressure metamorphic (UHP) belt. Acta Petrologica Sinica 23, 3137–3153 (in Chinese with English abstract).
Liu, F., Xu, Z., Katayama, I., Yang, J.S., Maruyama, S., Liou, J.G., 2001. Mineral inclusions in zircons of para- and orthogneiss from pre-pilot drillhole CCSD-PP1, Chinese continental scientific drilling project. Lithos 59, 199–215.
Liu, F., Xu, Z., Liou, J.G., Katayama, I., Masago, H., Maruyama, S., Yang, J.S., 2002a. Ultrahigh-pressure mineral inclusions in zircons from gneissic core samples of the Chinese continental scientific drilling site in eastern China. European Journal of Mineralogy 14, 499–512.
Liu, L., Sun, Y., Xiao, P.X., Chen, Z.C., Luo, J.H., Chen, D.L., Wang, Y., Zhang, A.D., 2002b. Discovery of ultrahigh-pressure magnesite-bearing garnet lherzolite (>3.8 GPa) in the Altyn Tagh, Northwest China. Chinese Science Bulletin 47, 881–886.
Liu, F., Xu, Z., Liou, J.G., Song, B., 2004a. SHRIMP U–Pb ages of ultrahigh-pressure and retrograde metamorphism of gneissic rocks, southwestern Sulu terrane, eastern China. Journal of Metamorphic Geology 22, 315–326.
Liu, F., Xu, Z., Xue, H., 2004b. Tracing the protolith, UHP metamorphism, and exhumation ages of orthogneiss from the SW Sulu terrane (eastern China): SHRIMP U–Pb dating of mineral inclusion-bearing orthogneiss. Lithos 78, 411–429.
Liu, X.C., Jahn, B.M., Liu, D.Y., Dong, S.W., Li, S.Z., 2004c. SHRIMP U–Pb zircon dating of a metagabbro and eclogites from western Dabieshan (Hong'an block), China, and its tectonic implications. Tectonophysics 394, 171–192.
Liu, F., Liou, J.G., Xu, Z., 2005. U–Pb SHRIMP ages recorded in the coesite-bearing zircon domains of paragneisses in the southwestern Sulu terrane, eastern China. New interpretation. American Mineralogist 90, 790–800.
Liu, F., Liou, J.G., Xue, H., 2006a. Identification of UHP and non-UHP orthogneisses in the Sulu UHP terrane (eastern China). Evidences from SHRIMP U–Pb dating on mineral inclusion-bearing zircons. International Geology Review 48, 1067–1086.
Liu, F., Gerdes, A., Liou, J.G., Xue, H., Liang, F.H., 2006b. SHRIMP U–Pb zircon dating from Sulu–Dabie dolomitic marble, eastern China: constraints on the prograde, UHP and retrograde metamorphic ages. Journal of Metamorphic Geology 24, 569–589.
Liu, D., Jian, P., Kröner, A., Xu, F.T., 2006c. Dating of prograde metamorphic events deciphered from episodic zircon growth in rocks of the Dabie–Sulu UHP complex, China. Earth and Planetary Sciences Letters 250, 650–666.
Liu, X.W., Jin, Z.M., Green, H.W., 2007a. Clinoenstatite exsolution in diopsidic augite of Dabieshan: garnet peridotite from depth of 300 km. American Mineralogist 92, 546–552.
Liu, Y.C., Li, S.G., Xu, S.T., 2007b. Zircon SHRIMP U–Pb dating for gneisses in northern Dabie high *T*/*P* metamorphic zone, central China: implications for decoupling with subducted continental crust. Lithos 96, 170–185.
Liu, F., Xu, Z., Liou, J.G., Dong, H., Xue, H., 2007c. Ultrahigh-pressure mineral assemblages in zircons from surface to 5158 m depth cores in the main drill hole of Chinese continental scientific drilling project, southwestern Sulu belt, China. International Geological Review 49, 454–478.
Liu, L., Zhang, J., Green, H.W., Jin, Z., Bozhilov, K.N., 2007d. Evidence of former stishovite in metamorphosed sediments, implying subduction to >350 km. Earth and Planetary Sciences Letters 263, 180–191.
Liu, F., Gerdes, A., Zeng, L., Xue, H., 2008a. SHRIMP U–Pb dating, trace elements and the Lu–Hf isotope system of coesite-bearing zircon from amphibolite in the SW Sulu UHP terrane, eastern China. Geochimica et Cosmochimica Acta 72, 2973–3000.
Liu, Y.S., Zong, K., Kellemen, B., Gao, S., 2008b. Geochemistry and magmatic history of eclogites and ultramafic rocks from the Chinese continental scientific drill hole: subduction and ultrahigh-pressure metamorphism of lower crustal cumulates. Chemical Geology 247, 133–153.
Lu, Z., Zhang, L., Du, J., Bucher, K., 2008. Coesite inclusions in garnet from eclogitic rocks in western Tianshan, NW China: convincing proof of deep subduction. American Mineralogist 93, 1845–1850.
Luth, R.W., 1997. Experimental study of the system phlogopite-diopside from 3.4–17 GPa. American Mineralogist 82, 1198–1209.
Mackenzie, J.M., Canil, D., Johnston, S.T., English, J., Mihalynuk, M.G., Grant, B., 2005. First evidence for ultrahigh-pressure garnet peridotite in the North American Cordillera. Geology 33, 105–108.
Malaspina, N., Hermann, J., Scambelluri, M., 2008. Fluid/mineral interaction in UHP garnet peridotite. Lithos. doi: 10.1016/j.lithos.2008.07.006.
Martens, U., Mattinson, C.G., Wooden, J., Liou, J.G., 2007. Protolith and metamorphic ages of gneiss hosting eclogite in the Chuacús complex, Central Guatemala, Eos Trans. AGU, vol. 88, no. 23. Joint Assembly Supplement Abstract U53A-08.
Maruyama, S.M., Liou, J.G., 1998. Initiation of UHP metamorphism and its significance on the Proterozoic/Phanerozoic boundary. Island Arc 7, 6–35.
Maruyama, S., Liou, J.G., 2005. From Snowball to Phanerozoic Earth. International Geology Review 47, 775–791.
Maruyama, S., Liou, J.G., Terabayashi, M., 1996. Blueschists and eclogites of the world, and their exhumation. International Geology Review 38, 485–594.
Masago, H., Rumble, D., Ernst, W.G., Parkinson, C., Maruyama, S., 2003. ^{18}O depletion in eclogites from the Kokchetav massif, northern Kazakhstan. Journal of Metamorphic Geology 21, 579–587.
Massonne, H.J., 1999. A new occurrence of microdiamonds in quartzofeldspathic rocks of the Saxonian Erzgebirge, Germany, and their metamorphic evolution. In: Proceedings of 7th International Kimberlite Conference, Capetown, vol. 2, pp. 533–539.
Massonne, H.J., 2001. First find of coesite in the ultrahigh-pressure metamorphic region of the Central Erzgebirge, Germany. European Journal of Mineralogy 13, 565–570.
Massonne, H.J., Bautsch, H.J., 2002. An unusual garnet pyroxenite from the Granulitgebirge, Germany: origin in the transition zone (>400 km depths) or in a shallower upper mantle region? International Geology Review 14, 779–796.
Massonne, H.J., Nasdala, L., 2003. Characterization of an early metamorphic stage through inclusions in zircon of a diamondferous quartzofeldspathic rock from the Erzgebirge, Germany. American Mineralogist 88, 883–889.
Massonne, H.J., O'Brien, P.J., 2003. The Bohemian Massif and the NW Himalaya. In: Carswell, D.A., Compagnoni, R. (Eds.), Ultra-High Pressure Metamorphism. European Mineralogical Union, Notes in Mineralogy, vol. 5, pp. 145–188.
Massonne, H.J., Kennedy, A., Nasdala, L., Theye, T., 2007. Dating of zircon and monazite from diamondiferous quartzofeldspathic rocks of the Saxonian Erzgebirge-hints at burial and exhumation velocities. Mineralogical Magazine 71, 407–425.
Mathez, E.A., Fogel, R.A., Hutcheon, I.D., 1995. Carbon isotopic composition and origin of SiC from kimberlites of Yakutia, Russia. Geochemica et Cosmochimica Acta 59, 781–791.
Mattinson, C.G., Zhang, R.Y., Tsujimori, T., Liou, J.G., 2004. Epidote-rich talc-kyanite-phengite eclogites, Sulu terrane, eastern China: P–T–f_{O_2} estimates and the significance of the epidote-talc assemblage in eclogite. American Mineralogist 89, 1772–1783.
Mattinson, C.G., Wooden, J.L., Liou, J.G., Bird, D.K., Wu, C.L., 2006. Age and duration of eclogite-facies metamorphism, North Qaidam HP/UHP terrane, western China. American Journal of Science 306, 683–711.
Mattinson, C.G., Menold, C.A., Zhang, J.X., Bird, D.K., 2007. High- and ultrahigh-pressure metamorphism in the North Qaidam and South Altyn terranes, Western China. International Geology Review 49, 969–995.
McClelland, W.C., Power, E.S., Gilotti, J.A., Mazdab, F.K., Wopenka, B., 2006. U–Pb SHRIMP geochronology and trace-element geochemistry of coesite-bearing zircons, North-East Greenland Caledonides. In: Hacker, B.R., McClelland, W., Liou, J.G. (Eds.), Ultrahigh-Pressure Metamorphism. Deep Continental Subduction. Geological Society of America Special Paper 403, 23–44.
Medaris Jr., L.G., 1980. Petrogenesis of the Lien peridotite and associated eclogites, Almklovdalen, Western Norway. Lithos 13, 339–353.
Medaris Jr., L.G., 1984. A geothermobarometric investigation of garnet peridotites in the Western Gneiss Region of Norway. Contributions to Mineralogy and Petrology 87, 72–86.
Medaris Jr., L.G., 1999. Garnet peridotite in Eurasian HP and UHP terranes: a diversity of origins and thermal histories. International Geology Review 41, 799–815.
Medaris Jr., L.G., Carswell, D.A., 1990. The petrogenesis of Mg–Cr garnet peridotites in European metamorphic belts. In: Carswell, D.A. (Ed.), Eclogite Facies Rocks. Chapman and Hall, New York, pp. 260–290.
Medaris Jr., L.G., Wang, H., Jelinek, E., Mihaljevic, M., Jakes, P., 2005. Characteristics and origins of diverse Variscan peridotites in the Gfohl nappe, Bohemian Massif, Czech Republic. Lithos 82, 1–23.
Medaris Jr., L.G., Beard, B.L., Jelinek, E., 2006. Mantle-derived, UHP garnet pyroxenite and eclogite in the Moldanubian Gfohl Nappe, Bohemian Massif: A geochemical review, new P-T determinations, and tectonic interpretation. International Geology Review 48, 765–777.
Menneken, M., Nemchin, A.A., Geisler, T., Pidgeon, R.T., Wilde, S.A., 2007. Hadean diamonds in zircon from Jack Hills, Western Australia. Nature 448, 917–920.
Mizukami, T., Wallis, S.R., Yamamoto, J., 2004. Natural examples of olivine lattice preferred orientation patterns with a flow-normal *a*-axis maximum. Nature 427, 432–436.
Monteleone, B.D., Baldwin, S.L., Webb, L.E., Fitzgerald, G., Grove, M., Schmitt, A.K., 2007. Late Miocene–Pliocene eclogite facies metamorphism. D'Entrecasteaux Islands, SE Papua New Guinea. Journal of Metamorphic Geology 25, 245–266.
Mosenfelder, J.L., Schertl, H.-P., Smyth, J., Liou, J.G., 2005. Factors in the preservation of coesite: the importance of fluid infiltration. American Mineralogist 90, 779–789.

Mposkos, E.D., Kostopoulos, D.K., 2001. Diamond, former coesite, and supersilicic garnet in metasedimentary rocks from the Greek Rhodope: a new ultrahigh-pressure metamorphic province established. Earth and Planetary Science Letters 192, 497–506.

Mposkos, E.D., Baziotis, I., Proyer, A., Hoinkes, G., 2006. Dolomitic marbles from the ultrahigh-pressure metamorphic Kimi complex in Rhodope, NE Greece. Mineralogy and Petrology 88, 341–362.

Mukherjee, B.K., Sachan, H.K., Ogasawara, Y., Muko, A., Yoshioka, N., 2003. Carbonate-bearing UHPM rocks from the Tso-Morari region, Ladakh, India: petrological implications. International Geology Review 45, 49–69.

Muko, A., Okamoto, K., Yoshioka, N., Zhang, R.Y., Parkinson, C.D., Ogasawara, Y., Liou, J.G., 2002. Petrogenesis of Ti-clinohumite-bearing garnetiferous ultramafic rocks from Kumdy-kol. In: Parkinson et al. (Eds.), The Diamond-bearing Kokchetav Massif, Kazakhstan: Petrochemistry and Tectonic Evolution of an Unique Ultrahigh-pressure Metamorphic Terrane. Universal Academy Press, Inc., Tokyo, Japan, pp. 343–360.

Murakami, M., Hirose, K., Yurimoto, H., Nakashima, S., 2002. Water in the Earth's lower mantle. Science 295, 1885–1887.

Nakano, N., Osanai, Y., Owada, M., Tguchi, S., Hodada, T., Nam, T.N., 2006. Ultrahigh-pressure metamorphism recorded in ultrahigh-temperature mafic granulite from the Kontum Massif, central Vietnam. 2006 International Mineralogical Association Meeting, Abstract Volume, p. 212.

Nakano, N., Osanai, Y., Owada, M., 2007. Multiple breakdown and chemical equilibrium of silicic clinopyroxene under extreme metamorphic conditions in the Kontum Massif, central Vietnam. American Mineralogist 92, 1844–1855.

O'Brien, P.J., 2006. The age of deep, steep continental subduction in the NW Himalaya: relating zircon growth to metamorphic history: comment. Earth and Planetary Science Letters 245, 814–816.

O'Brien, P.J., Rötzler, J., 2003. High-pressure granulites: formation, recovery of peak conditions, and implications for tectonics. Journal of Metamorphic Geology 21, 3–20.

O'Brien, P.J., Sachan, H.K., 2000. Diffusion modeling in garnet from Tso Morarj eclogite and implications for exhumation models. Earth Science Frontiers 7, 25–27.

O'Brien, P.J., Ziemann, M.A., 2008. Preservation of coesite in exhumed eclogite: insights from Raman mapping. European Journal of Mineralogy 20, 827–834.

O'Brien, P.J., Zotov, N., Law, R., Khan, M.A., Jan, M.Q., 2001. Coesite in Himalayan eclogite and implications for models of India–Asia collision. Geology 29, 435–438.

Ogasawara, Y., 2005. Microdiamonds in ultrahigh-pressure metamorphic rocks. Elements 1, 91–96.

Ogasawara, Y., Ohta, M., Fukasawa, K., Katayama, I., Maruyama, S., 2000. Diamond-bearing and diamond-free metacarbonate rocks from Kumdy-Kol in the Kokchetav massif, northern Kazakhstan. The Island Arc 9, 400–416.

Ogasawara, Y., Fukasawa, K., Maruyama, S., 2002. Coesite exsolution from supersilicic titanite in UHP marble from the Kokchetav Massif, northern Kazakhstan. American Mineralogist 87, 454–461.

Ohtani, E., 2005. Water in the mantle. Elements 1, 25–30.

Okay, A.I., 1993. Petrology of a diamond and coesite-bearing metamorphic terrain: Dabie Shan, China. European Journal of Mineralogy 5, 659–673.

Okamoto, K., Katayama, I., Maruyama, S., Liou, J.G., 2006. Zircon-inclusion mineralogy of a diamond-grade eclogites from the Kokchetav Massif, Northern Kazakhstan. International Geology Review 48, 882–891.

Ono, S., 1998. Stability limits of hydrous minerals in sediment and mid-oceanic ridge basalt compositions: implications for water transport in subduction zones. Journal of Geophysics Research 103, 18253–18267.

O'Reilly, S.Y., Griffin, W.L., 2006. Imaging global chemical and thermal heterogeneity in the subcontinental lithospheric mantle with garnets and xenoliths: geophysical implications. Tectonophysics 416, 289–309.

O'Reilly, S.Y., Griffin, W.L., Poudjom Djomani, Y., Morgan, P., 2001. Are lithospheres forever? Geological Society of America Today 11, 4–9.

Ortega-Gutiérrez, F., Solari, L.A., Solé, J., Martens, U., Gómez-Tuena, A., Morán-Ical, S., Reyes-Salas, M., Ortega-Obregón, C., 2004. Polyphase, high-temperature eclogite-facies metamorphism in the Chuacús Complex, Central Guatemala: petrology, geochronology, and tectonic implications. International Geology Review 46, 445–470.

Ortega-Obregón, C., Solari, L.A., Kepple, J.S., Ortega-Gutierrez, F., Sole, J., Moranlcal, S., 2008. Middle-Late Ordovician magmatism and Late Cretaceous collision in the southern Maya block, Rabinal-Salama area, central Guatemala: implications for North American–Caribbean plate tectonics. Geological Society of America Bulletin 120, 556–570.

Ota, T., Terabayashi, M., Katayama, I., 2004. Thermobaric structure and metamorphic evolution of the Iratsu eclogite body in the Sanbagawa belt, central Shikoku, Japan. Lithos 73, 95–126.

Ota, T., Kobayashi, K., Kunihiro, T., Nakamura, E., 2008. Boron cycling by subducted lithosphere; insights from diamondiferous tourmaline from the Kokchetav ultrahigh-pressure metamorphic belt. Geochemica et Cosmochemica Acta 72, 3531–3541.

Page, F.Z., Essene, E.J., Mukasa, S.B., 2005. Quartz exsolution in clinopyroxene is not proof of ultrahigh pressures: evidence from eclogites from the Eastern Blue Ridge, southern Appalachians. USA American Mineralogist 90, 1092–1099.

Palmeri, R., Ghiribelli, B., Talarico, F., Ricci, C.A., 2003. Ultrahigh-pressure metamorphism in felsic rocks: the garnet-phengite gneisses and quartzites from the Lanterman Rnage, Antarctica. European Journal of Mineralogy 15, 513–525.

Palmeri, R., Ghiribelli, B., Ranalli, G., Talarico, F., Ricci, C.A., 2007. Ultrahigh-pressure metamorphism and exhumation of garnet-bearing ultramafic rocks from the Lanterman Range (northern Victoria Land, Antarctica). Journal of Metamorphic Geology 25, 225–243.

Parkinson, C.D., Katayama, I., 1999. Metamorphic microdiamond and coesite from Sulawesi, Indonesia: evidence of deep subduction as SE Sundaland Margin. EOS, Transaction American Geophysics Union (abstract) F1181.

Parkinson, C.D., Miyazaki, K., Wakita, K., Barber, A.J., Carswell, D.A., 1998. An overview and tectonic synthesis of the very high pressure and associated rocks of Sulawesi, Java and Kalimanta, Indonesia. Island Arc 7, 184–200.

Parkinson, C.D., Motoki, A., Onishi, C.T., Maruyama, S., 2001. Ultrahigh-pressure pyrope-kyanite granulites and associated eclogites in Neoproterozoic Nappes of Southeast Brazil. UHPM Workshop 2001, Waseda University, pp. 87–90.

Parkinson, C.D., Katayama, I., Liou, J.G., Maruyama, S., 2002. The Diamond-bearing Kokchetav Massif. Kazakhstan: Petrochemistry and Tectonic Evolution of a Unique Ultrahigh-pressure Metamorphic Terrane. Universal Academy Press Inc., Tokyo, Japan. 527pp.

Parrish, R.R., Gough, S.J., Searle, M.P., Waters, D.J., 2006. Plate velocity exhumation of ultrahigh-pressure eclogites in the Pakistan Himalaya. Geology 34, 989–992.

Pawley, A.R., McMillan, P.F., Holloway, J.R., 1993. Hydrogen in stishovite, with implications for mantle water content. Science 261, 1024–1026.

Perraki, M., Proyer, A., Mposkos, E., Kaindl, R., Hoinkes, G., 2006. Raman micro-spectroscopy on diamond, graphite and other carbon polymorphs from the ultrahigh-pressure metamorphic Kimi Complex of the Rhodope Metamorphic Province, NE Greece. Earth and Planetary Science Letters 241, 672–685.

Pindell, J.L., Kennan, L., Maresch, W.V., Stanek, K.P., Draper, G., Higgs, R., 2005. Plate-kinematics and crustal dynamics of circum-Caribbean arc–continent interactions: tectonic controls on basin development in proto-Caribbean margins. In: Avé Lallemant, H.G., Sisson, V.B. (Eds.), Caribbean–South American plate interactions, Venezuela. Geological Society of America Special Paper 394, 7–52.

Poli, S., Schmidt, M.W., 2002. Petrology of subducted slabs. Annual Review of Earth and Planetary Science 30, 207–235.

Pullen, A., Kapp, P., Gehrels, G.E., Vervoort, J.D., Ding, L., 2008. Triassic continental subduction in central Tibet and Mediterranean-style closure of the Paleo-Tethys Ocean. Geology 36, 351–354.

Qi, X.X., Yang, J.S., Xu, Z.Q., Bai, W.J., Zhang, Z.M., Fang, Q.S., 2007. Discovery of moissanite in retrogressive eclogite from the pre-pilot hole of the Chinese continental scientific drilling project (CCSD-PP2) and its geological implication. Acta Petrologica Sinica 23, 3207–3214 (in Chinese with English abstract).

Ragozin, A.L., Liou, J.G., Shatsky, V.S., Sobolev, N.V., 2009. The timing of retrograde partial melting in the Kumdy-Kol region. Lithos 109, 274–284.

Reinecke, T., 1991. Very-high-pressure metamorphism and uplift of coesite-bearing metasediments from the Zermatt-Saas zone, Western Alps. European Journal of Mineralogy 3, 7–17.

Reisberg, L., Zindler, A., Jagoutz, E., 1989. Further Sr and Nd isotopic results from peridotites of the Ronda ultramafic complex. Earth and Planetary Science Letters 96, 161–180.

Reverdatto, V.V., Selyatitskiy, A.Y., Carswell, D.A., 2008. Geochemical distinction between "crustal" and mantle-derived peridotites/pyroxenites in high/ultrahigh pressure metamorphic complexes. Russian Geology and Geophysics 49, 73–90.

Ringwood, A.E., Major, A., 1971. Synthesis of majorite and other high pressure garnets and perovskites. Earth and Planetary Science Letters 12, 411–448.

Risold, A.C., Trommsdorff, V., Groberty, B., 2001. Genesis of ilmenite rods and palisades along humite type defects in olivine from Alpe Arami. Contributions to Mineralogy and Petrology 140, 619–628.

Rosenfeld, J.H., 1993. Sedimentary rocks of the Santa Cruz Ophiolite, Guatemala – a proto-Caribbean history. In: Pindell, J.L., Perkins, R.F. (Eds.), Mesozoic and Early Cenozoic development of the Gulf of Mexico and Caribbean Region – A Context for Hydrocarbon Exploration: Selected Papers Presented at the GCSSEPM Foundation Thirteenth Annual Research Conference, Gulf Coast Section SEPM, pp. 173–180.

Rubatto, D., 2002. Zircon trace element geochemistry: partitioning with garnet and the link between U–Pb ages and metamorphism. Chemical Geology 184, 123–138.

Rubatto, D., Hermann, J., 2001. Exhumation as fast as subduction? Geology 29, 3–6.

Rubatto, D., Hermann, J., 2007. Zircon behavior in deeply subducted rocks. Elements 3, 31–36.

Rumble, D., Giorgis, D., Oreland, T., Zhang, Z.M., Xu, H.F., Yui, T.F., Yang, J.S., Xu, Z.Q., Liou, J.G., 2002. Low $\delta^{18}O$ zircons, U–Pb dating, and the age of the Qinglongshan oxygen and hydrogen isotope anomaly near Donghai in Jiangsu province, China. Geochimica et Cosmochimica Acta 66, 2299–2306.

Rumble, D., Liou, J.G., Jahn, B.M., 2003. Continental crust subduction and UHP metamorphism. In: Rudnick, R.L. (Ed.), The Crust, Treatise on Geochemistry, vol. 3. In: Holland, H.D., Turekian, K.K. (Eds.). Elsevier, Oxford, pp. 293–320.

Sachan, H.K., Mucherjee, B.K., Ogasawara, Y., Maruyama, S., Ishida, H., Muko, A., Yoshioka, N., 2004. Discovery of coesite from Indus Suture Zone (TSZ), Ladakh, India: evidence for deep subduction. European Journal of Mineralogy 16, 235–240.

Scambelluri, M., Pettke, T., van Roermund, H.L.M., 2008. Majoritic garnets monitor deep subduction fluid flow and mantle dynamics. Geology 36, 59–62.

Schmädicke, E., 1991. Quartz pseudomorphs after coesite in eclogites from the Saxonian Erzgebirge. European Journal of Mineralogy 3, 231–238.

Schmädicke, E., Evans, B.W., 1997. Garnet-bearing ultramafic rocks from the Erzgebirge, and their relation to other settings in the Bohemian Massif. Contributions to Mineralogy and Petrology 127, 57–74.

Schmädicke, E., Mezger, K., Cosca, M.A., Okrusch, M., 1995. Variscan Sm–Nd and Ar–Ar ages of eclogite facies rocks from the Erzgebirge, Bohemian Massif. Journal of Metamorphic Geology 13, 537–552.

Schmidt, M.W., Poli, S., 1998. Experimentally based water budgets for dehydrating slabs and consequences for arc magma generation. Earth and Planetary Science Letters 163, 361–379.

Schmidt, A., Weyer, S., Mezger, K., Scherer, E.E., Xiao, Y., Hoefs, J., Brey, G.P., 2008. Rapid eclogitisation of the Dabie–Sulu UHP terrane: constraints from Lu–Hf garnet geochronology. Earth and Planetary Science Letters 273, 203–213.

Schneider, J., Bosch, D., Monie, P., Guillot, S., Carcía-Casco, A., Lardeaux, J.M., Torres-Roldán, L., Trujillo, G.M., 2004. Origin and evolution of the Escambray Massif (Central Cuba): an example of HP/LT rocks exhumed during intraoceanic subduction. Journal of Metamorphic Geology 22, 227–247.

Sharp, T.G., El Goresy, A., Wopenka, B., Chen, M., 1999. A post-stishovite SiO_2 polymorph in the Meteorite Shergotty: implications for impact events. Science 284, 1511–1513.

Shatsky, V.S., Sobolev, N.V., 2003. Reviews of representative UHPM terranes: the Kokchetav massif, Kazakhstan. In: Carswell, D.A., Compagnoni, R. (Eds.), Ultra-High Pressure Metamorphism. European Mineralogical Union, Notes in Mineralogy, vol. 5, pp. 75–104.

Shatsky, V.S., Sobolev, N.V., Vavilov, M.A., 1995. Diamond-bearing metamorphic rocks of the Kokchetav massif, N Kazakhstan. In: Coleman, R.G., Wang, X. (Eds.), Ultrahigh Pressure Metamorphism. Cambridge University Press, pp. 427–455.

Shimizu, R., Ogasawara, Y., 2005. Discovery of K-tourmaline in diamond-bearing quartz-rich rock from the Kokchetav Massif, Kazakhstan. Mitt Oterr Miner Ges 150, 141.

Smith, D.C., 1984. Coesite in clinopyroxene in the Caledonides and its implications for geodynamics. Nature 310, 641–644.

Sobolev, N.V., Shatsky, V.S., 1990. Diamond inclusions in garnets from metamorphic rocks: a new environment for diamond formation. Nature 343, 742–746.

Song, S.G., Yang, J.S., Xu, Z.Q., Liou, J.G., Shi, R.D., 2003a. Metamorphic evolution of eclogites in the Dulan ultrahigh-*P* metamorphic terrane and tectonic implications, North Qaidam, NW China. Journal of Metamorphic Geology 21, 631–644.

Song, S.G., Yang, J.S., Liou, J.G., Wu, C.L., Shi, R.D., Xu, Z.Q., 2003b. Petrology, geochemistry and isotopic ages of eclogites from the Dulan UHPM terrane, the North Qaidam, NW China. Lithos 70, 195–211.

Song, S.G., Zhang, L., Niu, Y., 2004. Ultra-deep origin of garnet peridotite from the North Qaidam ultrahigh-pressure belt, Northern Tibetan Plateau, NW China. American Mineralogist 89, 1330–1336.

Song, S.G., Zhang, L.F., Chen, J., Liou, J.G., Niu, Y.L., 2005a. Sodic amphibole exsolutions in garnet from garnet-peridotite, North Qaidam UHPM belt, NW China: Implications for ultradeep-origin and hydroxyl defects in mantle garnets. American Mineralogist 90, 814–820.

Song, S.G., Zhang, L., Niu, Y., Su, L., Jian, P., Liu, D., 2005b. Geochronology of diamond-bearing zircons from garnet peridotite in the North Qaidam UHPM belt, Northern Tibetan Plateau: a record of complex histories from oceanic lithosphere subduction to continental collision. Earth and Planetary Science Letters 234, 99–118.

Song, S.G., Zhang, L.F., Niu, Y., Su, L., Song, B., Liu, D.Y., 2006. Evolution from oceanic subduction to continental collision: a case study of the Northern Tibetan Plateau inferred from geochemical and geochronological data. Journal of Petrology 47, 435–455.

Song, S.G., Su, L., Niu, Y., Zhang, L.F., 2007. Petrological and geochemical constraints on the origin of Garnet Peridotite in the North Qaidam ultrahigh-pressure Metamorphic Belt, Northwestern China. Lithos 96, 243–265.

Spengler, D., van Roermund, H.L.M., Drury, M.R., Ottolini, L., Mason, R.D., Davies, G.R., 2006. Deep orogen and hot melting of an Archaean orogenic peridotite massif in Norway. Nature 440, 913–917.

Stöckhert, B., Duyster, J., Trepmann, C., Massonne, H.J., 2001. Microdiamond daughter crystals precipitated from supercritical COH + silicate fluids included in garnet, Erzegebirge, Germany. Geology 29, 391–394.

Sun, S.S., McDonough, W.F., 1989. Chemical and isotopic systematics of oceanic basalts: implications for mantle composition and processes. In: Sanders, A.D. and Norry, M.J. (Eds.), Magmatism in the Ocean Basins. Geological Society of London Special Publication 42, 313–346.

Tagiri, M., Yano, T., Bakirov, A., Nakajima, T., Uchiumi, S., 1995. Mineral parageneses and metamorphic *P–T* paths of ultrahigh-pressure eclogites from Kyrghyzstan Tien-Shan. The Island Arc 4, 280–292.

Tang, J., Zheng, Y.-F., Gong, B., Wu, Y.-B., Gao, T.-S., Yuan, H.L., Wu, F.-Y., 2008a. Extreme oxygen isotope signature of meteoric water in magmatic zircon from metagranite in the Sulu orogen, China: implications for Neoproterozoic rift magmatism. Geochimica et Cosmochimica Acta 72, 3139–3169.

Tang, J., Zheng, Y.-F., Wu, Y.-B., Gong, B., Zha, X.P., Liu, X.-M., 2008b. Zircon U–Pb age and geochemical constraints on the tectonic affinity of the Jiaodong terrane in the Sulu orogen, China. Precambrian Research 161, 389–418.

Terabayashi, M., Okamoto, K., Yamamoto, H., Kaneko, Y., Ota, T., Maruyama, S., Komia, T., Ishikawa, A., Anama, R., Ozawa, H., Windley, B., Liou, J.G., 2005. Accretionary complex origin of the mafic–ultramafic bodies of the Sanbagawa belt, central Shikoku, Japan. International Geology Review 47, 1058–1073.

Terry, M.P., Robinson, P., Krogh Ravana, E.J., 2000. Kyanite eclogite thermobarometry and evidence for thrusting of UHP over HP metamorphic rocks, Nordoyane, Western Gneiss Region, Norway. American Mineralogist 85, 1637–1650.

Treloar, J., O'Brien, J., Parrish, R.R., Khan, M.A., 2003. Exhumation of early Tertiary coesite-bearing eclogites from the Pakistan Himalaya. Journal of the Geological Society of London 160, 367–376.

Tsai, C.-H., Liou, J.G., 2000. Eclogite-facies relics and inferred ultrahigh-pressure metamorphism in the North Dabie Complex, central-eastern China. American Mineralogist 85, 1–8.

Tsujimori, T., Sisson, B., Liou, J.G., Harlow, G.E., Sorensen, S.S., 2006a. Very low-temperature record in subduction process: a review of global lawsonite-eclogites. Lithos 92, 609–624.

Tsujimori, T., Sisson, V.B., Liou, J.G., Harlow, G.E., Sorensen, S.S., 2006b. Petrologic characterizations of Guatemalan lawsonite-eclogite: direct information on eclogitization of subducted oceanic crust in a cold subduction zone. In: Hacker, B.R., McClelland, W., Liou, J.G. (Eds.), Ultrahigh-Pressure Metamorphism: Deep Continental Subduction. Geological Society of America Special Paper 403, 147–168.

Ulmer, R., Stalder, R., 2001. The Mg(Fe)SiO_3 orthoenstatite–clinoenstatite transitions at high pressure and temperature determined by Raman-spectroscopy on quenched samples. American Mineralogist 86, 1267–1274.

Ulmer, P., Trommsdorff, V., 1997. Titanium content of mantle olivine: an experimental study to 10 GPa. Terra Nova 9, 39.

Ulmer, P., Trommsdorff, V., 1999. Phase relations of hydrous mantle subducting to 300 km. Geochemical Society of London Special Publication 6, 1–23.

Usui, T., Nakamura, E., Kobayashi, K., Maruyama, S., 2003. Fate of the subducted Farallon plate inferred from eclogite xenoliths in the Colorado Plateau. Geology 31, 589–592.

Usui, T., Nakamura, E., Helmstaedt, H., 2006. Petrology and geochemistry of eclogite xenoliths from the Colorado plateau: implications for the evolution of subducted oceanic crust. Journal of Petrology 47, 929–964.

van Roermund, H.L.M., Drury, M.R., 1998. Ultra-high pressure ($P > 6$ Gpa) garnet peridotites in western Norway: exhumation of mantle rocks from >185 km depth. Terra Nova 10, 295–301.

van Roermund, H.L.M., Drury, M.R., Barnhoom, A., Ronde, A., 2000. Super-silicic garnet microstructures from an orogenic garnet peridotite, evidence for an ultra-deep, >6 GPa origin. Journal of Metamorphic Geology 18, 135–148.

van Roermund, H.L.M., Carswell, D.A., Drury, M.R., Heijboer, T.C., 2002. Microdiamonds in a megacrystic garnet websterite pod from Bardane on the island of Fjortoft, western Norway: evidence for diamond formation in mantle rocks during deep continental subduction. Geology 30, 959–962.

Wain, A., 1997. New evidence for coesite in eclogite and gneisses: defining an ultrahigh-pressure province in the Western Gneiss Region of Norway. Geology 25, 927–930.

Wan, Y.S., Li, R.W., Wilde, S.A., Liu, D.Y., Chen, Z.Y., Yan, L.L., Song, T.R., Yin, X.Y., 2005. UHP metamorphism and exhumation of the Dabie Orogen, China: evidence from SHRIMP dating of zircon and monazite from a UHP granitic gneiss cobble from the Hefei Basin. Geochimica et Cosmochimica Acta 69, 4333–4348.

Wei, C.J., Powell, R., Zhang, L.F., 2003. Eclogites from the south Tianshan, NW China: petrological characteristic and calculated mineral equilibria in the Na_2O–CaO–FeO–MgO–Al_2O_3–SiO_2–H_2O system. Journal of Metamorphic Geology 21, 163–180.

Wu, X.-L., Meng, D.-W., Hanm, Y.-J., 2005. α-PbO_2-type nanophase of TiO_2 from coesite-bearing eclogite in the Dabie Mountains, China. American Mineralogist 90, 1458–1461.

Wu, Y.-B., Zheng, Y.-F., Zhao, Z.-F., Gong, B., Liu, X.-M., Wu, F.-Y., 2006. U–Pb, Hf and O isotope evidence for two episodes of fluid-assisted zircon growth in marble-hosted eclogites from the Dabie orogen. Geochimica et Cosmochimica Acta 70, 3743–3761.

Wu, Y.-B., Zheng, Y.-F., Tang, J., Gong, B., Zhao, Z.-F., Liu, X.M., 2007. Zircon U–Pb dating of water–rock interaction during Neoproterozoic rift magmatism in South China. Chemical Geology 246, 65–86.

Wunder, B., 1998. Equilibrium experiments in the system MgO ± SiO_2 ± H_2O (MSH); stability fields of clinohumite-OH [$Mg_9Si_4O_{16}(OH)_2$], chondrodite-OH [$Mg_5Si_4(OH)_2$] and phase A ($Mg_7Si_2O_8(OH)_6$). Contributions to Mineralogy and Petrology 132, 111–120.

Wunder, B., Rubie, C., Ross II, C.R., Medenbach, O., Seifert, E., Schreyer, W., 1993. Synthesis, stability, and properties of $Al_2SiO_4(OH)_2$: a fully hydrated analogue of topaz. American Mineralogist 78, 285–297.

Xia, Q.X., Zheng, Y.F., Zhou, I.G., 2008. Dehydration and melting during continental collision: constraints from element and isotope geochemistry of low-T/UHP granitic gneiss in the Dabie orogen. Chemical Geology 247, 36–65.

Xu, S.-T., Okay, A.I., Ji, S.-Y., Sengor, A.M.C., Su, W., Liu, Y.-C., Jiang, L.-L., 1992. Diamond from the Dabie Shan metamorphic rocks and its implication for tectonic setting. Science 256, 80–82.

Xu, S.-T., Liu, Y.-C., Chen, G.-B., Ji, S.-Y., Ni, P., Xiao, W.-S., 2005. Microdiamonds, their classification and tectonic implications for the host eclogites from the Dabie and Su-Lu regions in central eastern China. Mineralogical Magazine 69, 509–520.

Xu, S.T., Wu, W.P., Xiao, W.S., 2006a. Natural moissanite from southern Dabie Mountains. Acta Petrological et Mineralogica 25, 314–322.

Xu, Z., Zeng, L., Zhang, Z., Liu, F., Yang, J., Chen, F., Liang, F., McWilliams, M., Liou, J.G., 2006b. Polyphase structural deformation and a dynamic model for the formation of Sulu high to ultrahigh-pressure (HP–UHP) metamorphic belt: from subduction to exhumation. In: Hacker, B.R., McClelland, W., Liou, J.G.

(Eds.), Deep Continental Subduction. Geological Society of America Special Paper 403, 93–113.

Yamamoto, S., Maruyama, S., Windley, B.F., Omori, S., Shibuya, T., Kawai, T., Sawaki, Y., 2007. An ultrahigh-pressure origin of podiform chromitites in the Ballantrae Complex ophiolite, SW Scotland: silicate exsolution lamellae in chromites. In: 29th International Eclogite Field Symposium in Lochalsh Scotland Programme and Abstracts, p. 126.

Yamamoto, S., Komiya, T., Hirose, K., Maruyama, S., 2009. Coesite and clinopyroxene exsolution lamellae in chromites: in situ ultrahigh-pressure evidence from podiform chromitites in the Luobusa ophiolite, southern Tibet. Lithos 109, 314–322.

Yamato, P., Burov, E., Agard, P., Le Pourhiet, L., Jolivert, L., 2008. HP–UHP exhumation during slow continental subduction: self-consistent thermodynamically and thermomechanically coupled model with application to the Western Alps. Earth and Planetary Sciences Letters 271, 63–74.

Yang, J.J., Jahn, B.M., 2000. Ultra-deep subduction of the Su-Lu garnet peridotite and its isotopic and mineral chemical consequences. Journal of Metamorphic Geology 18, 167–180.

Yang, J.J., Powell, R., 2008. Ultrahigh-pressure garnet peridotites from the devolatilization of sea-floor hydrated ultramafic rocks. Journal of Metamorphic Geology 26, 695–716.

Yang, J.J., Godard, G., Kienast, J.R., Lu, Y., Sun, J., 1993. Ultrahigh-pressure, 60 kbar magnesite-bearing garnet peridotite from Northeastern Jiangsu, China. Journal of Geology 101, 541–554.

Yang, J.S., Xu, Z., Song, S., Zhang, J., Shi, R., Li, H., Brunel, M., 2001. Discovery of coesite in the North Qaidam Early Paleozoic ultrahigh pressure (UHP) metamorphic belt, NW China. Comptes Rendus de l'Academie des Sciences, Paris. Sciences de la Terre et des Planets 333, 719–724.

Yang, J.S., Xu, Z., Dobrzhnestskaya, L.F., Green, H.W., Shi, R., Pei, X., Wu, C., Wooden, J.L., Zhang, J., Li, H., 2003a. Discovery of metamorphic diamond in central China: an indication of a >4000 km-long-zone of deep subduction resulting from multiple continental collisions. Terra Nova 15, 370–379.

Yang, J.S., Wooden, J.L., Wu, C.L., Liu, F.L., Xu, Z.Q., Shi, R.D., Katayama, I., Liou, J.G., Maruyama, S., 2003b. SHRIMP U–Pb dating of coesite-bearing zircons from ultrahigh-pressure metamorphic rocks in the Sulu belt, east China. Journal of Metamorphic Geology 21, 551–560.

Yang, J.S., Bai, W.J., Rong, H., Zhang, Z.M., Xu, Z., Fang, Q.S., Yang, B.G., Li, T.F., Ren, Y.F., Chen, S.Y., Hu, J.Z., Mao, H.K., 2005. Discovery of Fe_2P alloy in garnet peridotite from the Chinese continental scientific drilling project (CCSD) main hole. Acta Petrologica Sinica 21, 271–276 (in Chinese with English abstract).

Yang, J.S., Zhang, R.Y., Li, T-F., Zhang, Z.M., Liou, J.G., 2007a. Petrogenesis of the garnet peridotite and garnet-free peridotite of the Zhimafang ultramafic body in the Sulu ultrahigh pressure metamorphic belt, eastern China. Journal of Metamorphic Geology 25, 187–206.

Yang, J.S., Dobrzhinetskaya, L., Bai, W.J., Fang, Q.S., Robinson, P.T., Zhang, J.F., Green, H.W., 2007b. Diamond- and coesite-bearing chromitites from the Luobusa ophiolite, Tibet. Geology 35, 875–878.

Ye, K., Cong, B.L., Ye, D.N., 2000. The possible subduction of continental material to depths greater than 200 km. Nature 407, 734–736.

Yin, A., Manning, C.E., Lovera, O., Menold, C.A., Chen, X.H., Gehrels, G.E., 2007. Early Paleozoic tectonic and thermomechanical evolution of ultrahigh-pressure (UHP) metamorphic rocks in the northern Tibetan Plateau, northwest China. International Geology Review 49, 681–716.

Yoshino, T., Matsuzaki, T., Yamashita, S., Katsura, T., 2006. Hydrous olivine unable to account for conductivity anomaly at the top of the asthenosphere. Nature 443, 973–976.

Yoshino, T., Manthilake, G., Matsuzaki, T., Katsura, T., 2008. Dry mantle transition zone inferred from the conductivity of wadsleyite and ringwoodite. Nature 451, 326–329.

Yuan, H., Gao, S., Rudnick, R.L., Jin, Z., Liu, Y., Puchtel, I.S., Walker, R.J., Yu, R., 2007. Re–Os evidence for the age and origin of peridotites from the Dabie–Sulu ultrahigh pressure metamorphic belt, China. Chemical Geology 236, 323–338.

Yui, T.F., Rumble, D., Lo, C.H., 1995. Unusually low 18O ultrahigh-pressure metamorphic rocks from Su-Lu terrane China. Geochimica et Cosmochimica Acta 59, 2859–2864.

Zhang, R.Y., Liou, J.G., 1996. Significance of coesite inclusions in dolomite from eclogite in the southern Dabie Mountains, China. American Mineralogist 81, 181–186.

Zhang, R.Y., Liou, J.G., 1997. Transformation of gabbro to coesite-bearing eclogites from Yangkou, the Sulu terrane, eastern China. Journal of Metamorphic Geology 15, 183–202.

Zhang, R.Y., Liou, J.G., 1998. Dual origin of garnet peridotites of the Dabie–Sulu UHP terrane, eastern-central China. Episodes 21, 229–234.

Zhang, R.Y., Liou, J.G., 2003. Clinopyroxene from the Sulu garnet clinopyroxenite, China: origin and evolution of garnet exsolution in clinopyroxene. American Mineralogist 88, 1591–1619.

Zhang, R.Y., Liou, J.G., Cong, B., 1994. Petrogenesis of garnet-bearing ultramafic rocks and associated eclogites in the Su-Lu ultrahigh-pressure metamorphic terrane, China. Journal of Metamorphic Geology 12, 169–186.

Zhang, R.Y., Hirajima, T., Banno, S., Cong, B., Liou, J.G., 1995a. Petrology of ultrahigh-pressure rocks from the southern Sulu region, eastern China. Journal of Metamorphic Geology 13, 659–675.

Zhang, R.Y., Liou, J.G., Cong, B.L., 1995b. Talc-, magnesite- and Ti–clinohumite-bearing ultrahigh-pressure mafic and ultramafic complex in the Dabie Mountains, China. Journal of Petrology 36, 1011–1037.

Zhang, R.Y., Liou, J.G., Tsai, C.H., 1996. Petrogeneses of a high-temperature metamorphic belt: a new tectonic interpretation for the north Dabieshan, Central China. Journal of Metamorphic Geology 14, 319–333.

Zhang, R.Y., Rumble, D., Liou, J.G., Wang, Q.C., 1998. Low $\delta^{18}O$ ultrahigh-P garnet-bearing mafic and ultramafic rocks from Dabie Shan, China. Chemical Geology 150, 161–170.

Zhang, R.Y., Shu, J.F., Mao, H.K., Liou, J.G., 1999. Magnetite lamellae in olivine and clinohumite from Dabie UHP ultramafic rocks, central China. American Mineralogist 84, 564–569.

Zhang, R.Y., Liou, J.G., Yang, J.S., Yui, T.F., 2000. Petrochemical constraints for dual origin of garnet peridotites from the Dabie–Sulu UHP terrane, eastern-central China. Journal of Metamorphic Geology 18, 149–166.

Zhang, J.X., Zhang, Z.M., Xu, Z.Q., Yang, J.S., Cui, J.W., 2001. Petrology and geochronology of eclogites from the western segment of the Altyn Tagh, Northwestern China. Lithos 56, 187–206.

Zhang, R.Y., Shau, Y.H., Liou, J.G., Lo, C.H., 2002a. Discovery of clinoenstatite in garnet pyroxenites from the Dabie–Sulu ultrahigh-pressure terrane, east-central China. American Mineralogist 87, 867–874.

Zhang, R.Y., Liou, J.G., Shau, J.F., 2002b. Hydroxyl-rich topaz in high-pressure and ultrahigh-pressure kyanite quartzites, with retrograde woodhouseite, from the Sulu terrane, eastern China. American Mineralogist 87, 445–453.

Zhang, L., Ellis, D.J., Jiang, W., 2002c. Ultrahigh-pressure metamorphism in western Tianshan, China: Part I. Evidence from inclusions of coesite pseudomorphs in garnet and from quartz exsolution lamellae in omphacite in eclogites. Part II. Evidence from magnesite in eclogite. American Mineralogist 87, 853–860. 860–866.

Zhang, R.Y., Liou, J.G., Ye, K., Yang, J., 2003a. Ultrahigh-pressure metamorphism in the forbidden zone. The Xugou garnet peridotite, Sulu terrane, eastern China. Journal of Metamorphic Geology 21, 539–550.

Zhang, R.Y., Liou, J.G., Zheng, Y.F., Fu, B., 2003b. Transition of UHP eclogites to gneissic rocks of low-grade amphibolite facies during exhumation. Evidence from the Dabie terrane, central China. Lithos 70, 269–291.

Zhang, R.Y., Zhai, S.M., Fei, Y.W., Liou, J.G., 2003c. Titanium solubility in coexisting garnet and clinopyroxene at very high pressure. The significance of exsolved rutile in garnet. Earth and Planetary Science Letters 216, 591–601.

Zhang, L., Ellis, D.J., Arculus, R.J., Jiang, W., 2003d. Forbidden zone' subduction of sediments to 150 km depth – the reaction of dolomite to magnesite + aragonite in the UHPM metapelites from western Tianshan, China. Journal of Metamorphic Geology 21, 523–529.

Zhang, R.Y., Liou, J.G., Yang, J.S., Liu, L., Jahn, B.M., 2004a. Garnet peridotites in UHP mountain belts of China. International Geology Review 46, 981–1004.

Zhang, R.Y., Liou, J.G., Zheng, J.P., 2004b. Ultrahigh-pressure corundum-rich garnetite in garnet peridotite, Sulu terrane, China. Contributions to Petrology and Mineralogy 147, 21–31.

Zhang, R.Y., Yang, J.S., Wooden, J.L., Liou, J.G., Li, T.F., 2005a. U–Pb SHRIMP geochronology of zircon in garnet peridotite from the Sulu UHP terrane, China: implication for mantle metasomatism and subduction-zone UHP metamorphism. Earth and Planetary Science Letters 237, 729–734.

Zhang, R.Y., Liou, J.G., Zheng, J.P., Yui, Z-F, Griffin, W.L., O'Reilly, S.Y., 2005b. Petrogenesis of the Yangkou ultramafic complex with rhythmic layering structure from the Sulu UHP terrane, China. American Mineralogist 90, 801–813.

Zhang, Z.M., Xiao, Y.L., Hoefs, J., Xu, Z.Q., Liou, J.G., 2005c. Petrogenesis of UHP metamorphic crustal and mantle rocks from the Chinese continental scientific drilling pre-pilot hole 1, Sulu belt, Eastern China. International Geology Review 47, 1160–1177.

Zhang, Z.M., Rumble, D., Liou, J.G., Xiao, Y.L., Gao, Y.J., 2005d. Oxygen isotope geochemistry of rocks from the pre-pilot hole of the Chinese continental scientific drilling project (CCSD-PPH1). American Mineralogist 90, 857–863.

Zhang, Z.M., Xiao, Y., Liu, F., Liou, J.G., Hoefs, J., 2005e. Petrogeneses of UHP metamorphic rocks from Qinglongshan, Southern Sulu, East-Central China. Lithos 73, 189–207.

Zhang, Z.M., Shen, K., Xiao, Y., Kerkhof, A.M., van den Hoefs, J., Liou, J.G., 2005f. Fluid composition and evolution of UHP metamorphism: a case study of fluid inclusions of the drill cores in southern Sulu, Eastern China. International Geology Review 47, 297–309.

Zhang, L., Song, S., Liou, J.G., Ai, Y., Li, X., 2005g. Relict coesite exsolution in omphacite from Western Tianshan eclogites, China. American Mineralogist 90, 181–186.

Zhang, Z.M., Xiao, Y., Xu, Z., Hoefs, J., Yang, J., Liu, F., Liou, J.G., 2006a. UHP metamorphic rocks from the main hole (0–2050 m) of Chinese continental scientific drilling project – I. Petrology and geochemistry. Contributions to Mineralogy and Petrology 152, 421–441.

Zhang, Z.M., Liou, J.G., Zhao, S., Shi, Z., 2006b. Petrogenesis of Maobei Fe–Ti rich eclogites from the Southern Sulu UHP metamorphic belt, east-central China. Journal of Metamorphic Geology 24, 727–741.

Zhang, Z.M., Xiao, Y.L., Zhao, X.D., Shi, C., 2006c. Fluid–rock interaction during the continental deep subduction: oxygen isotopic profile of the main hole of the CCSDD project. Acta Petrologica Sinica 22, 1941–1951 (in Chineses with English abstract).

Zhang, Z.M., Shen, K., Xiao, Y., Hoefs, J., Liou, J.G., Zu, Z., 2006d. Mineral and fluid inclusions in zircon of UHP metamorphic rocks from the CCSD-main hole. A record of metamorphic evolution and fluid activity. Lithos 92, 378–398.

Zhang, K.J., Cai, J.X., Zhang, Y.X., Zhao, T.P., 2006e. Eclogites from central Qiangtang, northern Tibet (China) and tectonic implication. Earth and Planetary Science Letters 245, 722–729.

Zhang, R.Y., Liou, J.G., Ernst, W.G., 2007a. Ultrahigh-pressure metamorphic belts in China: major progress in the past several years. International Geology Review 49, 504–519.

Zhang, R.Y., Li, T., Rumble, D., Yui, T-F., Li, L., Yang, J.S., Pan, Y., Liou, J.G., 2007b. Multiple mantle metasomatisms in the Sulu ultrahigh-*P* garnet peridotite constrained by petrological and geochemical investigation. Journal of Metamorphic Geology 25, 149–164.

Zhang, L., Ai, Y., Li, X., Rubatto, D., Song, B., Williams, S., Song, S., Ellis, D., Liou, J.G., 2007c. Triassic collision of western Tianshan orogenic belt, China: evidences from the SHRIMP U–Pb dating of zircons from HP/UHP eclogitic rocks. Lithos 96, 266–280.

Zhang, Z.M., Shen, K., Liou, J.G., Zhao, X., 2007d. Fluid inclusions associated with exsolution quartz needles in omphacite of UHP eclogites from the main hole of Chinese continental scientific drilling project. International Geology Review 49, 479–486.

Zhang, Zhong M., Yang, J.S., Rong, H., Hu, J.Z., Su, J.F., Mao, H.K., 2007e. Discovery of diamond in eclogite from the Chinese continental scientific drilling project main hole (CCSD-MH) in the Sulu UHPM belt. Acta Petrologica Sinica 23, 3201–3206 (in Chinese with English abstract).

Zhang, L.F., Ai, Y.L., Song, S., Liou, J.G., Wei, C.J., 2007f. A brief review of UHP metamorphic rocks, southeastern Tianshan, western China. International Geology Review 49, 811–823.

Zhang, R.Y., Liou, J.G., Ernst, W.G., 2007g. Ultrahigh-pressure metamorphic belts in China: Major progress in the past several years. International Geology Review 49, 487–503.

Zhang, J.X., Mattinson, C.G., Meng, F., Wan, Y., Tung, K., 2008a. Polyphase tectonothermal history recorded in granulized gneiss from the North Qaidam HP/UHP terrane, western China: evidence from zircon U–Pb geochronology. Geological Society of American Bulletin 120, 732–749.

Zhang, Z.M., Shen, K., Liu, Y.S., Sun, W.D., Liou, J.G., 2008b. Fluids in the deeply subducted continental crust: a study of petrology, mineral chemistry and fluid inclusion of UHP metamorphic veins from the Sulu orogen, eastern China. Acta Geochemica et Cosmochimica 72, 3200–3228.

Zhang, R.Y., Liou, J.G., Iizuka, Y. Yang, J.S., in press-a. First record of K-cymrite in North Qaidam UHP eclogite, Western China. American Mineralogist.

Zhang, Z.M., Xu, Z., Shen, K., Shi, C., Dong, H., in press-b. Petrological and geochronological constraints on the formation and subduction of the continental crust in the southern Sulu orogen, eastern-central China. Tectonophysics.

Zhao, R.X., Liou, J.G., Zhang, R.Y., 2005. SHRIMP U–Pb dating of zircon from the Xugou UHP eclogite, Sulu terrane, eastern China. International Geology Review 47, 805–814.

Zhao, R.X., Liou, J.G., Zhang, R.Y., Li, T.F., 2006a. SHRIMP U–Pb zircon dating of the Rongcheng eclogite and associated peridotite: new constraints for ultrahigh-pressure metamorphism of mantle-derived mafic-ultramafic bodies from the Sulu terrane. In: Hacker, B.R., McClelland, W.C., Liou, J.G. (Eds.), Ultrahigh-Pressure Metamorphism: Deep Continental Subduction. Geological Society of America Special Paper 403, 115–125.

Zhao, Z.-F., Zheng, Y.-F., Gao, T.-S., Wu, Y.-B., Chen, B., Chen, F.K., Wu, F.-Y., 2006b. Isotopic constraints on age and duration of fluid-assisted high-pressure eclogite-facies recrystallization during exhumation of deeply subducted continental crust in the Sulu orogen. Journal of Metamorphic Geology 24, 687–702.

Zhao, R.X., Liou, J.G., Tsujimori, T., Zhang, R.Y., 2007a. Petrology and U–Pb SHRIMP geochronology of a garnet peridotite, Sulu UHP terrane, east-central China. International Geology Review 49, 732–752.

Zhao, R.X., Zhang, R.Y., Liou, J.G., Booth, A.L., Pope, E.C., Chamberlain, C., 2007b. Petrochemistry, oxygen isotopes and U–Pb SHRIMP geochronology of mafic-ultramafic bodies from the Sulu UHP terrane, China. Journal of Metamorphic Geology 25, 207–224.

Zhao, Z.-F., Zheng, Y.-F., Chen, R.-X., Xia, Q.-X., Wu, Y.-B., 2007c. Element mobility in mafic and felsic ultrahigh-pressure metamorphic rocks during continental collision. Geochimica et Cosmochimica Acta 71, 5244–5266.

Zhao, Z.-F., Chen, B., Zheng, Y.-F., Chen, R.-X., Wu, Y.-B., 2007d. Mineral oxygen isotope and hydroxyl content changes in ultrahigh-pressure eclogite–gneiss transition from the Chinese continental scientific drilling core samples. Journal of Metamorphic Geology 25, 165–186.

Zhao, Z.-F., Zheng, Y.-F., Wei, C.S., Chen, F.K., Liu, X.M., Wu, F.-Y., 2008. Zircon U–Pb ages, Hf and O isotopes constrain the crustal architecture of the ultrahigh-pressure Dabie orogen in China. Chemical Geology 253, 222–242.

Zheng, Y.-F., 2008. A perspective view on ultrahigh-pressure metamorphism and continental collision in the Dabie–Sulu orogenic belt. Chinese Science Bulletin 53, 3081–3104.

Zheng, Y.-F., Fu, B., Gong, B., Li, L., 2003a. Stable isotope geochemistry of ultrahigh-pressure metamorphic rocks from the Dabie–Sulu orogen in China: implications for geodynamics and fluid regime. Earth Science Review 62, 105–161.

Zheng, Y.-F., Yang, J.-J., Gong, B., Jahn, B.-m., 2003b. Partial equilibrium of radiogenic and stable isotope systems in garnet peridotite during UHP metamorphism. American Mineralogist 88, 1633–1643.

Zheng, Y.-F., Wu, Y.-B., Chen, F.-K., Gong, B., Li, L., Zhao, Z.-F., 2004. Zircon U–Pb and oxygen isotope evidence for a large-scale 18O depletion event in igneous rocks during the Neoproterozoic. Geochimica et Cosmochimica Acta 68, 4145–4165.

Zheng, J.P., Zhang, R.Y., Liou, J.G., Griffin, W.L., O'Reilly, S.Y., 2005a. Heterogeneous and metasomatised mantle recorded by trace elements in minerals of the Donghai garnet peridotites, Sulu UHP terrane, China. Chemical Geology 221, 243–259.

Zheng, Y.-F., Wu, Y.-B., Zhao, Z.-F., Zhang, S.-B., Xu, Z., Wu, F.-Y., 2005b. Metamorphic effect on zircon Lu–Hf and U–Pb isotope systems in ultrahigh-pressure metagranite and metabasite. Earth and Planetary Science Letters 240, 378–400.

Zheng, J.P., Griffin, W.L., O'Reilly, S.Y., Yang, J.S., Zhang, R.Y., 2006a. A refractory mantle protolith in younger continental crust, east-central China: age and composition of zircon in the Sulu ultrahigh-pressure peridotite. Geology 34, 705–708.

Zheng, J.P., Griffin, W.L., O'Reilly, S.Y., Yang, J.S., Li, T.F., Zhang, M., Zhang, R.Y., Liou, J.G., 2006b. Mineral chemistry of peridotites from Paleozoic, Mesozoic and Cenozoic lithosphere. Constraints on mantle evolution beneath eastern China. Journal of Petrology 46, 1–24.

Zheng, Y.-F., Zhao, Z.-F., Wu, Y.-B., Zhang, S.-B., Liu, X.-M., Wu, F.-Y., 2006c. Zircon U–Pb age, Hf and O isotope constraints on protolith origin of ultrahigh-pressure eclogite and gneiss in the Dabie orogen. Chemical Geology 231, 135–158.

Zheng, Y.-F., Wu, Y.-B., Gong, B., Chen, R.-X., Tang, J., Zhao, Z.-F., 2007a. Tectonic driving of Neoproterozoic glaciations: evidence from extreme oxygen isotope signature of meteoric water in granite. Earth and Planetary Science Letters 256, 196–210.

Zheng, Y.-F., Gao, T.-S., Wu, Y.-B., Gong, B., 2007b. Fluid flow during exhumation of deeply subducted continental crust: zircon U–Pb age and O isotope studies of quartz vein in eclogite. Journal of Metamorphic Geology 25, 267–283.

Zheng, Y.-F., Zhang, S.-B., Zhao, Z.-F., Wu, Y.-B., Li, X.-H., Li, Z.-X., Wu, F.-Y., 2007c. Contrasting zircon Hf and O isotopes in the two episodes of Neoproterozoic granitoid in South China: implications for growth and reworking of continental crust. Lithos 96, 127–150.

Zheng, Y.-F., Chen, R.X., Zhao, Z.F., in press. Chemical geodynamics of continental subduction-zone metamorphism: insights from the studies of the Chinese continental scientific drilling (CCSD) core samples. Tectonophysics. doi: 10.1016/j.tecto.2008.09.014.